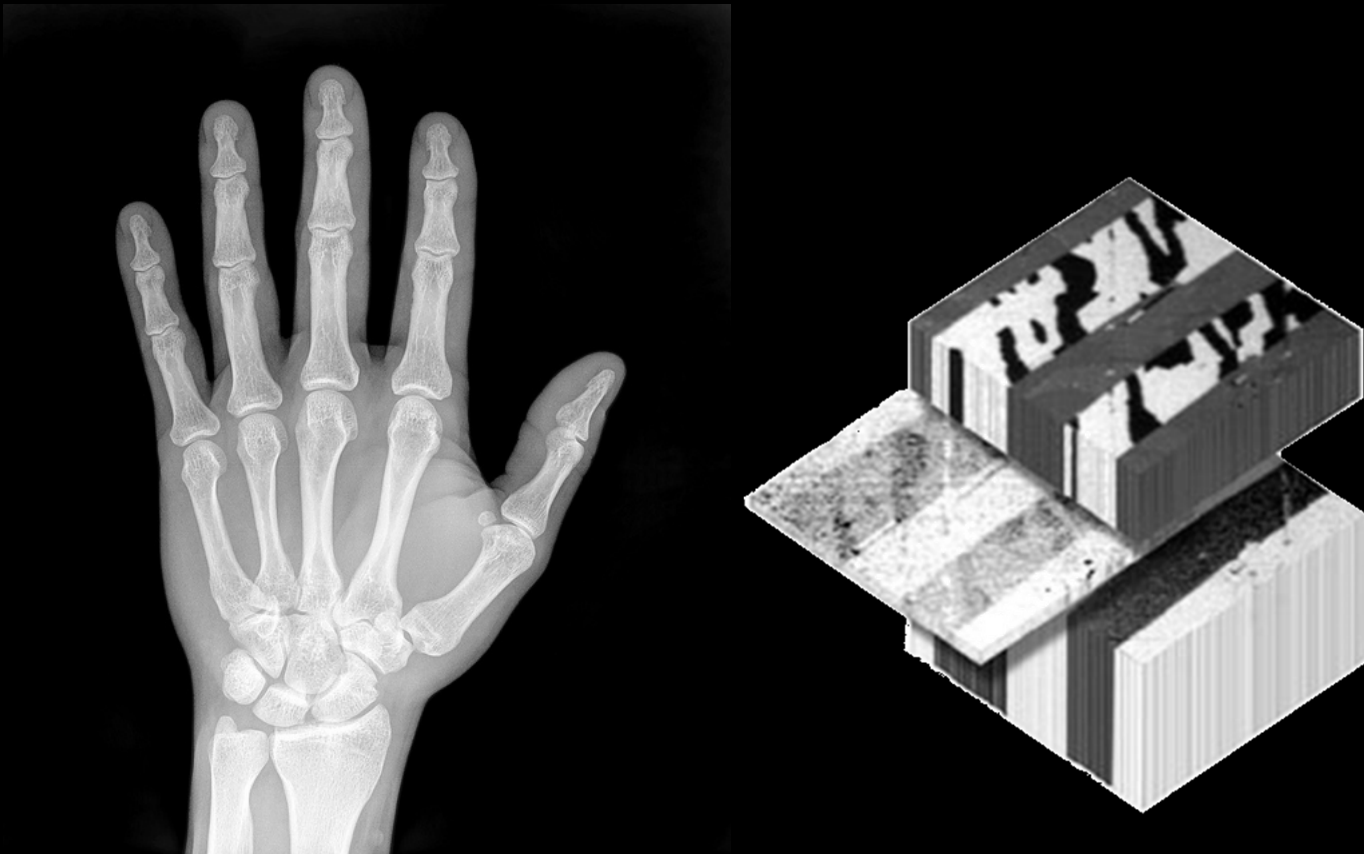


Magnetism as seen with X-Rays

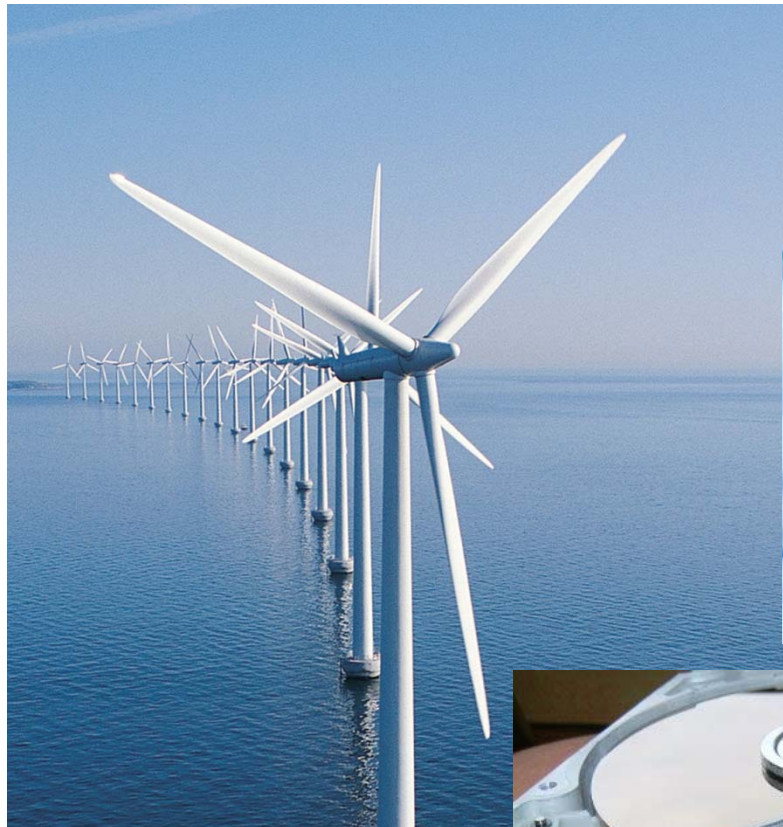


Elke Arenholz

Lawrence Berkeley National Laboratory
and

Department of Material Science and Engineering, UC Berkeley

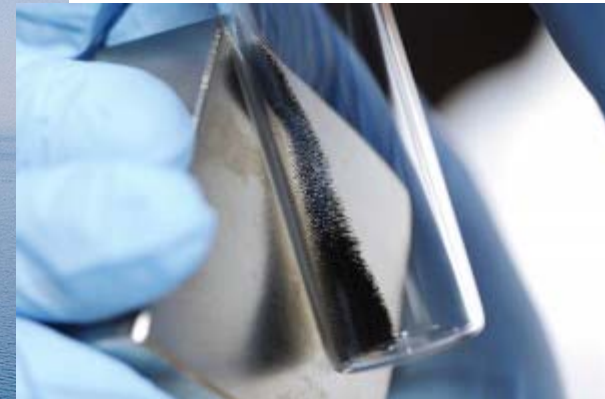
Magnetic Materials Today



**Magnetic thin films
for
information storage
and processing**



**Magnetic materials
for
energy applications**



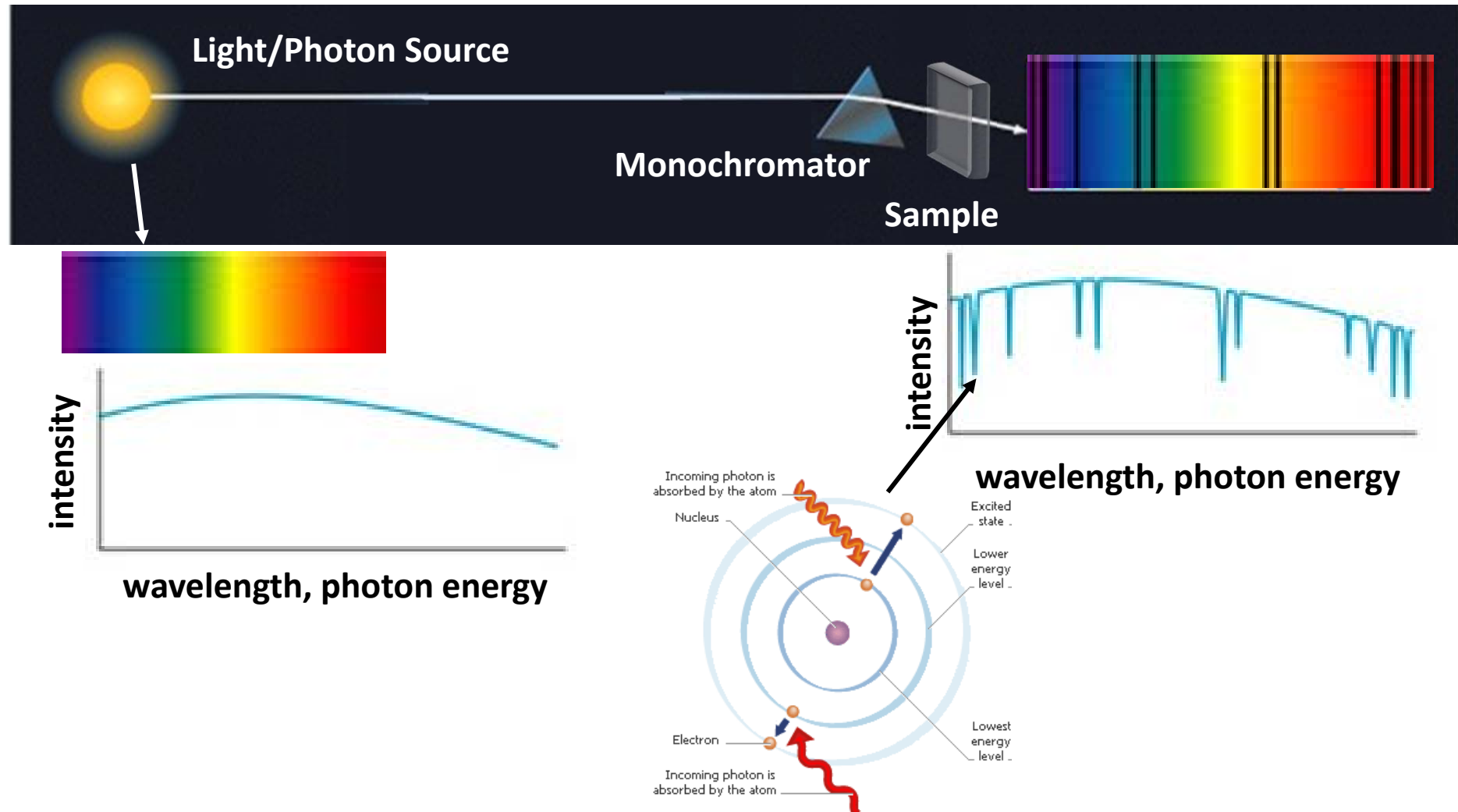
**Magnetic
nanoparticles
for
biomedical and
environmental
applications**

Magnetic Materials Characterization Wish List

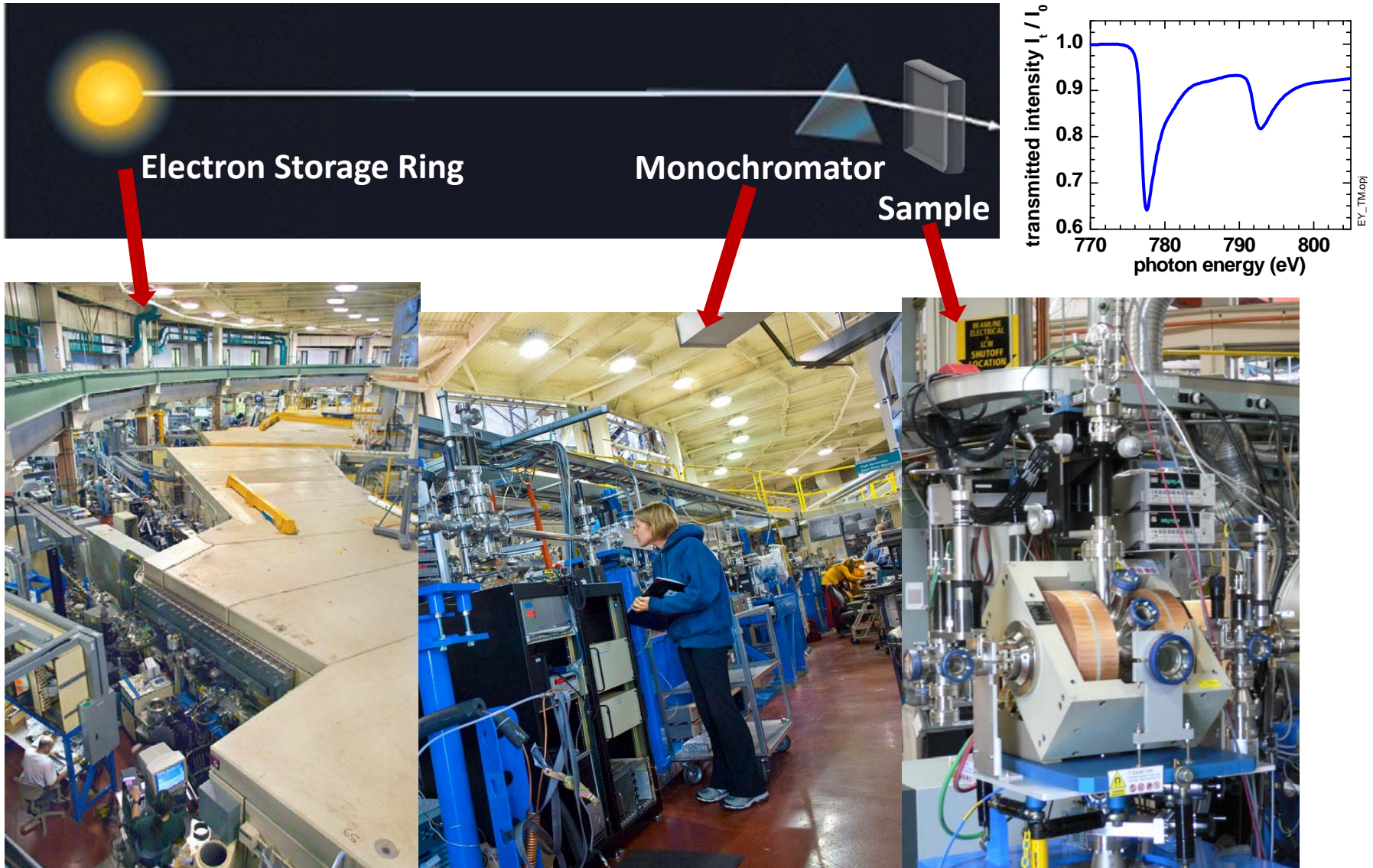


Soft X-Ray Spectroscopy and Microscopy

Spectroscopy

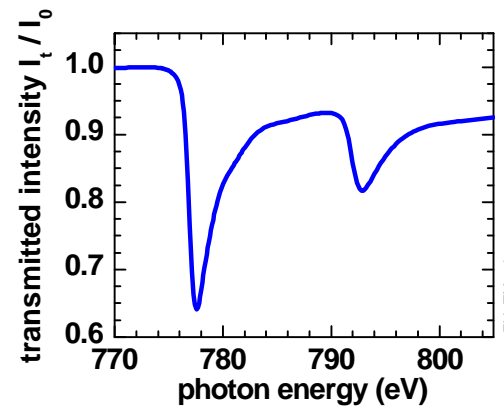
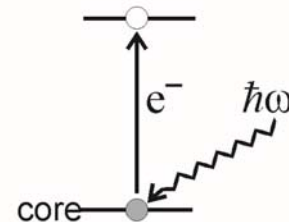
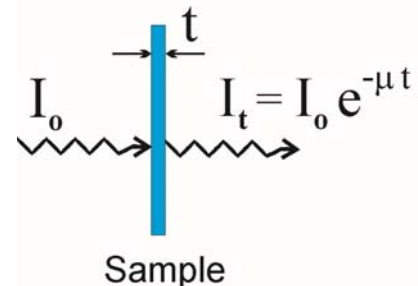


Soft X-Ray Spectroscopy ($h\nu \approx 500\text{-}1000\text{eV}$, $\lambda \approx 1\text{-}2\text{nm}$)



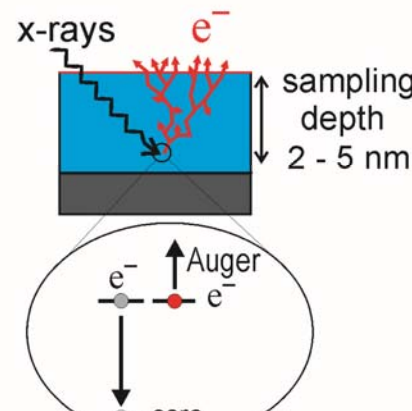
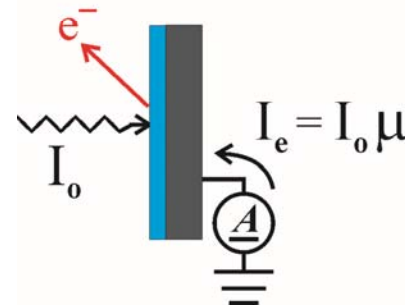
X-Ray Absorption – Detection Modes

Transmission

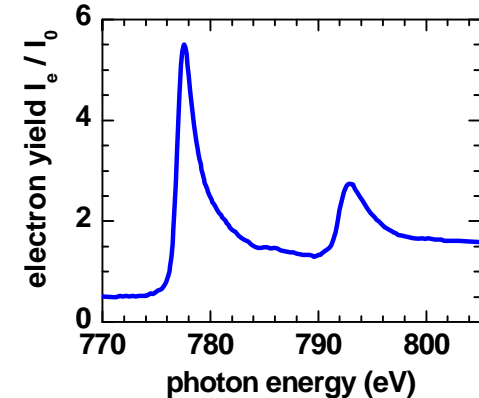


photons
absorbed

Electron Yield



Magnetism (Springer)

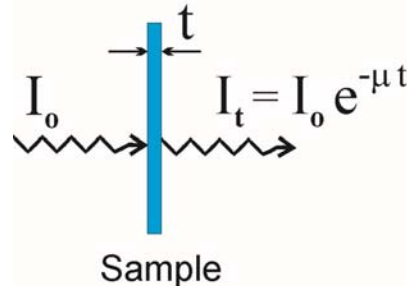


electrons
generated

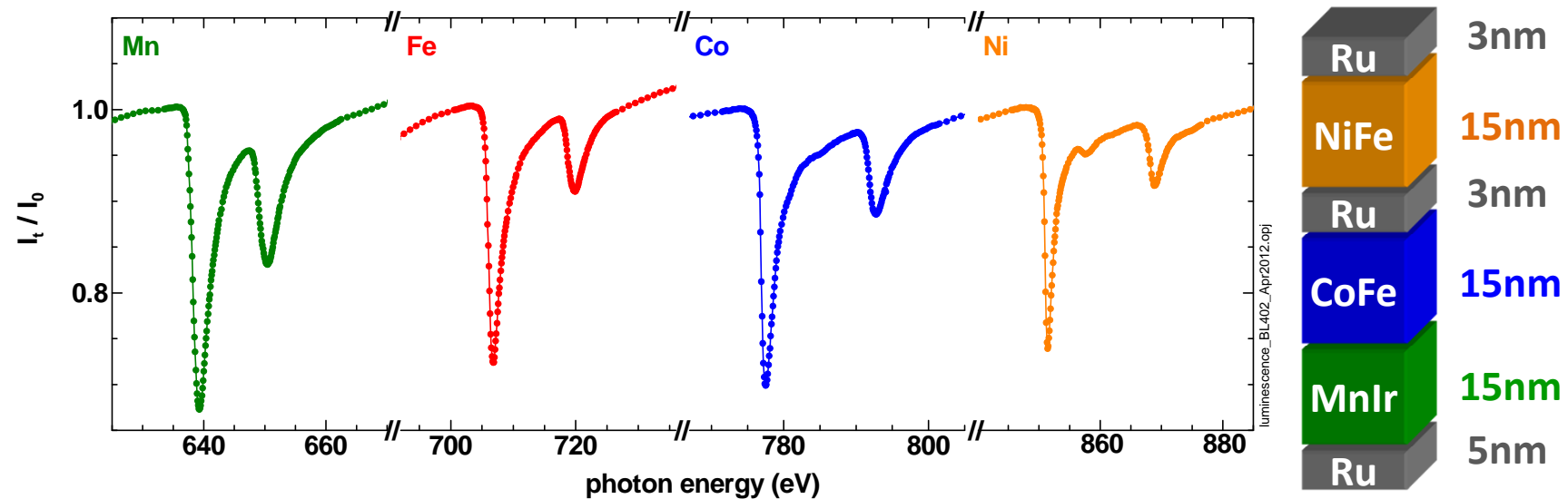
Electron yield:

- + Absorbed photons create core holes subsequently filled by Auger electron emission
- + Auger electrons create low-energy secondary electron cascade through inelastic scattering
- + Emitted electrons \propto probability of Auger electron creation \propto absorption probability

Soft X-Ray Absorption – Probing Depth

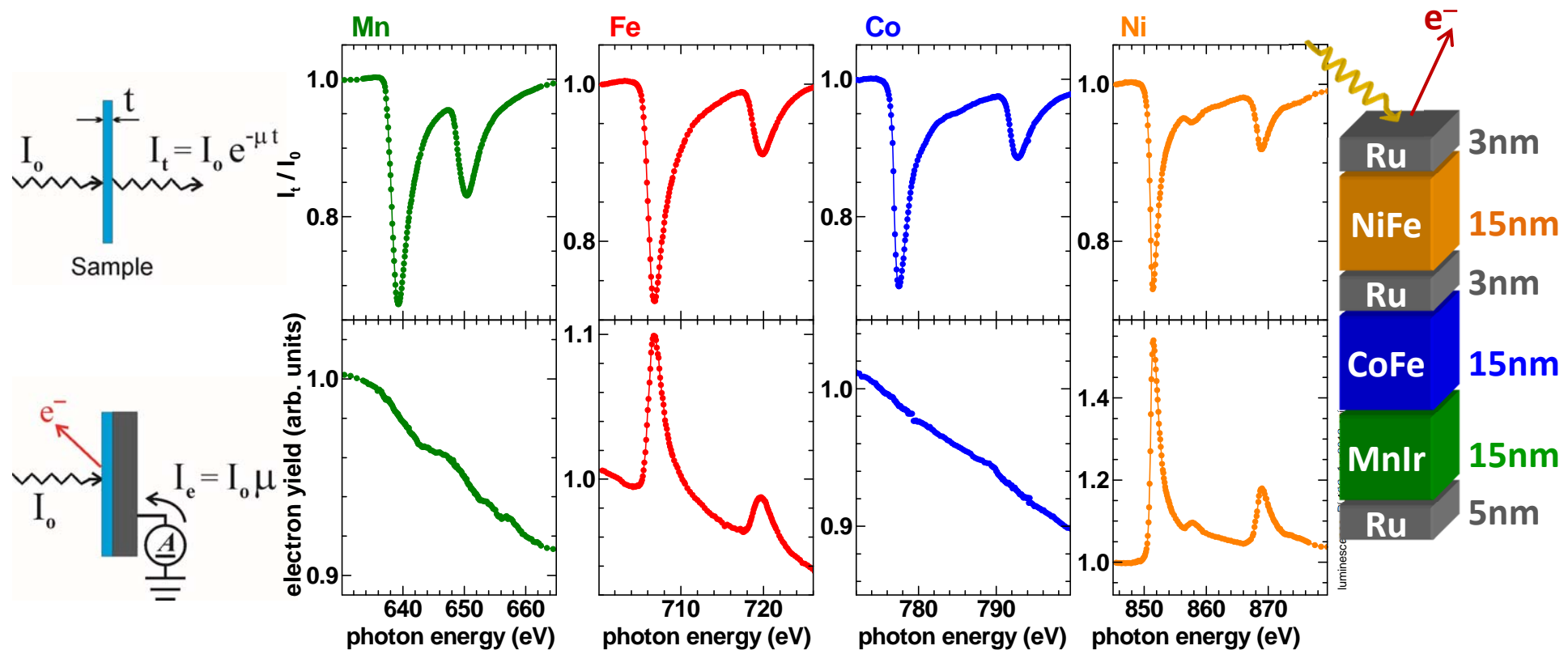


Element	10 eV below L_3 1/ μ [nm]	at L_3 1/ μ [nm]	40 eV above L_3 1/ μ [nm]
Fe	550	17	85
Co	550	17	85
Ni	625	24	85



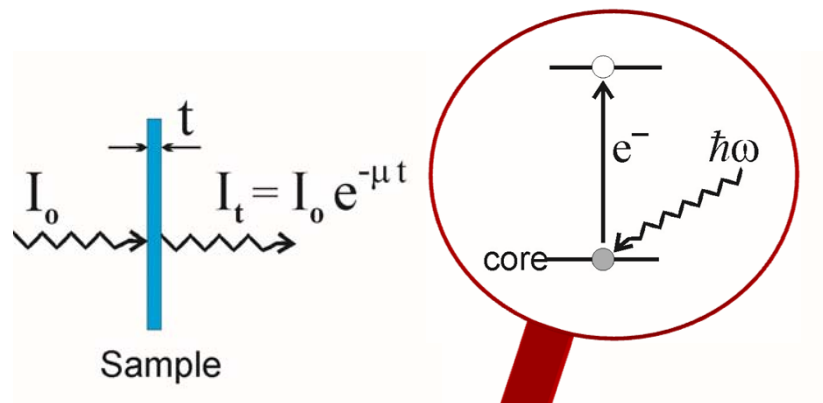
~10-20 nm layer thick films supported by substrates transparent to soft x-rays

X-Ray Absorption – Detection Modes and Probing Depth



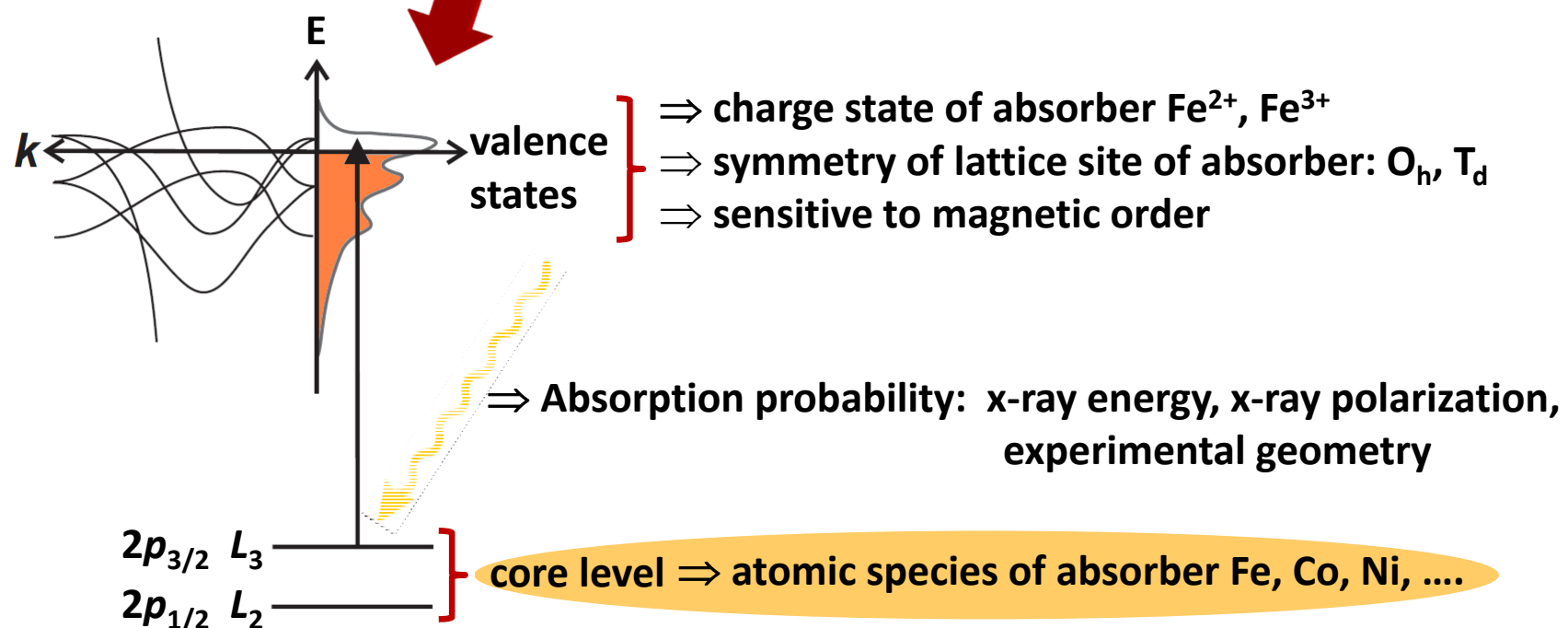
- + Electron sample depth: 2-5 nm in Fe, Co, Ni
 \Rightarrow 60% of the electron yield originates from the topmost 2-5 nm

X-Ray Absorption – Fundamentals

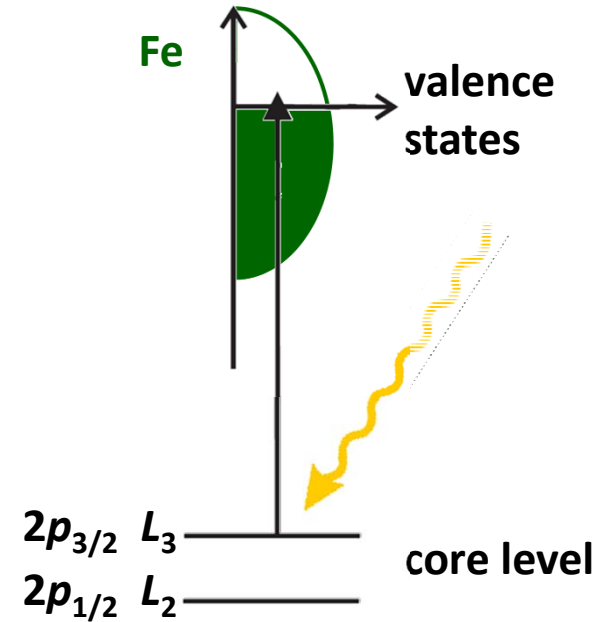
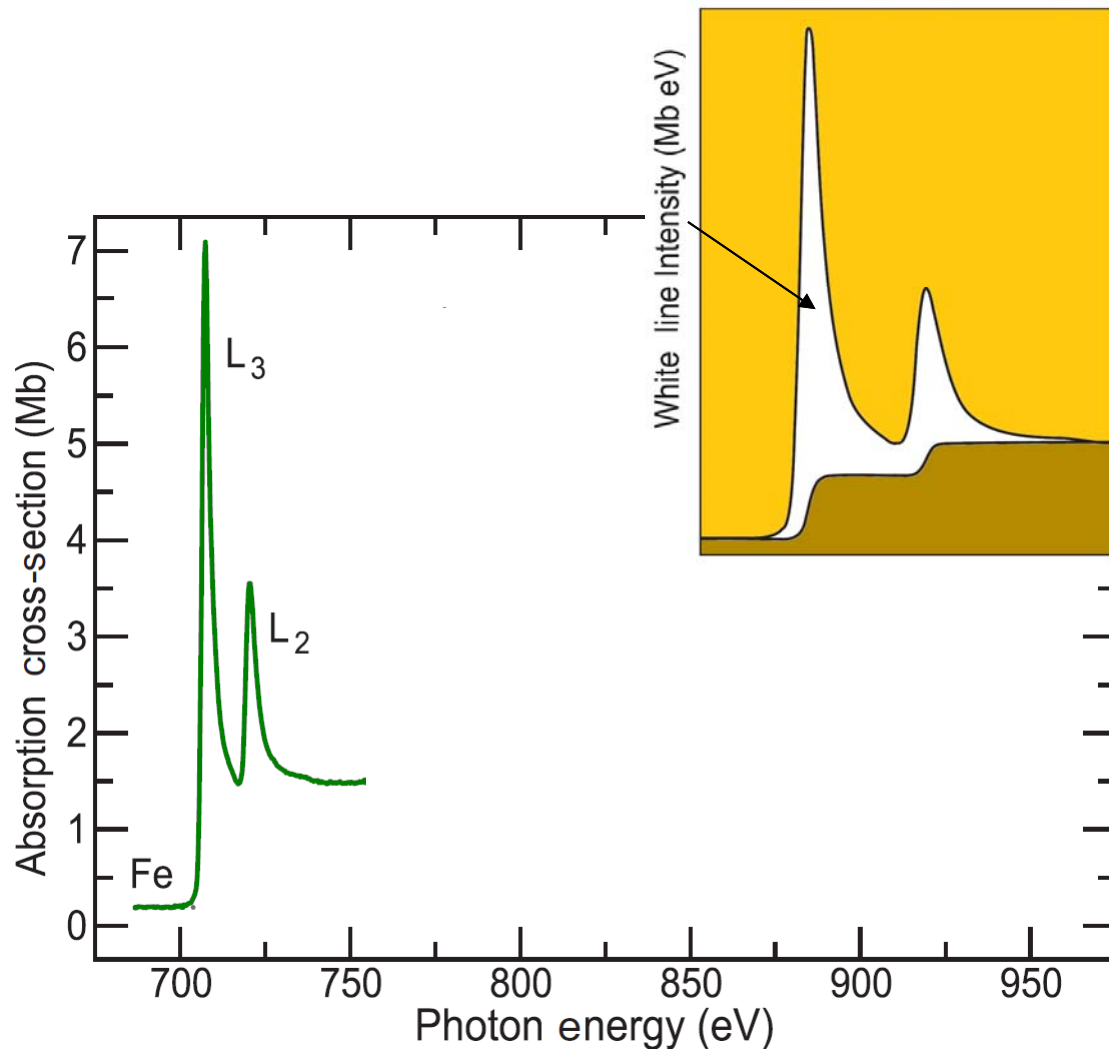


Experimental Concept:

Monitor reduction in x-ray flux transmitted through sample as function of photon energy

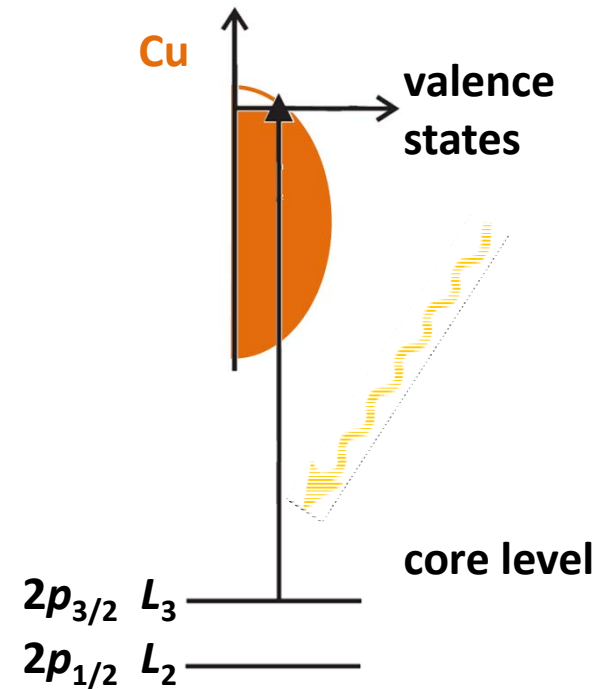
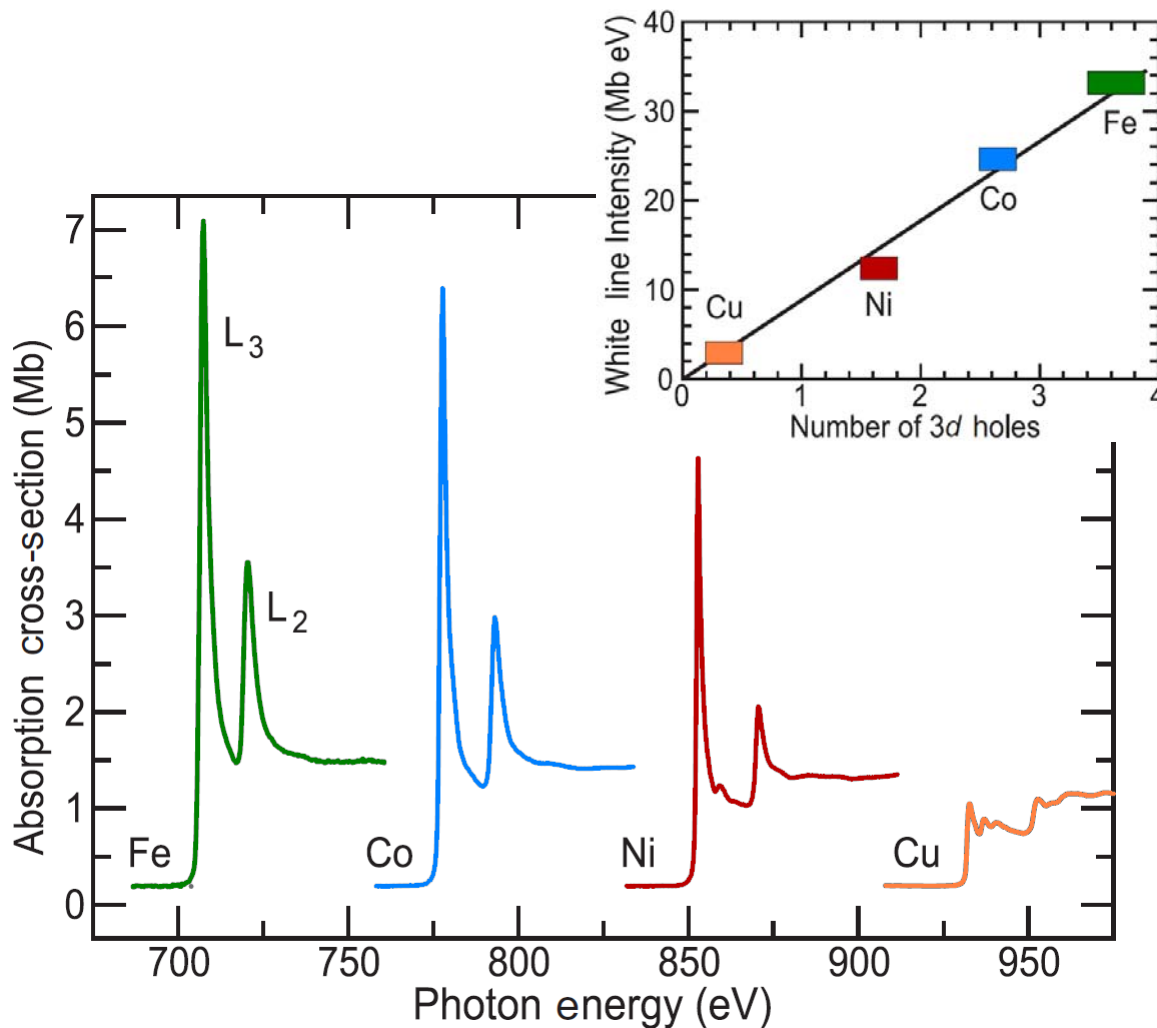


'White Line' Intensity



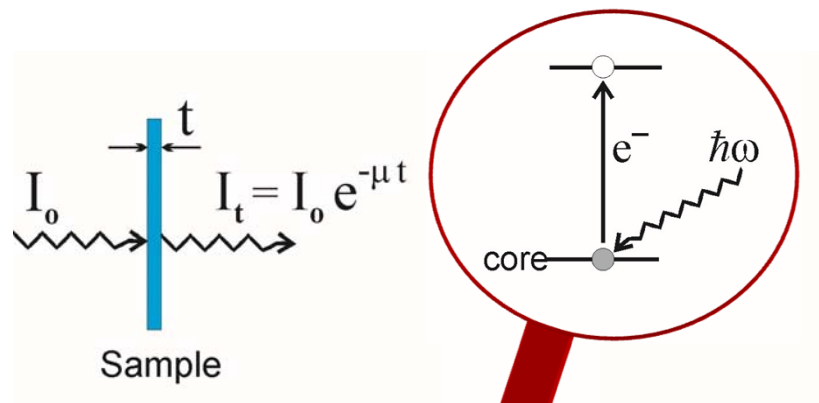
Intensity of $L_{3,2}$ resonances is proportional to number of d states above the Fermi level, i.e. number of holes in the d band.

'White Line' Intensity



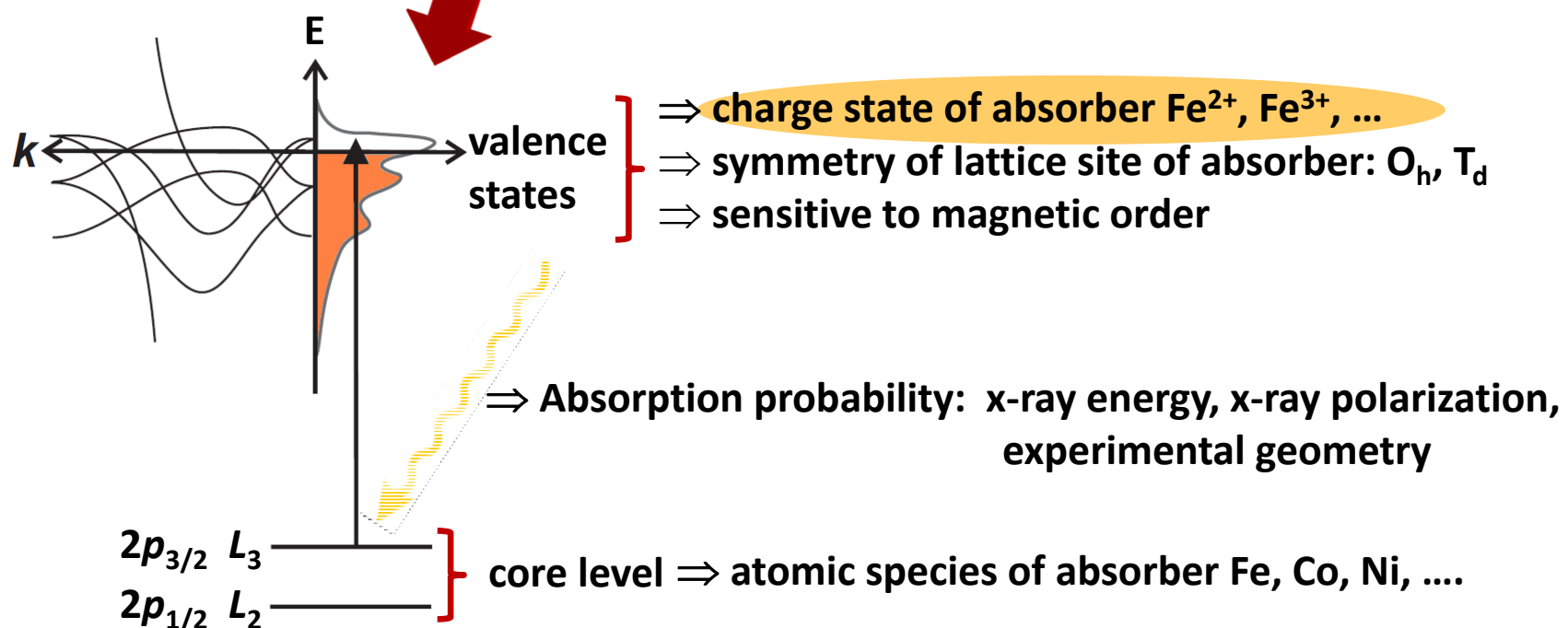
Intensity of $L_{3,2}$ resonances is proportional to number of d states above the Fermi level, i.e. number of holes in the d band.

X-Ray Absorption – Fundamentals

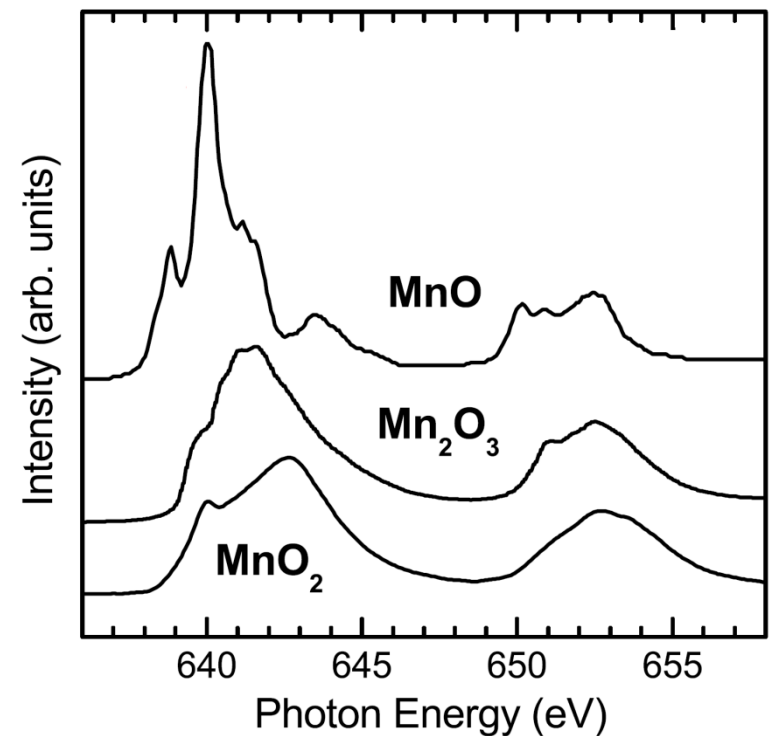
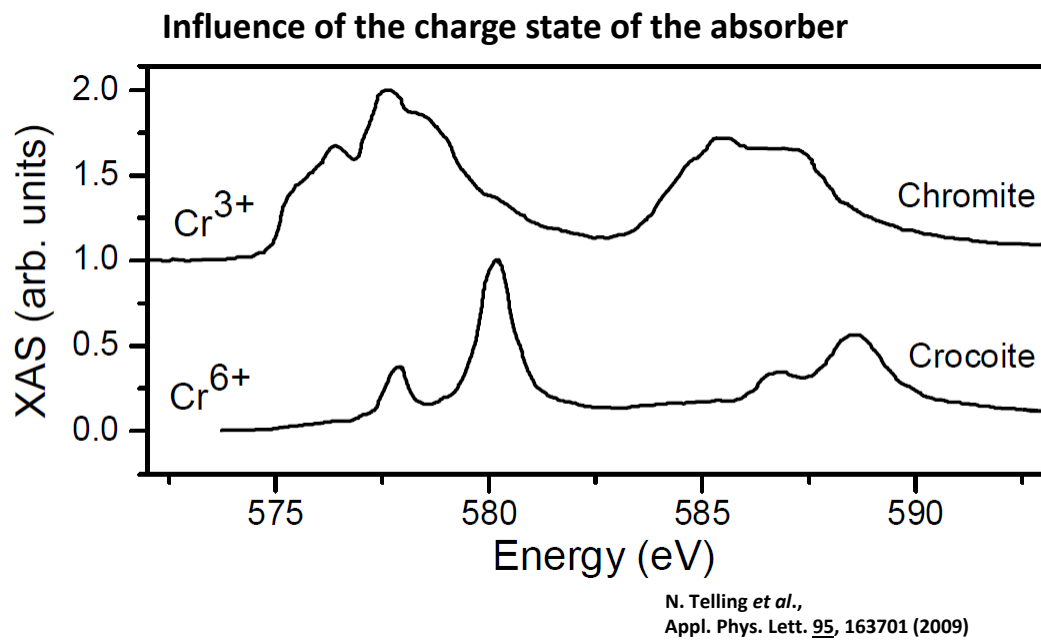


Experimental Concept:

Monitor reduction in x-ray flux transmitted through sample as function of photon energy

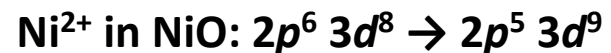


X-ray Absorption – Valence State



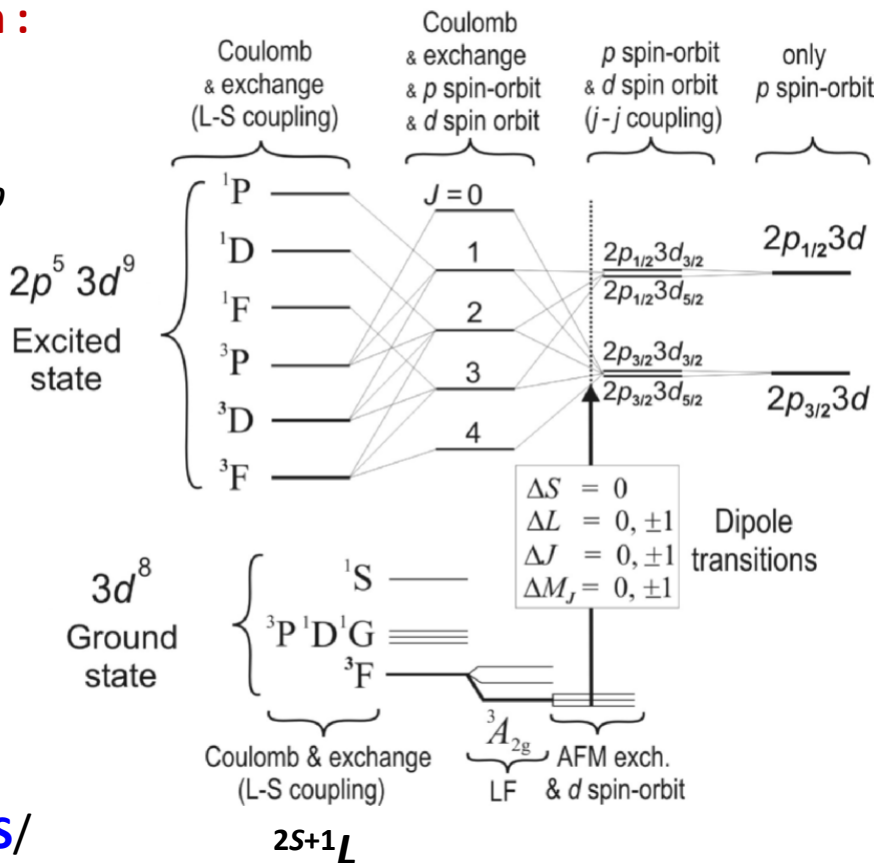
J.-S. Kang *et al.*, Phys. Rev. B **77**, 035121 (2008)

X-Ray Absorption – Configuration Model



Configuration model, e.g. L edge absorption :

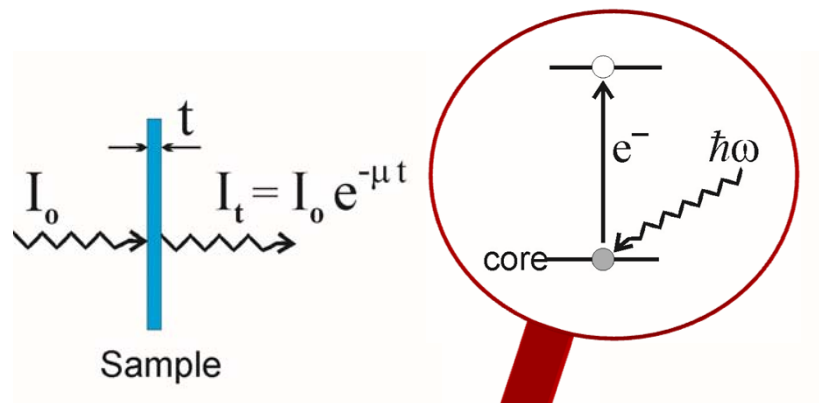
- + Excited from ground/initial state configuration, $2p^6 3d^8$ to excited/final state configuration, $2p^5 3d^9$
- + Omission of all full subshells (spherical symmetric)
- + Takes into account correlation effects in the ground state as well as in the excited state
- + Leads to multiplet effects/structure



<http://www.anorg.chem.uu.nl/CTM4XAS/>

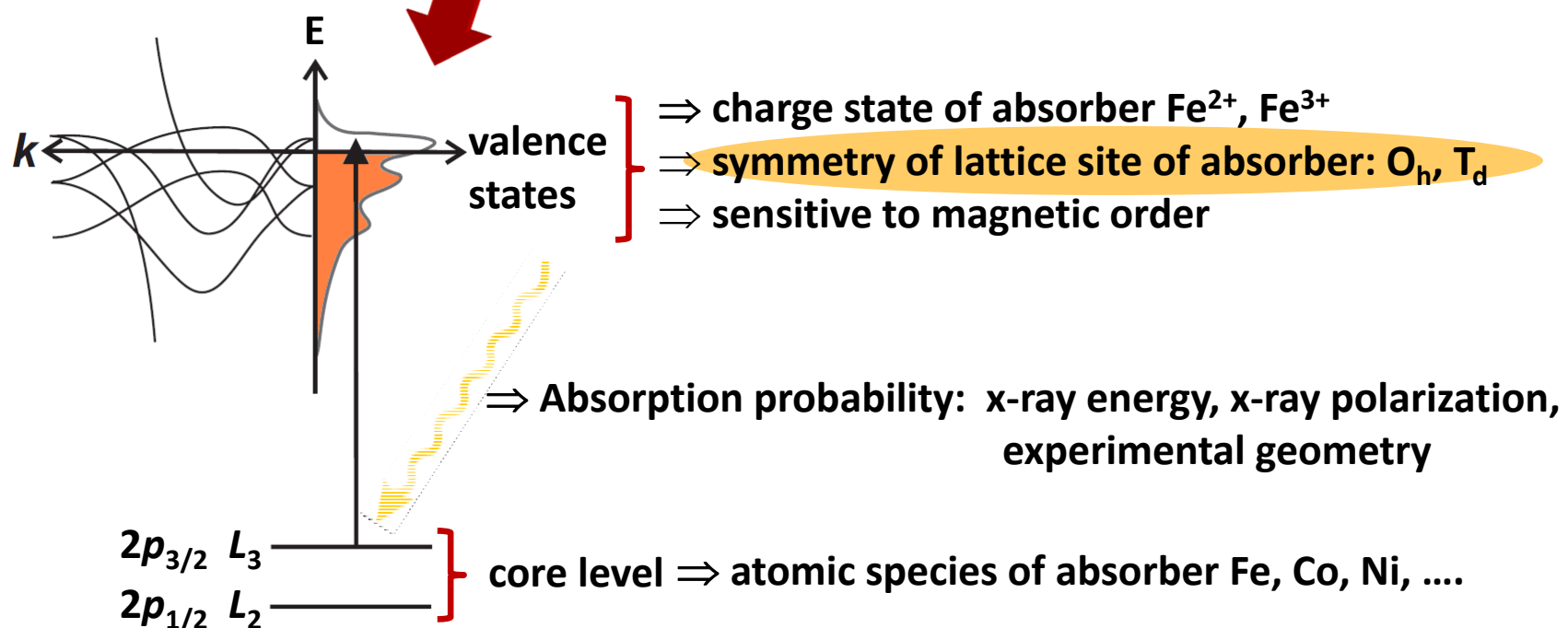
J. Stöhr, H.C. Siegmann,
Magnetism (Springer)

X-Ray Absorption – Fundamentals

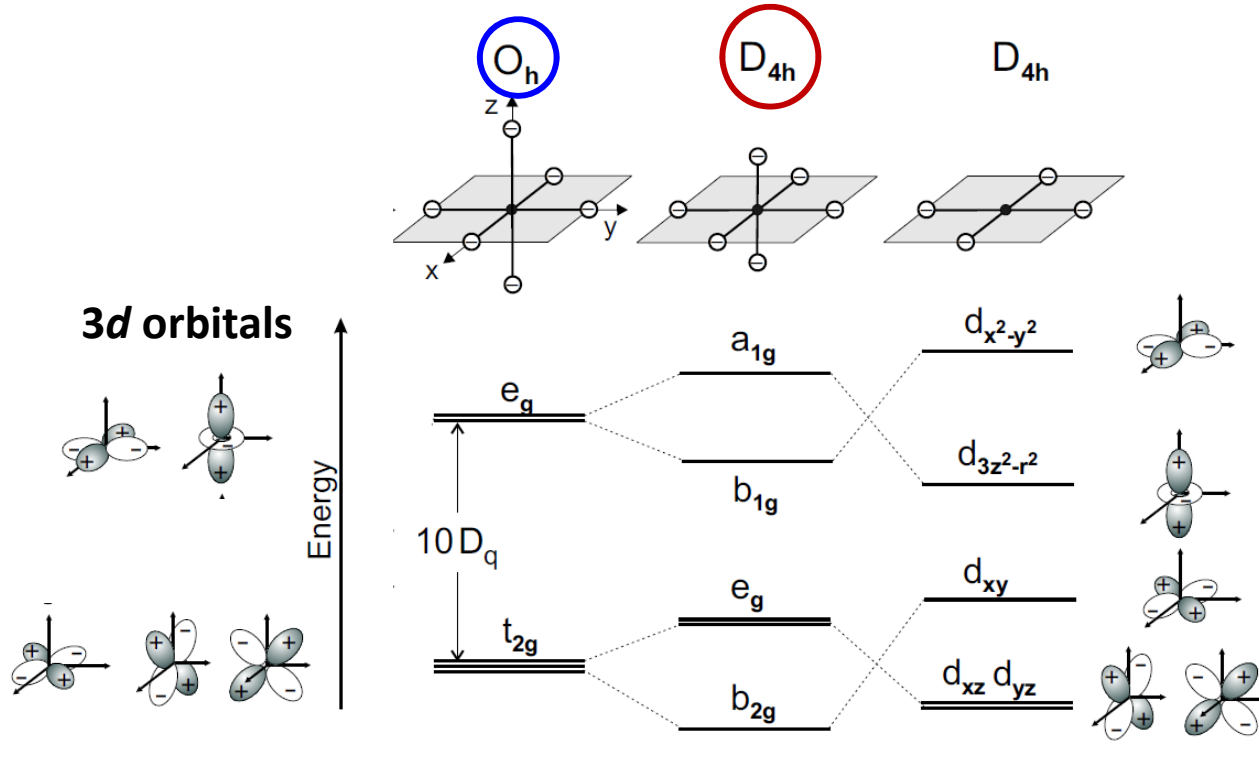


Experimental Concept:

Monitor reduction in x-ray flux transmitted through sample as function of photon energy



Sensitivity To Site Symmetry: $\text{Ti}^{4+} L_{3,2}$



+ Electric dipole transitions: $d^0 \rightarrow 2p^5 3d^1$

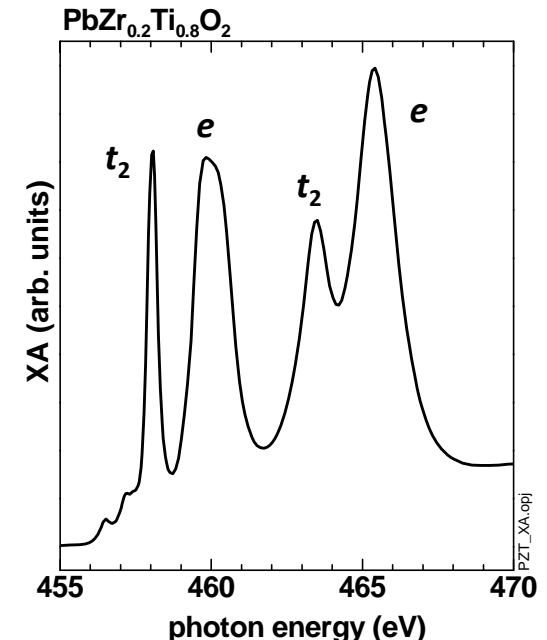
+ Crystal field splitting $10Dq$ acting on 3d orbitals:

Octahedral symmetry:

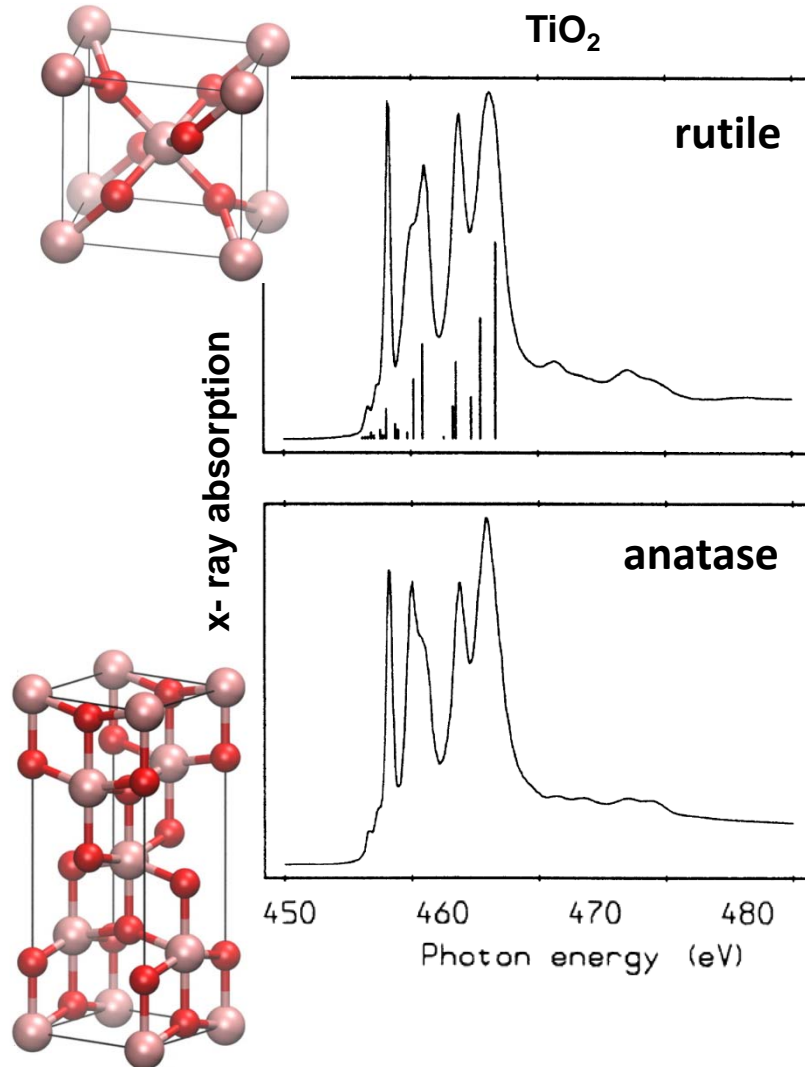
e orbitals towards ligands \rightarrow higher energy
 t_2 orbitals between ligands \rightarrow lower energy

Tetragonal symmetry:

e orbitals $\rightarrow b_2 = d_{xy}, e = d_{yz}, d_{yz}$
 t_2 orbitals $\rightarrow b_1 = d_{x^2-y^2}, a_1 = d_{3z^2-r^2}$



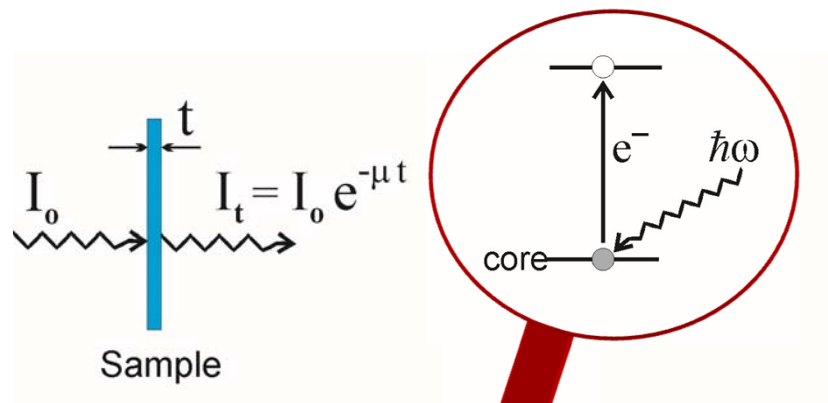
X-Ray Absorption – Lattice Symmetry



Influence of lattice site symmetry at the absorber

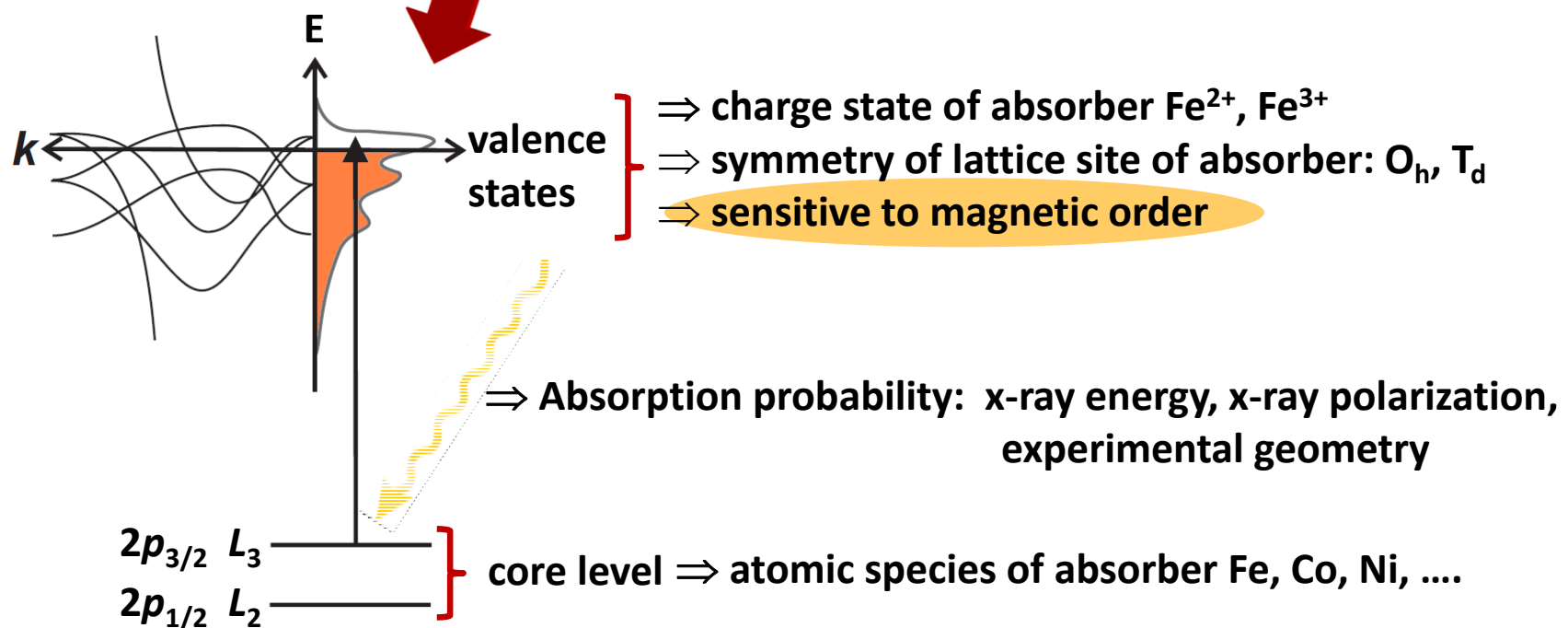
G. Van der Laan
Phys. Rev. B 41, 12366 (1990)

X-Ray Absorption – Fundamentals

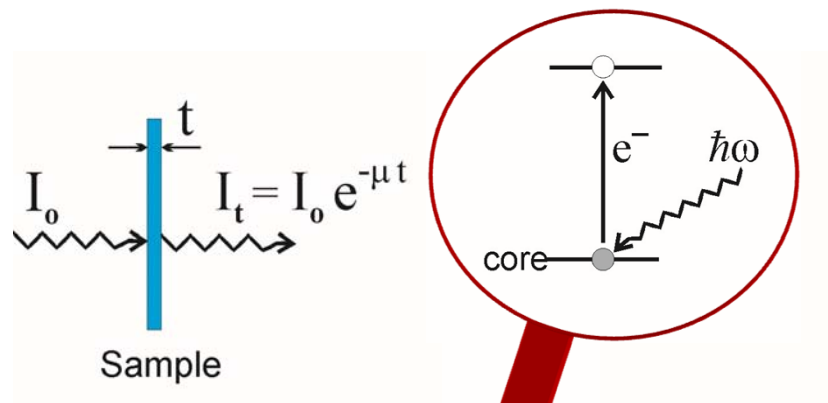


Experimental Concept:

Monitor reduction in x-ray flux transmitted through sample as function of photon energy

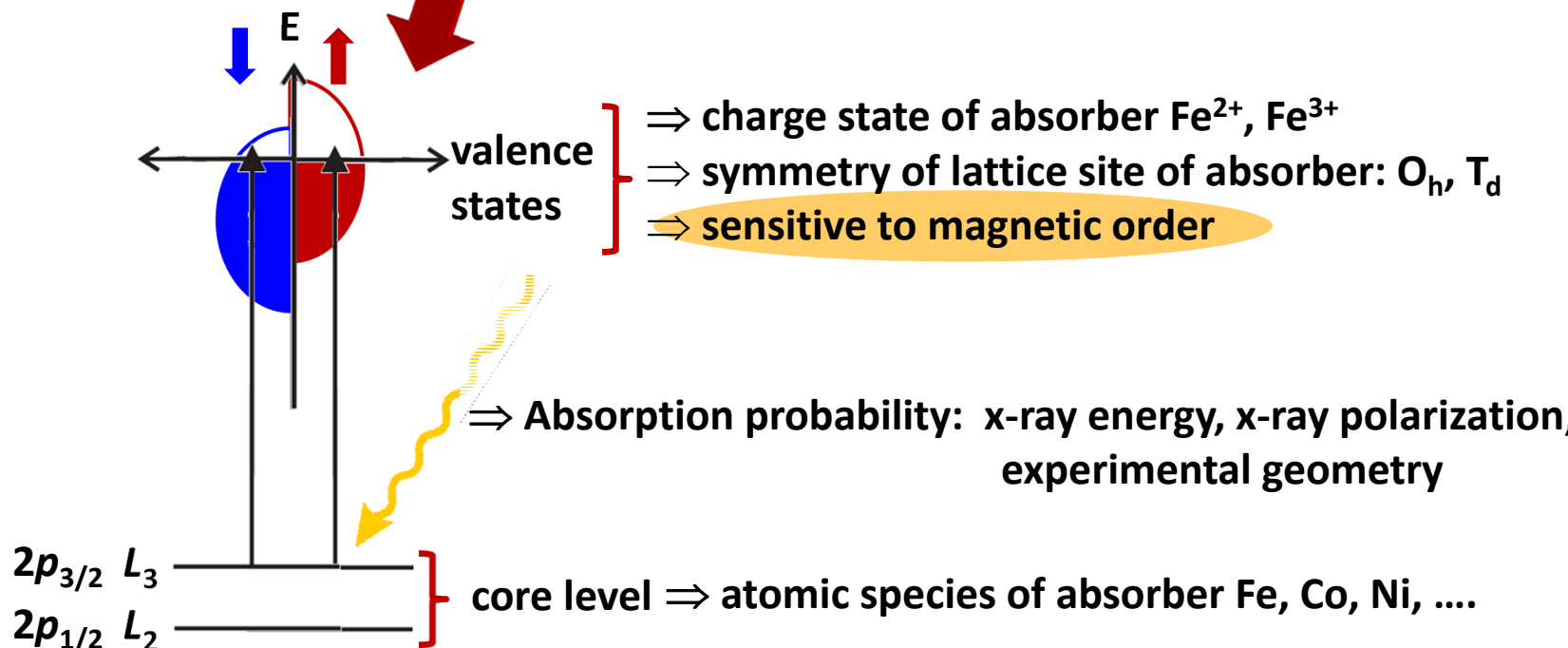


X-Ray Absorption – Fundamentals

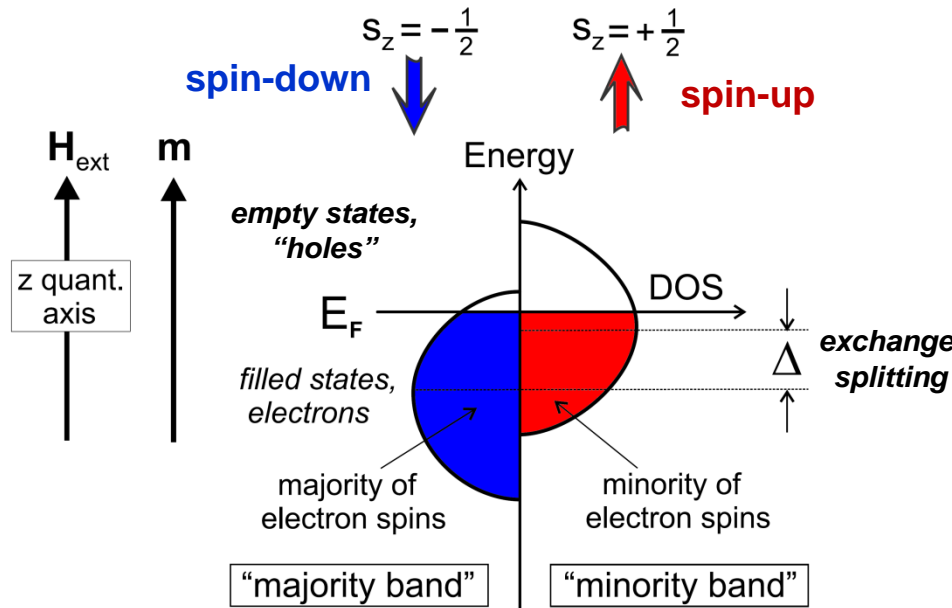


Experimental Concept:

Monitor reduction in x-ray flux transmitted through sample as function of photon energy



Stoner Model For Ferromagnetic Metals



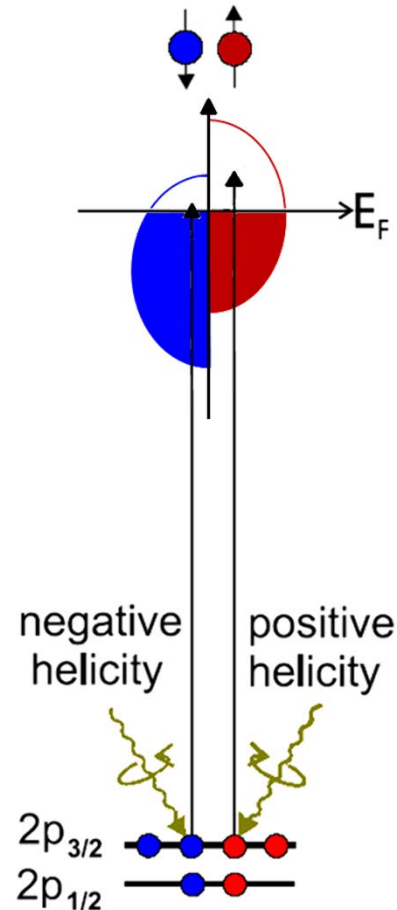
J. Stöhr, H.C. Siegmann,
Magnetism (Springer)

3d shell

- + Magnetic moments in Fe, Co, Ni well described by Stoner model: d -bands containing up and down spins shifted relative to each other by exchange splitting
- + Spin-up and spin-down bands filled according to Fermi statistics
- + Magnetic moment $|m|$ determined by difference in number of electrons in majority and minority bands

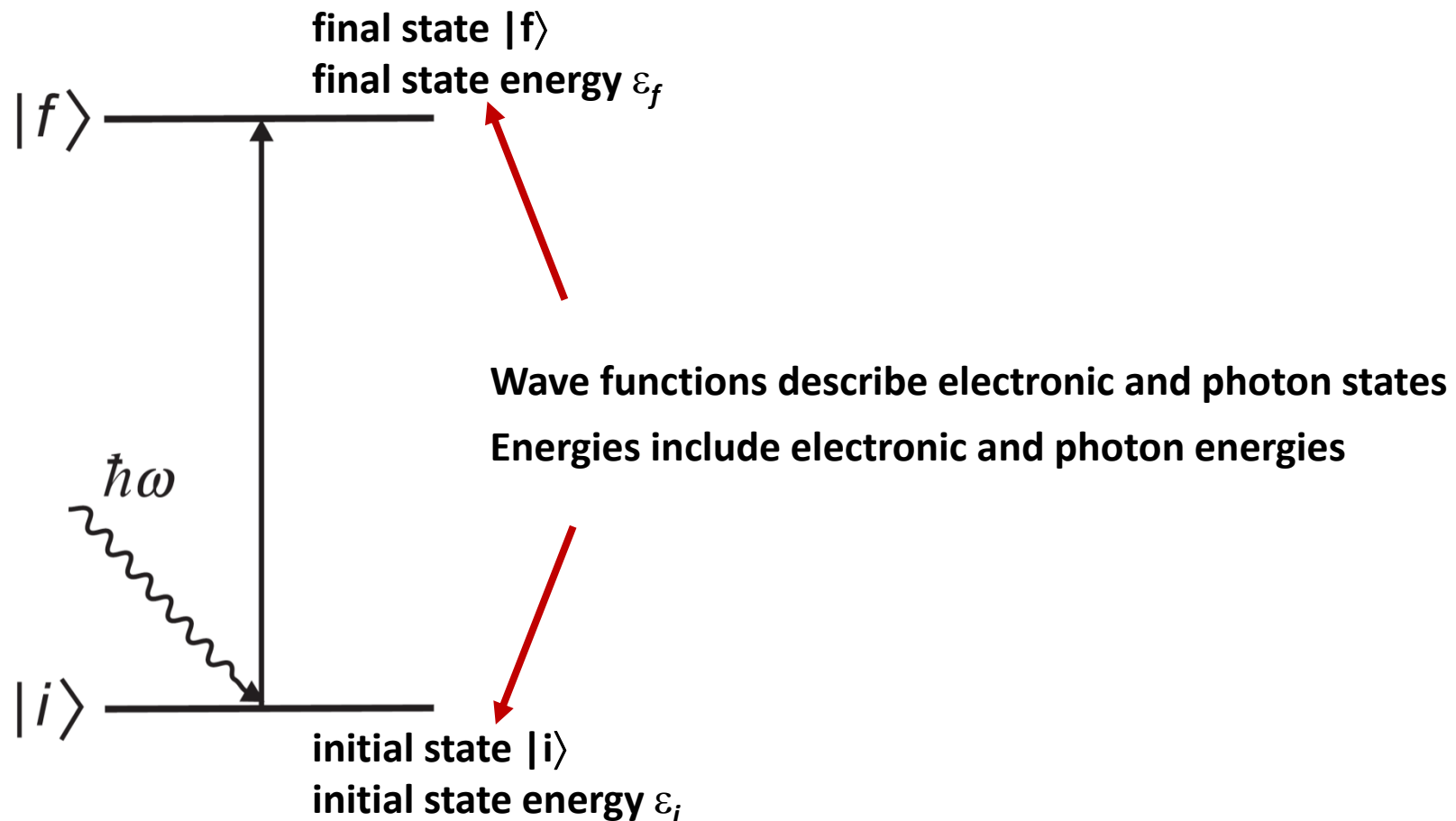
$$|m| \propto \mu_B (n_e^{\text{maj}} - n_e^{\text{min}})$$

Origin of X-ray Magnetic Circular Dichroism

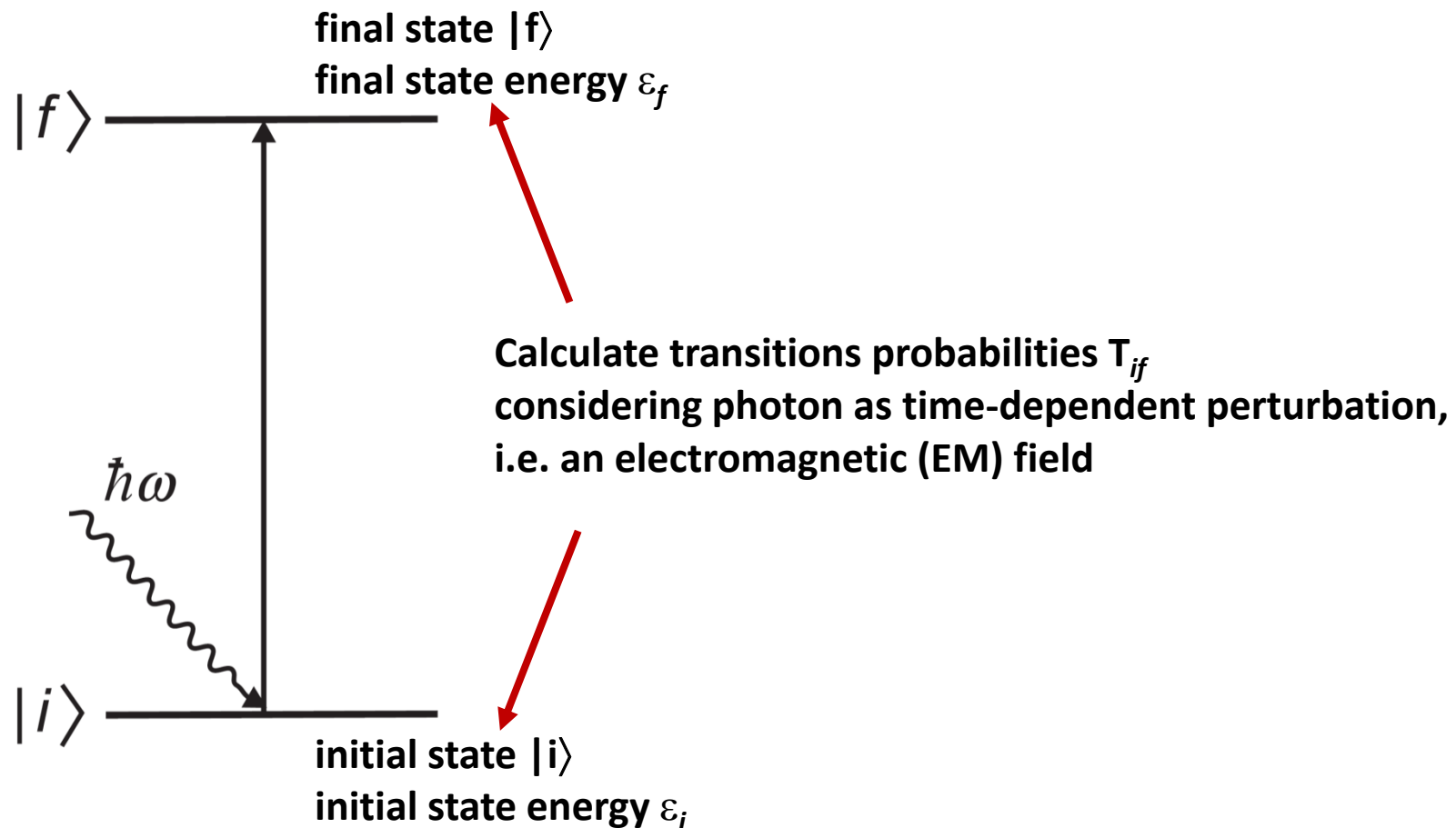


- + Calculate transition probabilities from filled $2p_{3/2}$ and $2p_{1/2}$ states to empty states in d -band for circularly polarized x rays using **Fermi's Golden Rule**

Origin of X-ray Magnetic Circular Dichroism



Origin of X-ray Magnetic Circular Dichroism



Origin of X-ray Magnetic Circular Dichroism

Transition probability per unit time, T_{if} , from a state i to a state f

$$T_{if} = \frac{2\pi}{\hbar} \left| \langle f | \mathcal{H}_{\text{int}} | i \rangle \right|^2 \delta(\varepsilon_i - \varepsilon_f) \rho(\varepsilon_f)$$

Fermi's Golden Rule

T_{if} Dimension [time $^{-1}$]

Initial state: wavefunction $|i\rangle$, energy ε_i

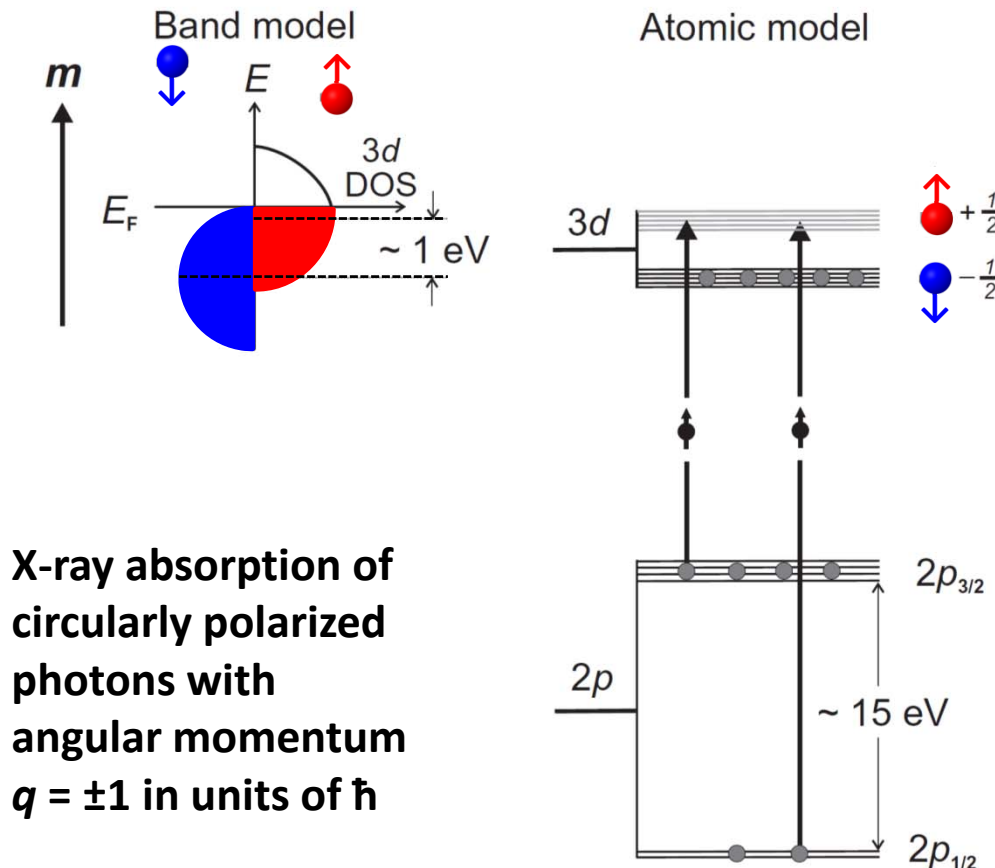
Final state: wavefunction $|f\rangle$, energy ε_f

$\rho(\varepsilon_f)$ = density of final states per unit energy

\mathcal{H}_{int} interaction Hamiltonian,
product of momentum operator p and vector potential A

$$\mathcal{H}_{\text{int}} = \frac{e}{m_e} \mathbf{p} \cdot \mathbf{A}$$

Origin of X-ray Magnetic Circular Dichroism

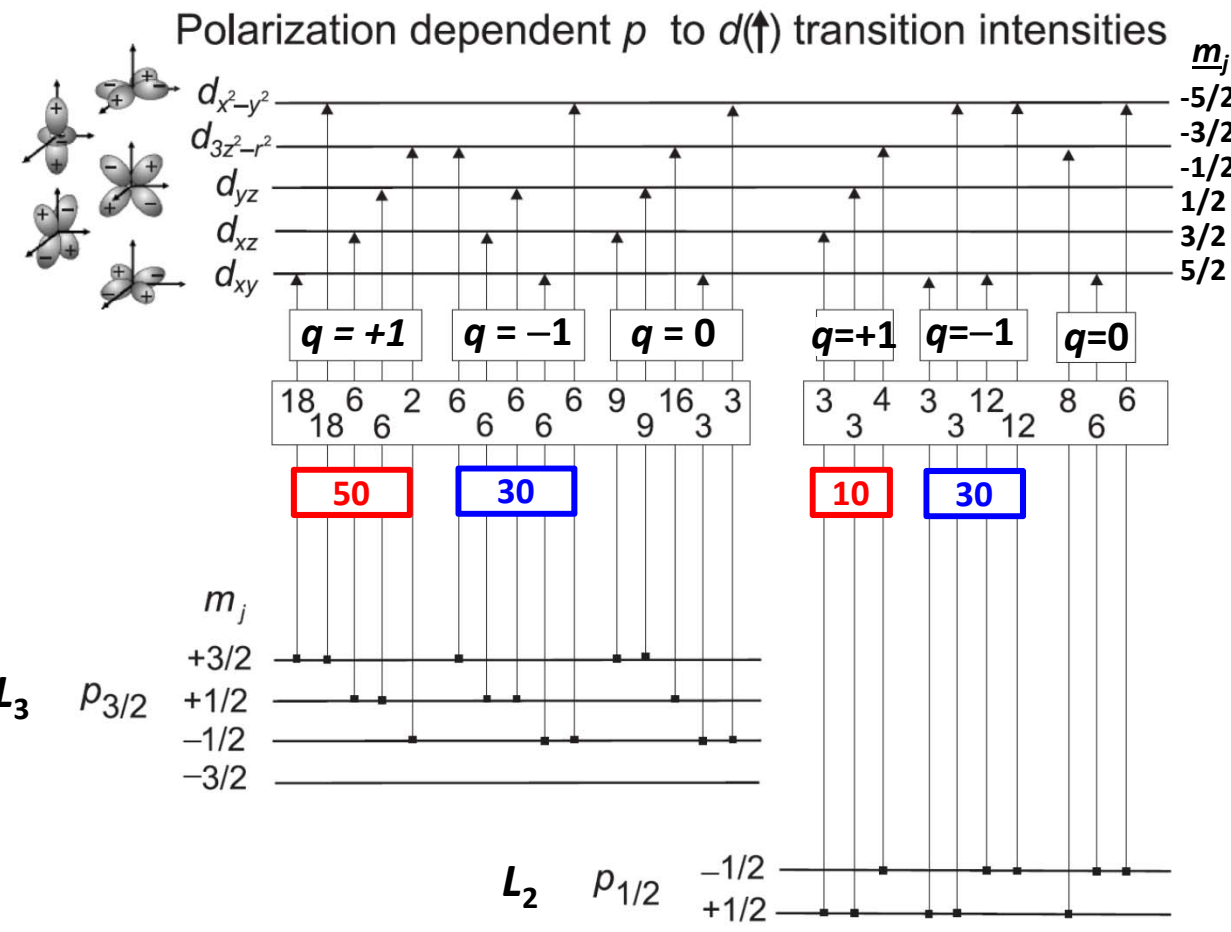


X-ray absorption of
circularly polarized
photons with
angular momentum
 $q = \pm 1$ in units of \hbar

- + Consider strong ferromagnet with one filled spin band:
 - All spin down d states filled
 - Spin up d states partially filled
- + This specific case:
Only spin up electron excited

J. Stöhr, H.C. Siegmann,
Magnetism (Springer)

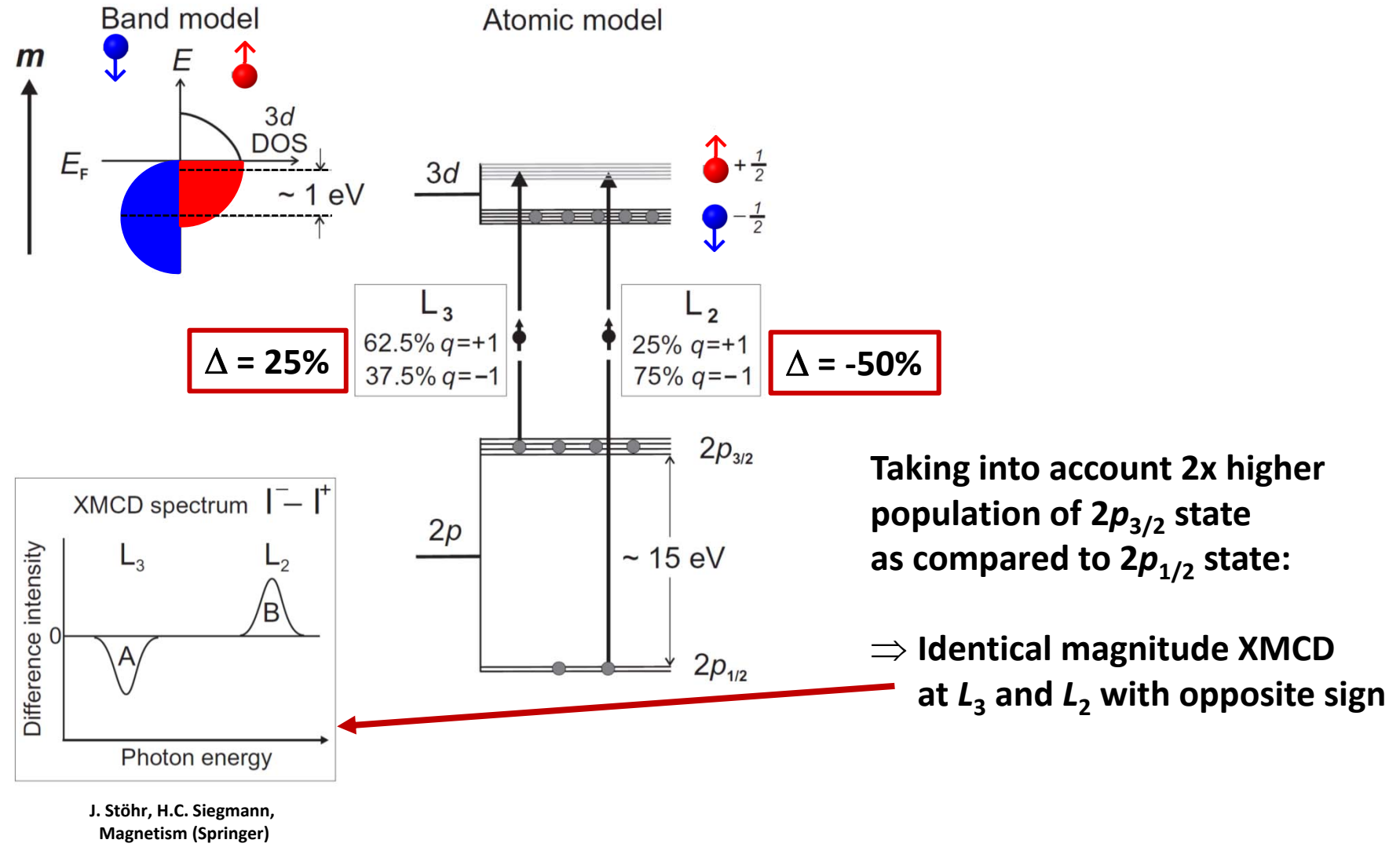
Origin of X-ray Magnetic Circular Dichroism



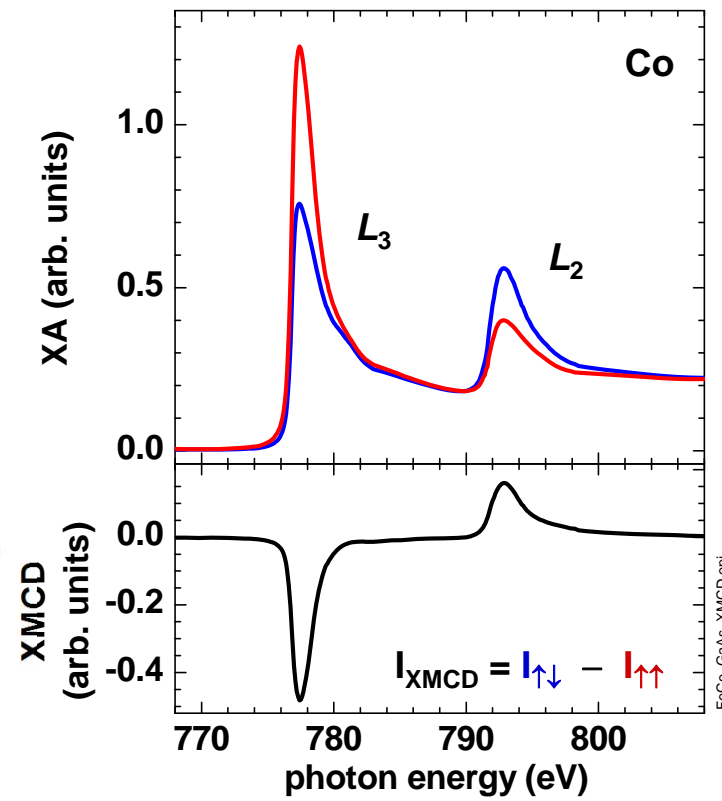
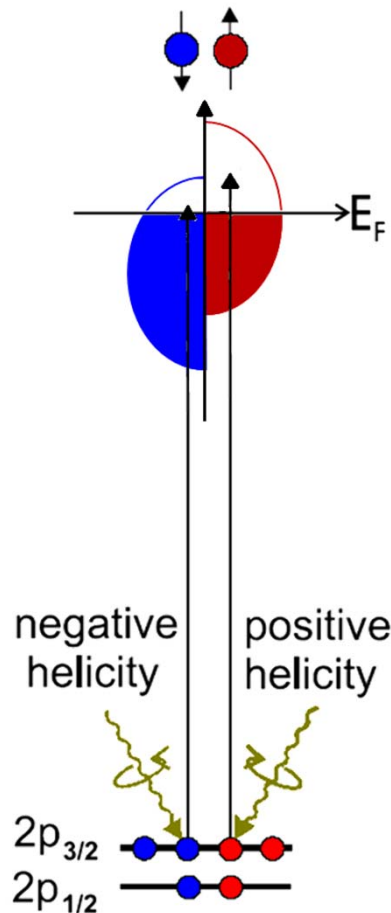
J. Stöhr, H.C. Siegmann,
Magnetism (Springer)

L_3 : X rays with $q = +/−1$ excite 62.5%/37.5% of the spin up electrons
 L_2 : X rays with $q = +/−1$ excite 25%/75% of the spin up electrons

Origin of X-ray Magnetic Circular Dichroism



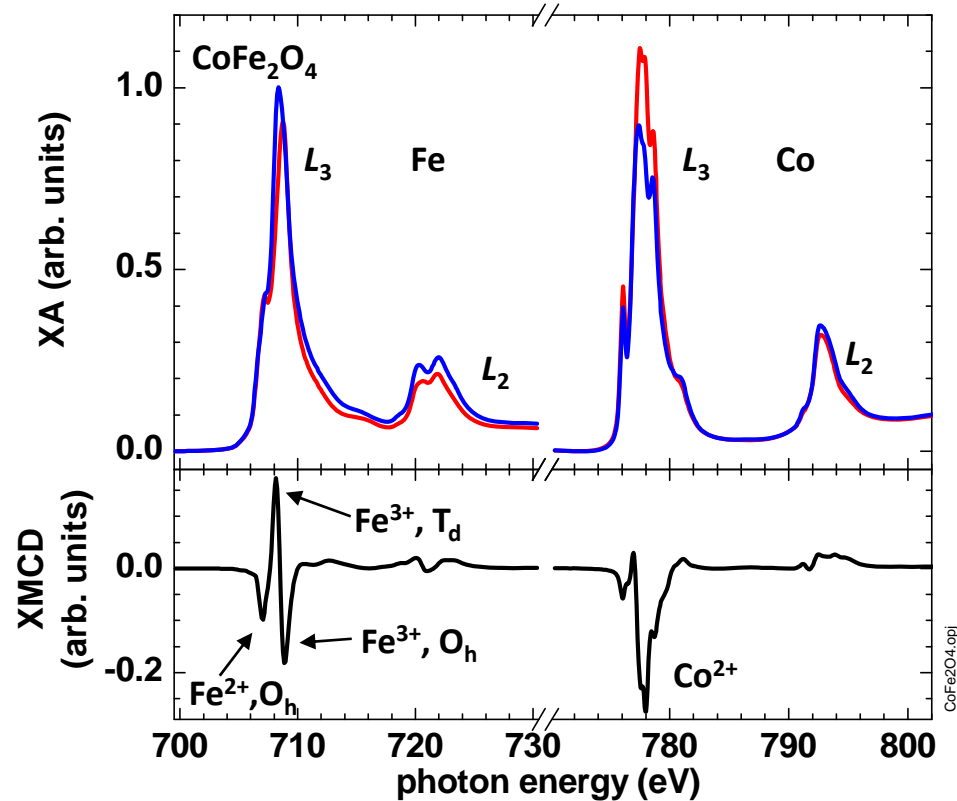
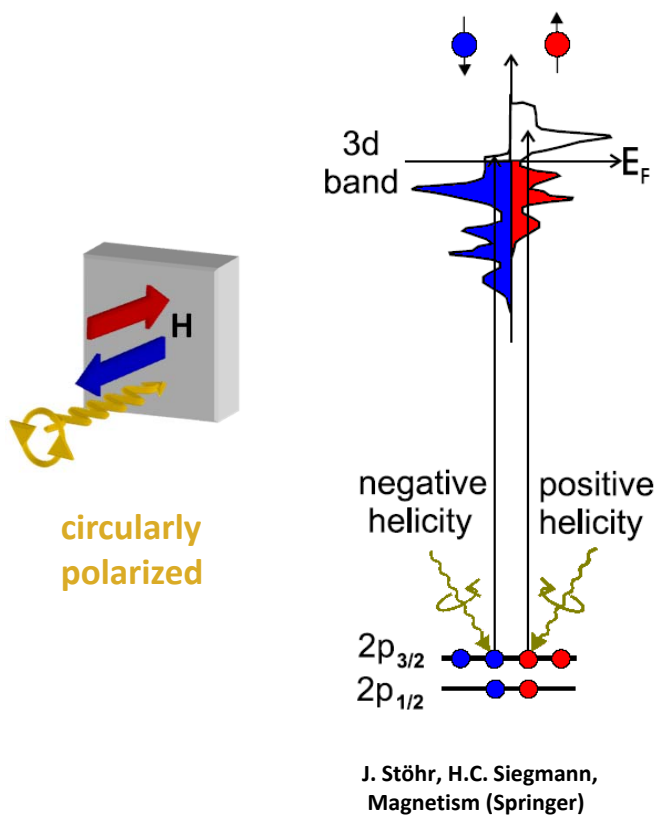
X-Ray Magnetic Circular Dichroism (XMCD)



Magnitude of XMCD depends on

- + expectation value of $3d$ magnetic moment
- + degree of circular photon polarization, P_{circ}
- + geometry

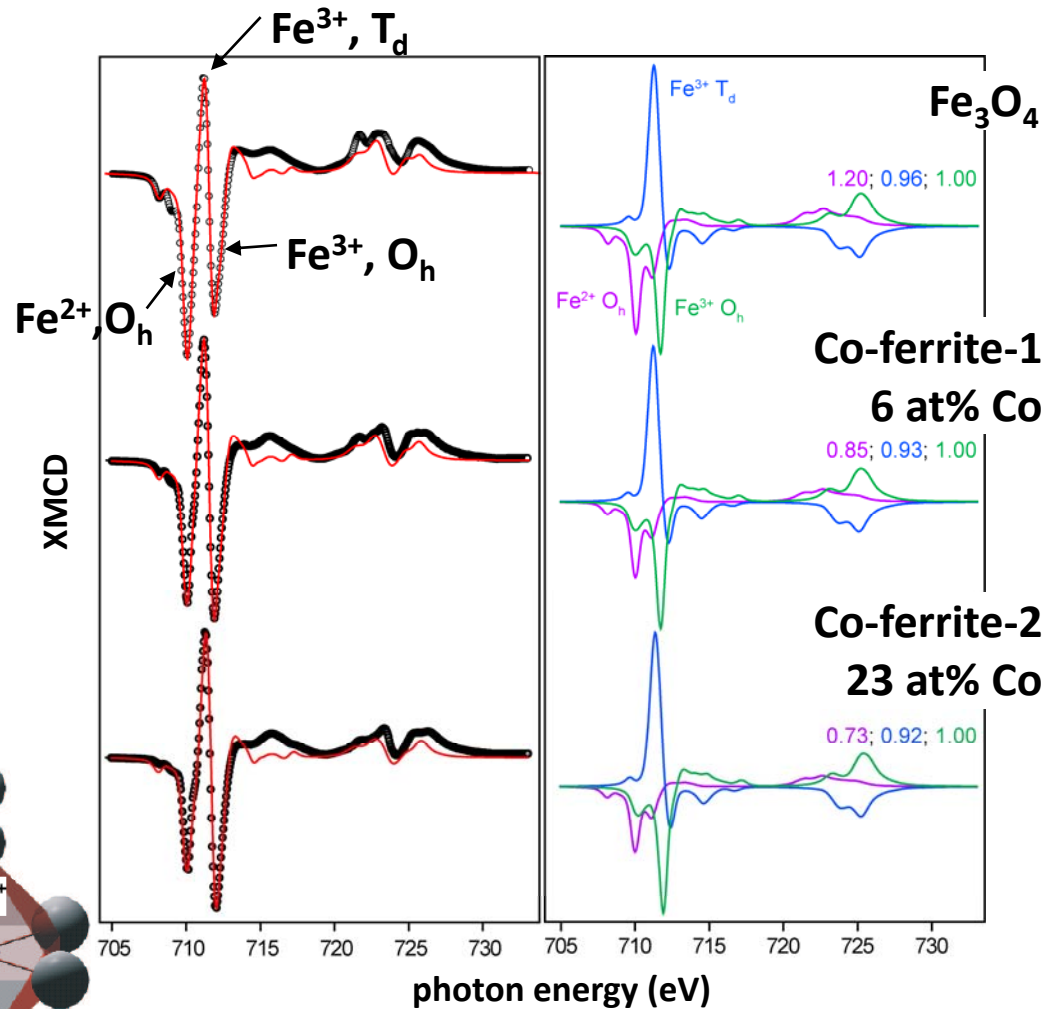
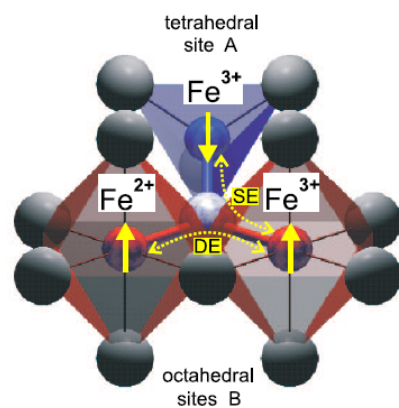
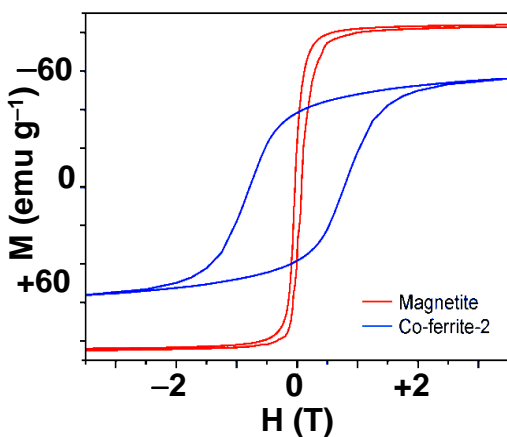
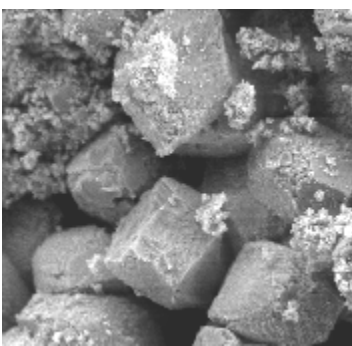
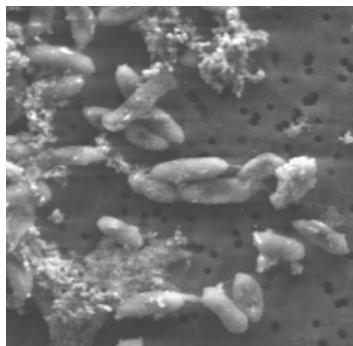
X-Ray Magnetic Circular Dichroism (XMCD)



- + XMCD provides magnetic information resolving elements Fe, Co, ...
valence states: Fe^{2+} , Fe^{3+} , ...
lattice sites: octahedral, O_h , tetrahedral, T_d ,

Magnetic Bionanospinels

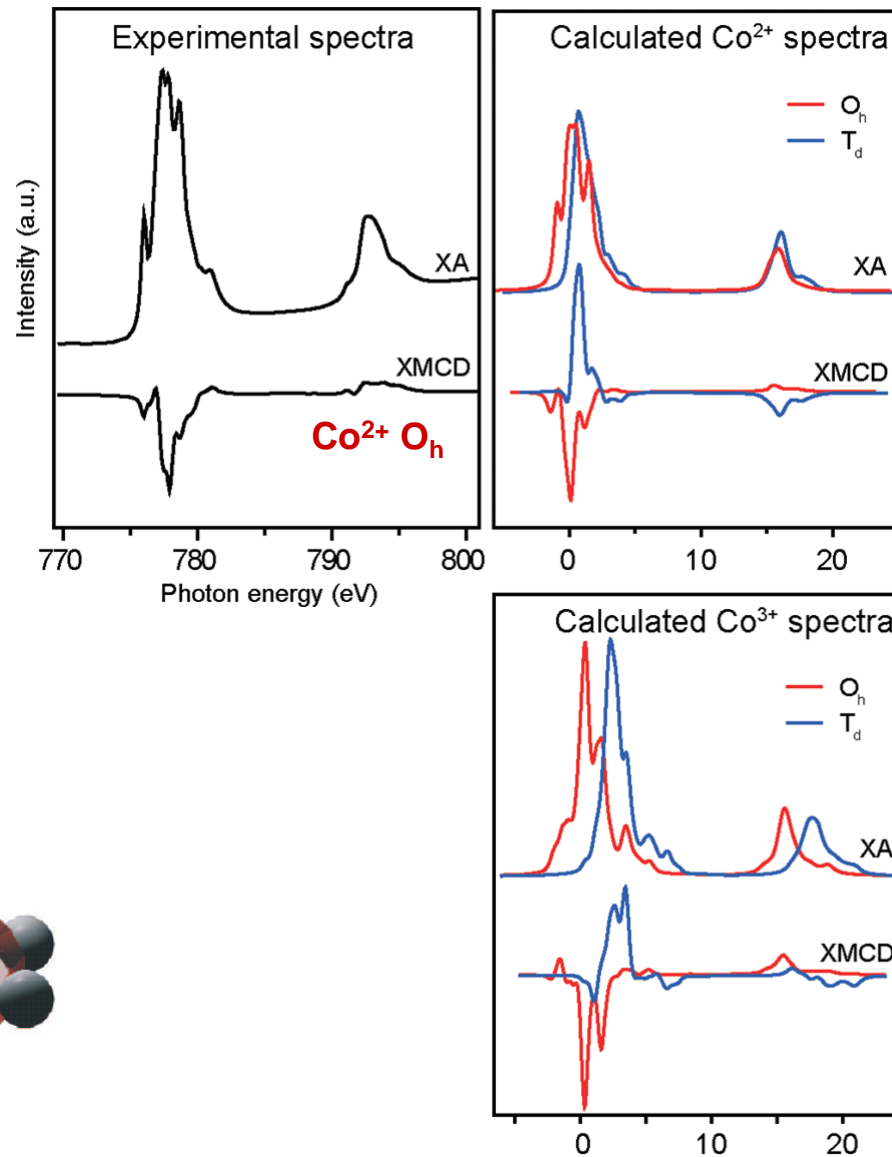
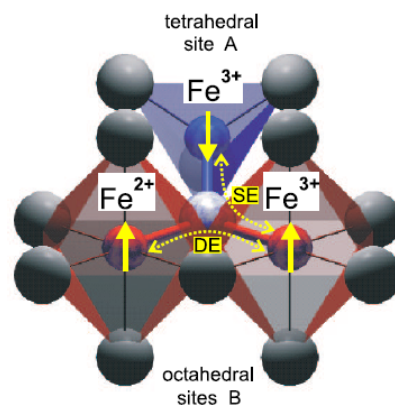
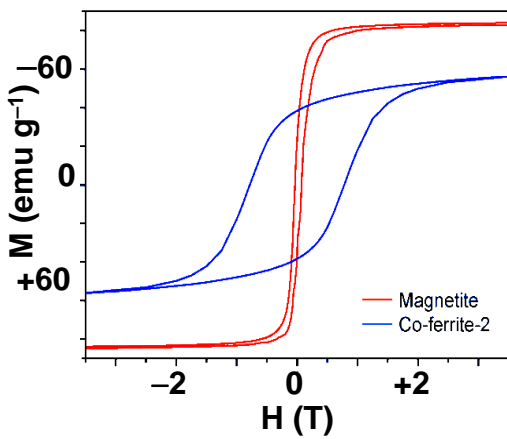
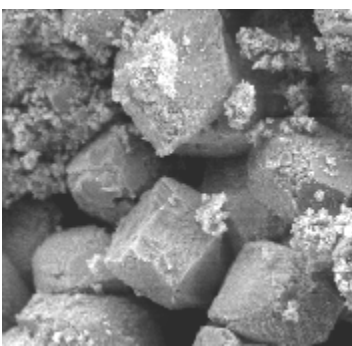
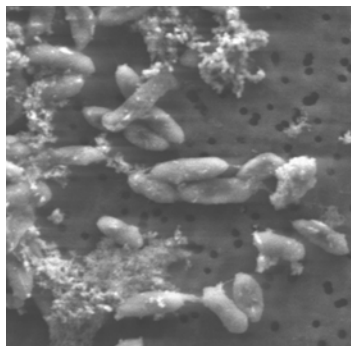
+ **Geobacter sulfurreducens** bacteria form magnetite nanocrystals (15nm) via extracellular reduction of amorphous Fe(III)-bearing minerals



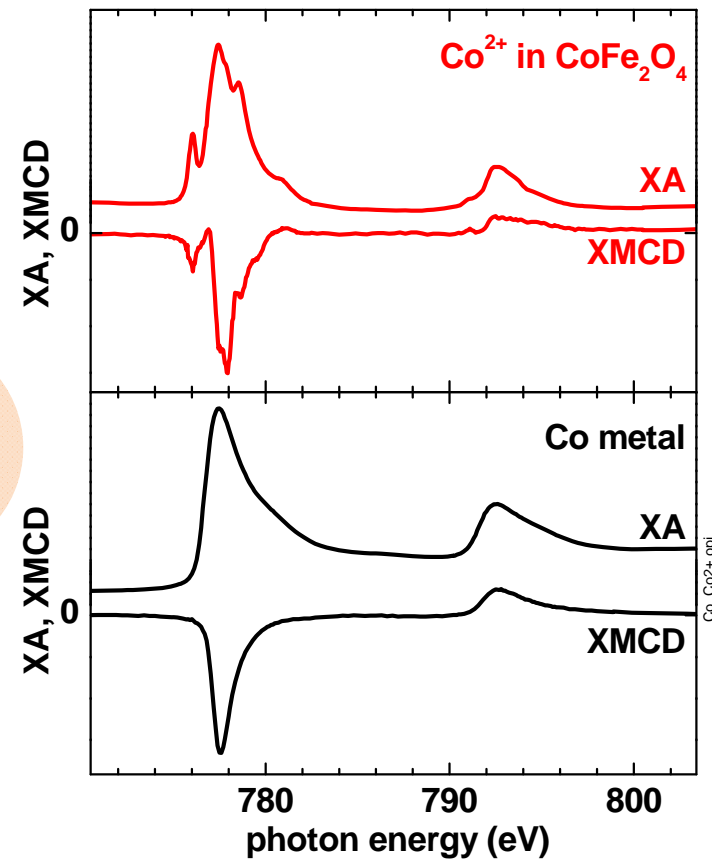
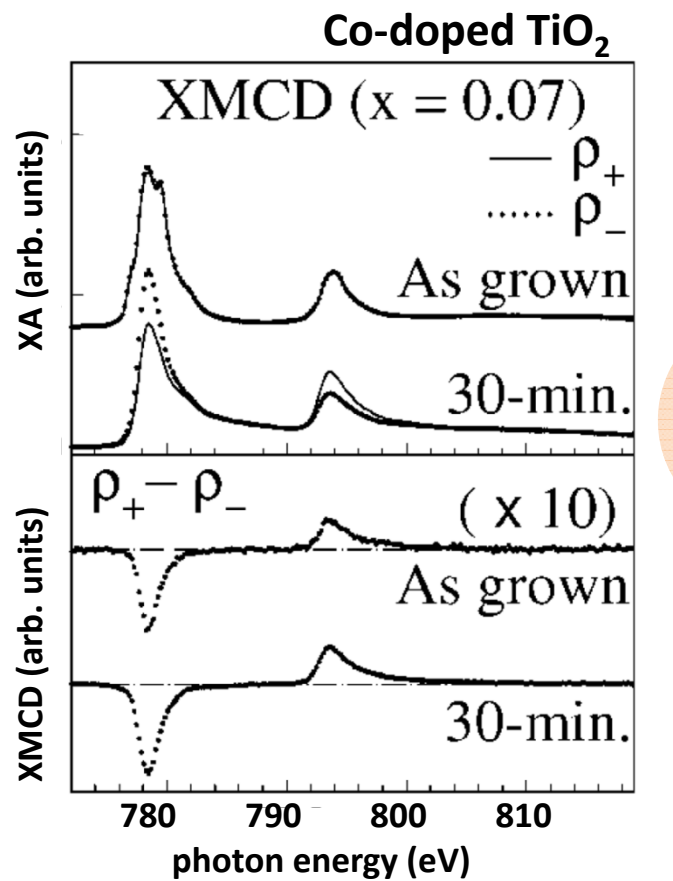
V. Cocker et al.,
Eur. J. Mineral. **19**, 707–716 (2007)

Magnetic Bionanospinels

+ **Geobacter sulfurreducens bacteria form magnetite nanocrystals (15nm) via extracellular reduction of amorphous Fe(III)-bearing minerals**



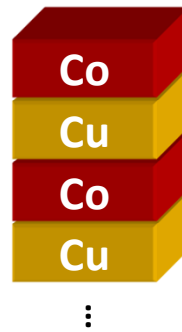
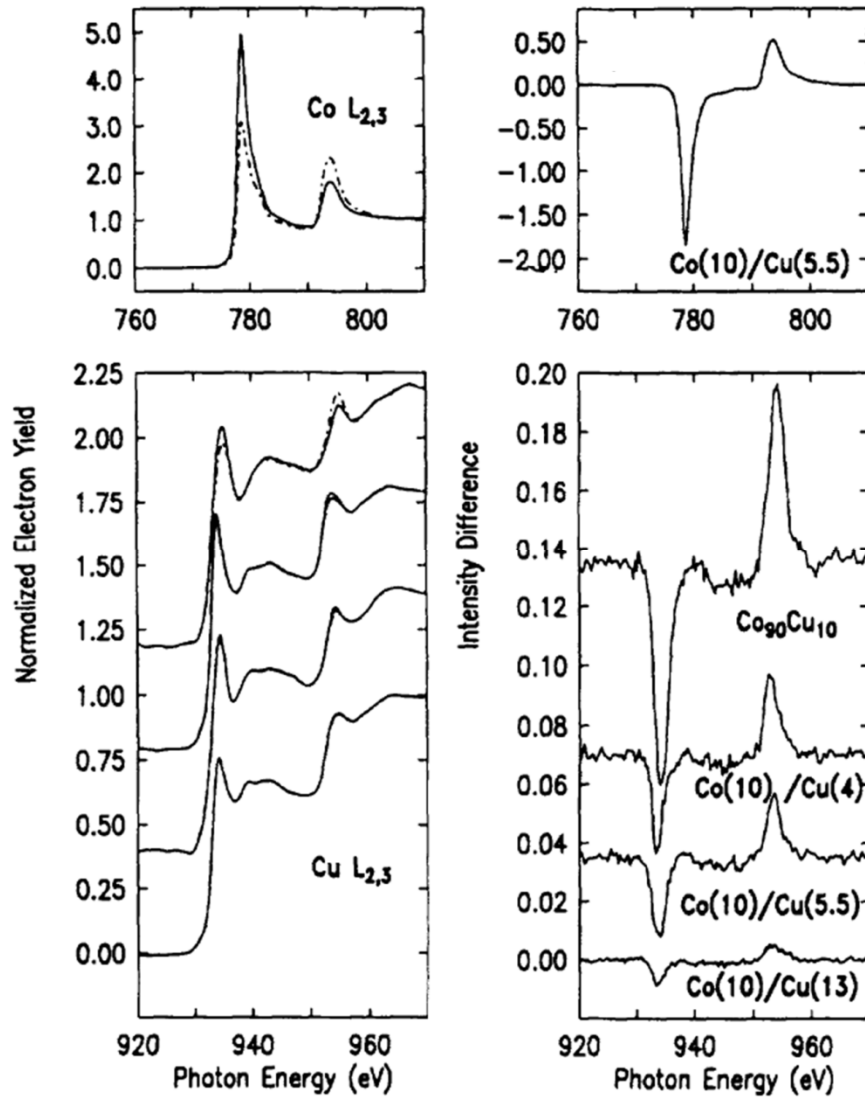
Co-doped TiO₂



J.-Y. Kim *et al.*,
Phys. Rev. Lett. **90**, 017401 (2003)

- + Comparing XMCD spectra with model compounds and/or calculations
- ⇒ Identifying magnetic phases

Induced Moments At Co/Cu Interfaces

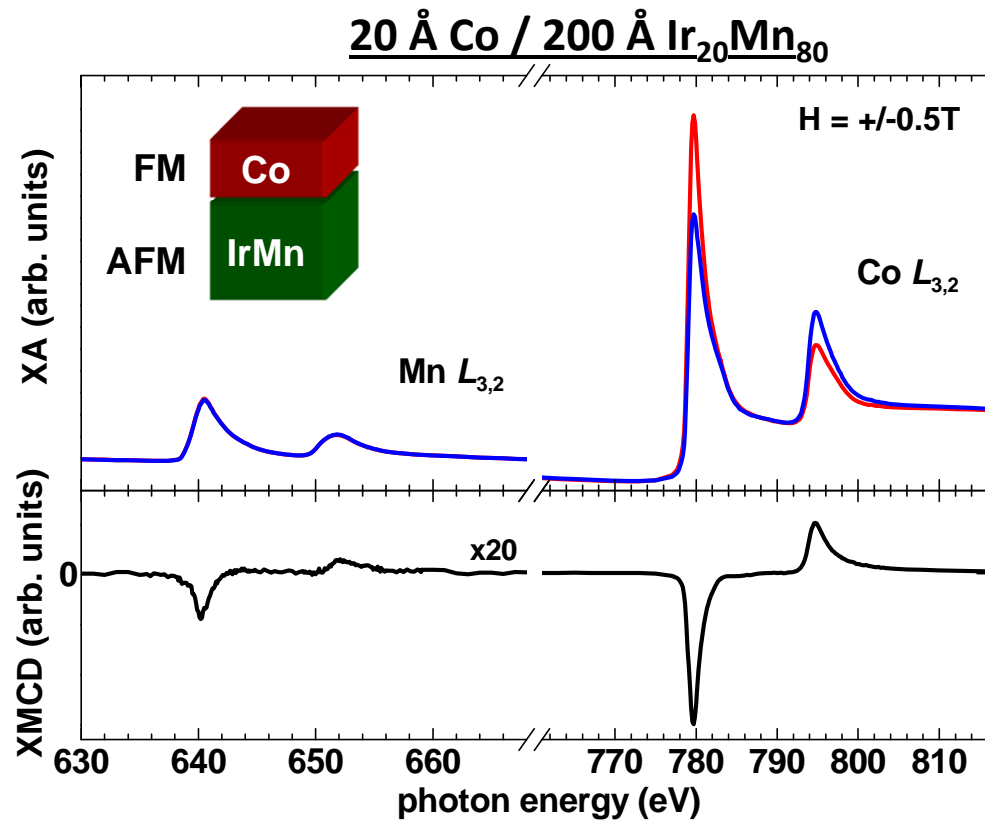


+ The element-specificity makes XMCD measurements an ideal tool to determine induced moments at interfaces between magnetic and non-magnetic elements.

M. G. Samant *et al.*,
Phys. Rev. Lett. 72, 1112 (1994)

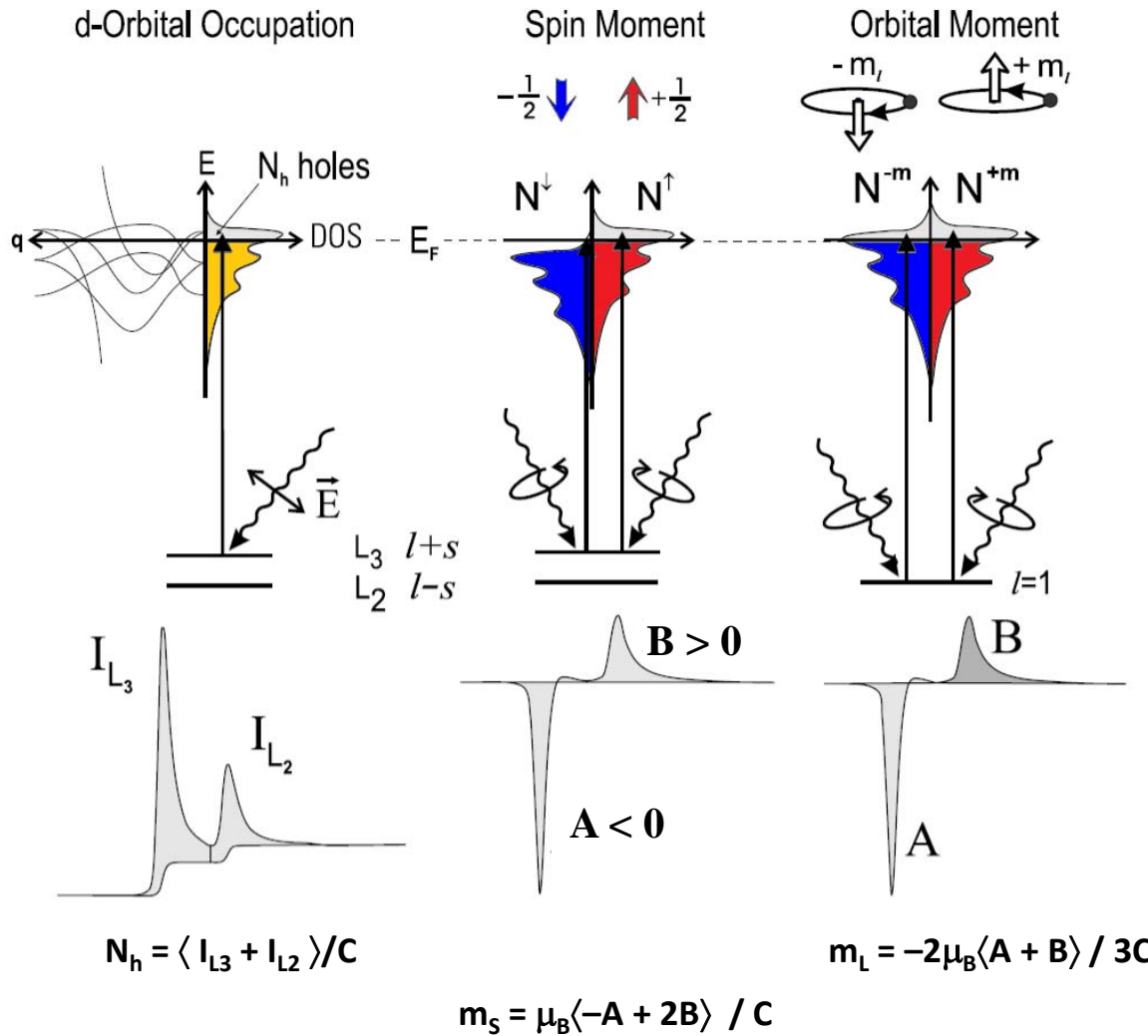
Magnetic Interfaces

- + Weak Mn XMCD signal
⇒ Uncompensated Mn at Co/IrMn interface
- + Same sign of XMCD signal for Co and Mn
⇒ Parallel coupling of Co and Mn moments
- + Nominal thickness of uncompensated interface moments: $(0.5 \pm 0.1) \text{ML}$



H. Ohldag et al.,
Phys. Rev. Lett. 91, 017203 (2003)

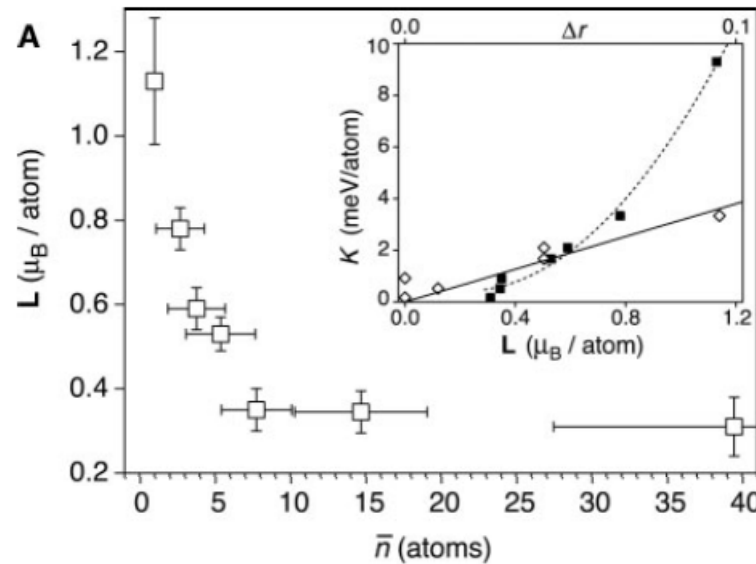
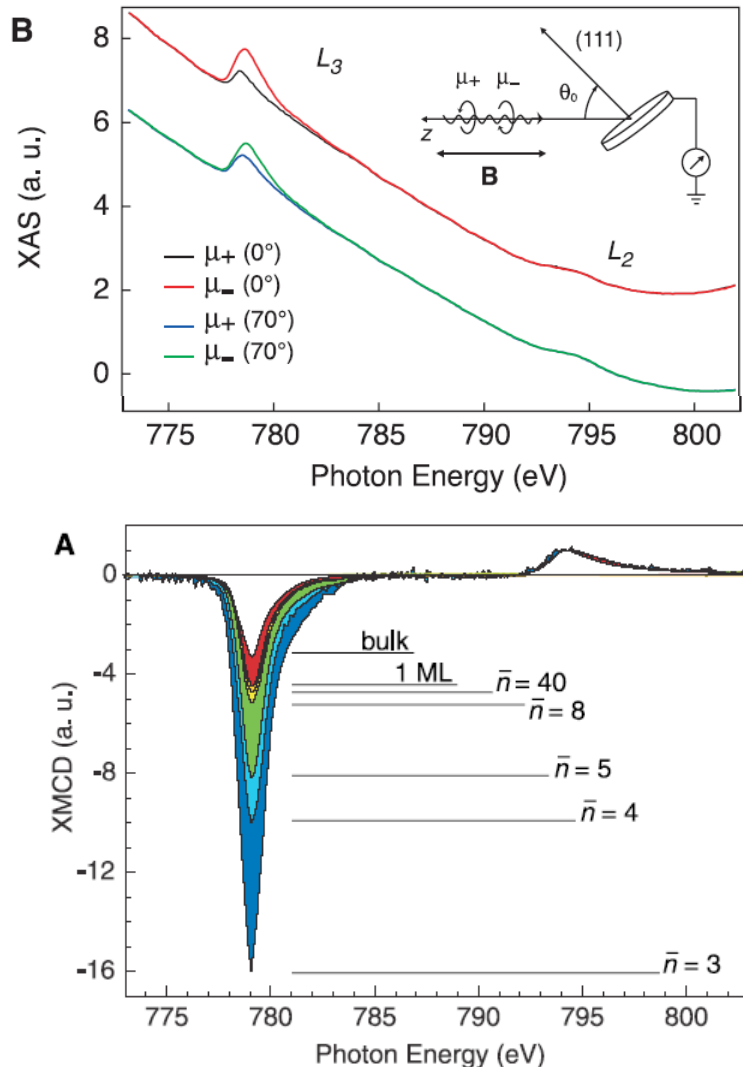
Sum Rules



+ Theoretically derived sum rules correlate XMCD spectra with spin and orbital moment providing unique tool for studying magnetic materials.

J. Stöhr, H.C. Siegmann,
Magnetism (Springer)

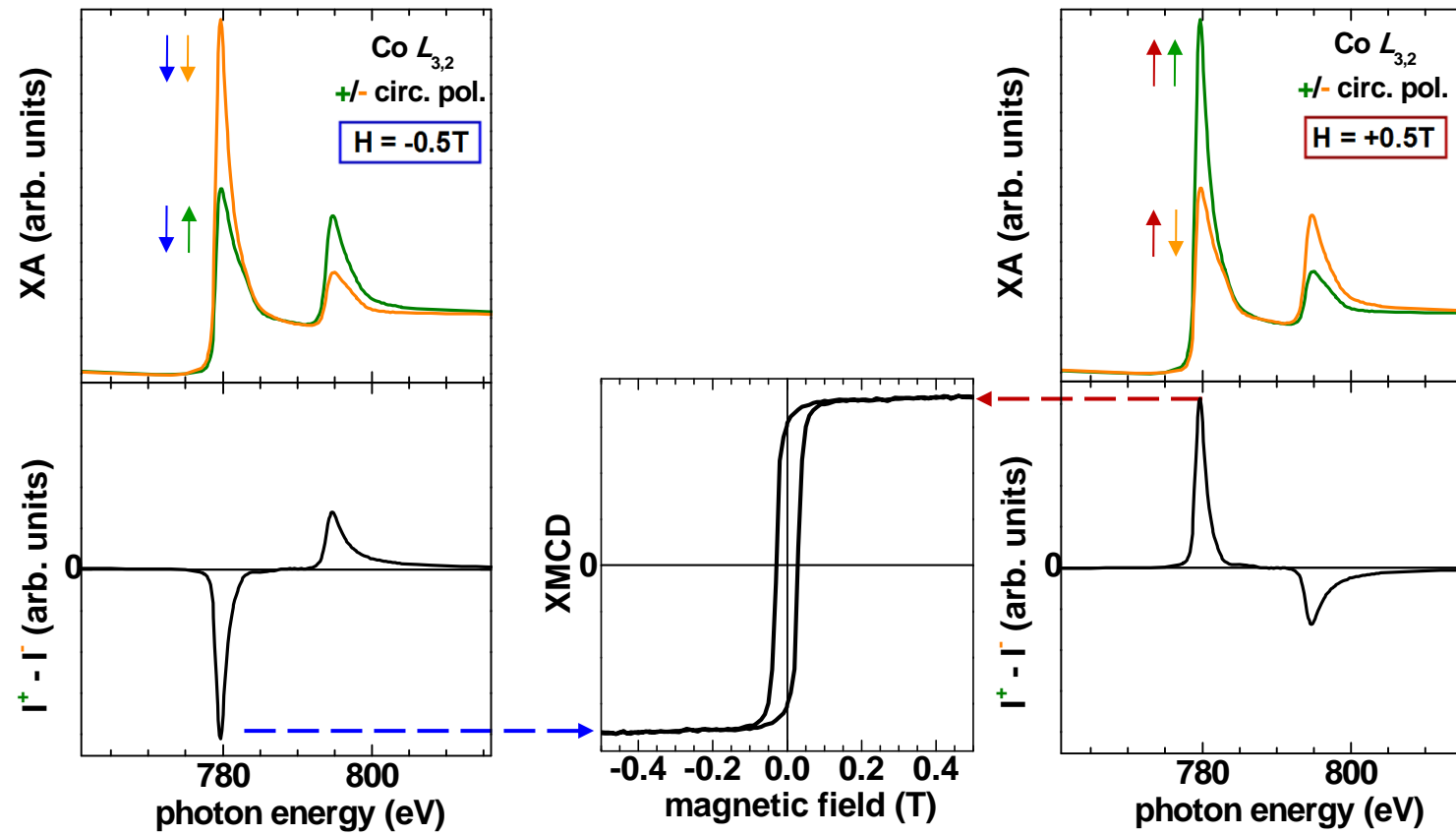
Orbital Moment Of Co Nanoparticles



- + Strong variation of orbital and spin magnetic moment observable as change in relative L_3 and L_2 intensity in XMCD spectrum.
- + Co atoms and nanoparticles on Pt have enhanced orbital moments up to $1.1 \mu_B$

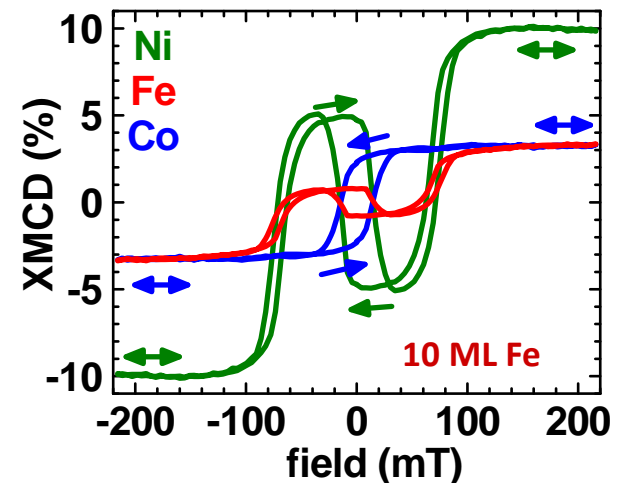
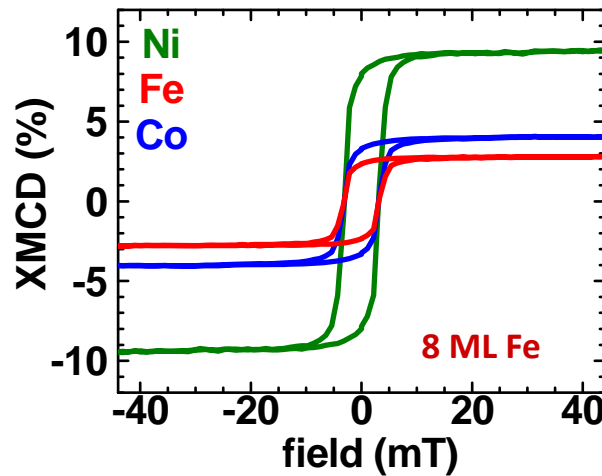
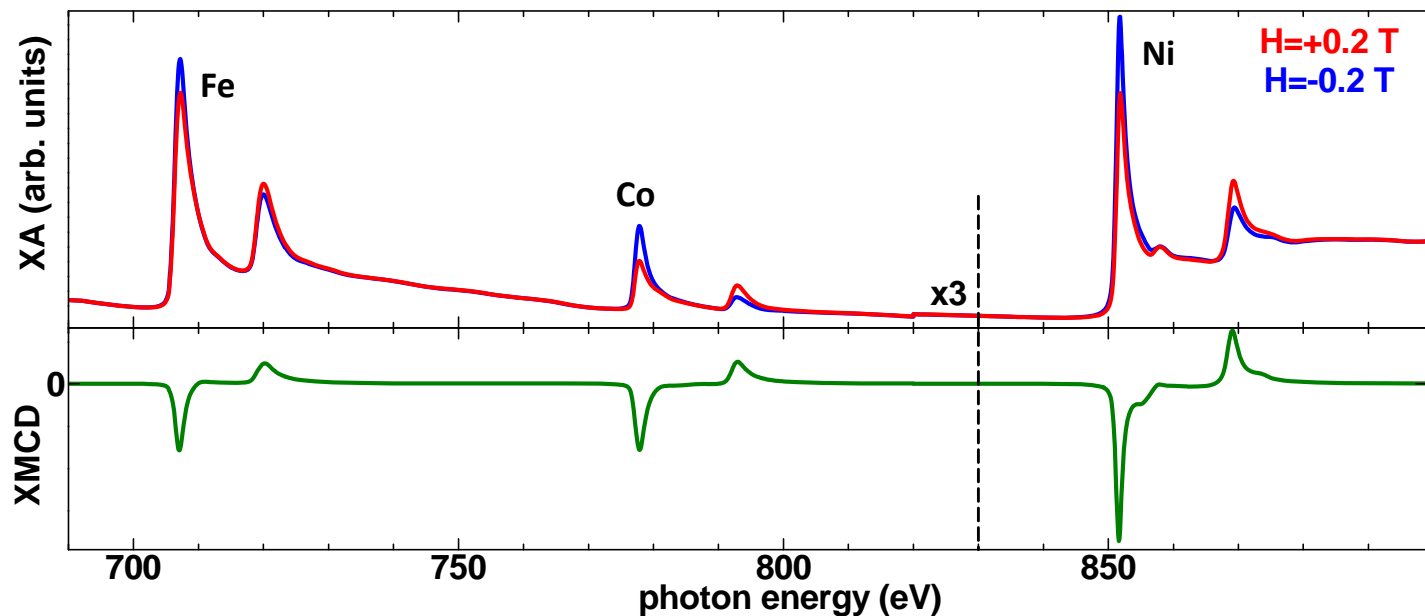
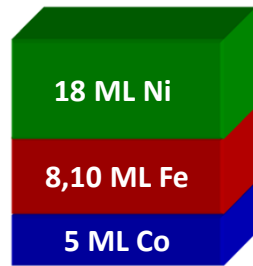
P. Gambardella *et al.*,
Science 300, 1130 (2003)

Element-specific Magnetization Reversal

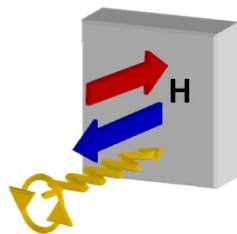


- + Monitoring field dependence of XMCD
- ⇒ Element-specific information on magnetization reversal in complex magnetic nanostructures.

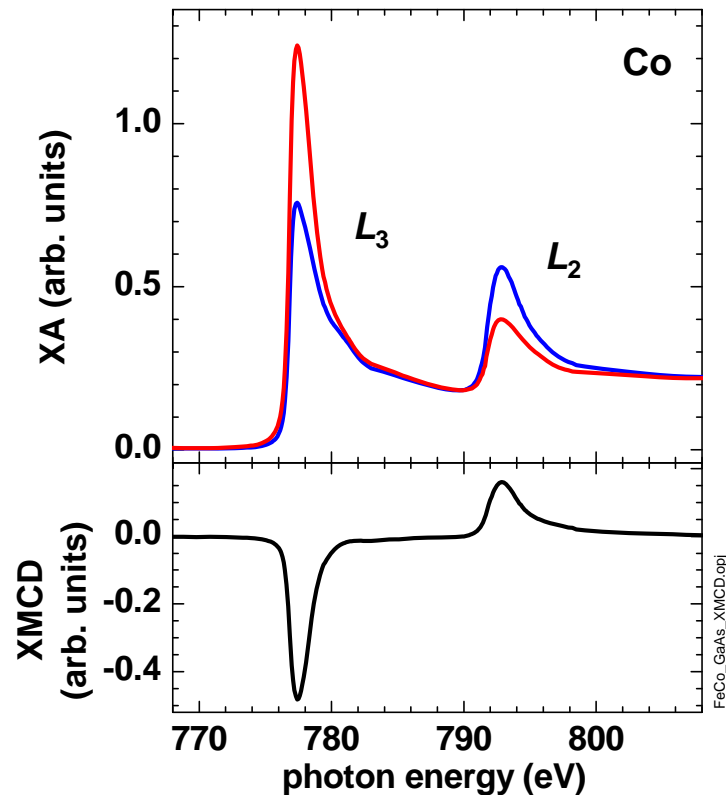
Element-specific Magnetization Reversal



X-Ray Ferromagnetic Resonance

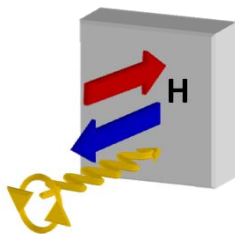


circularly
polarized

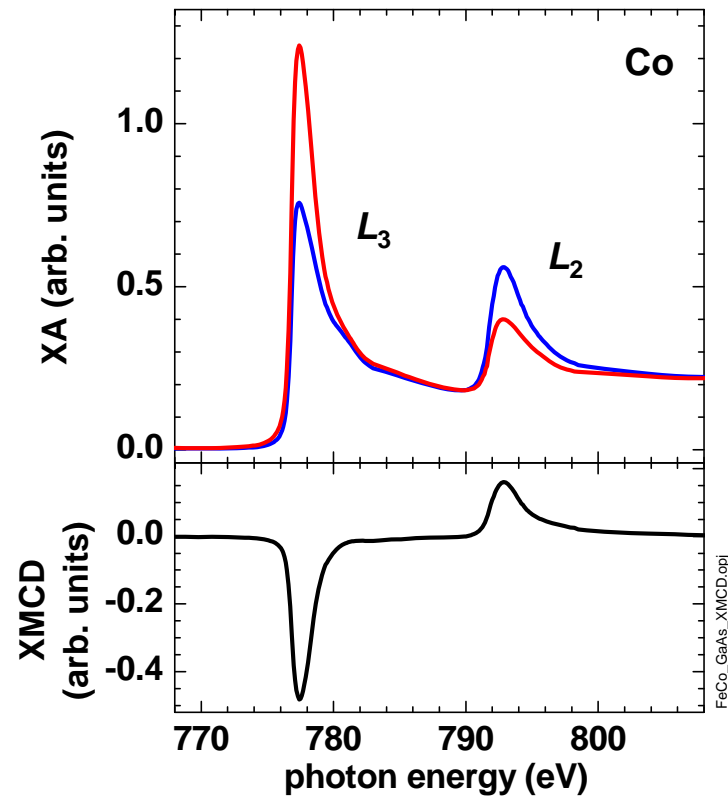


- + XMCD is the difference in x-ray absorption between antiparallel and parallel orientation of magnetic moment and photon spin.
- + The XMCD magnitude reflects the magnetic moment aligned parallel to the x ray beam.

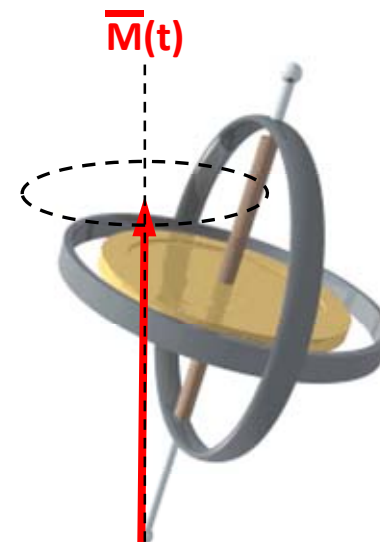
X-Ray Ferromagnetic Resonance



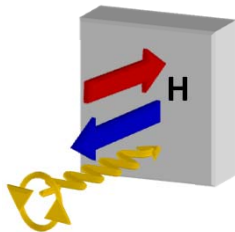
circularly
polarized



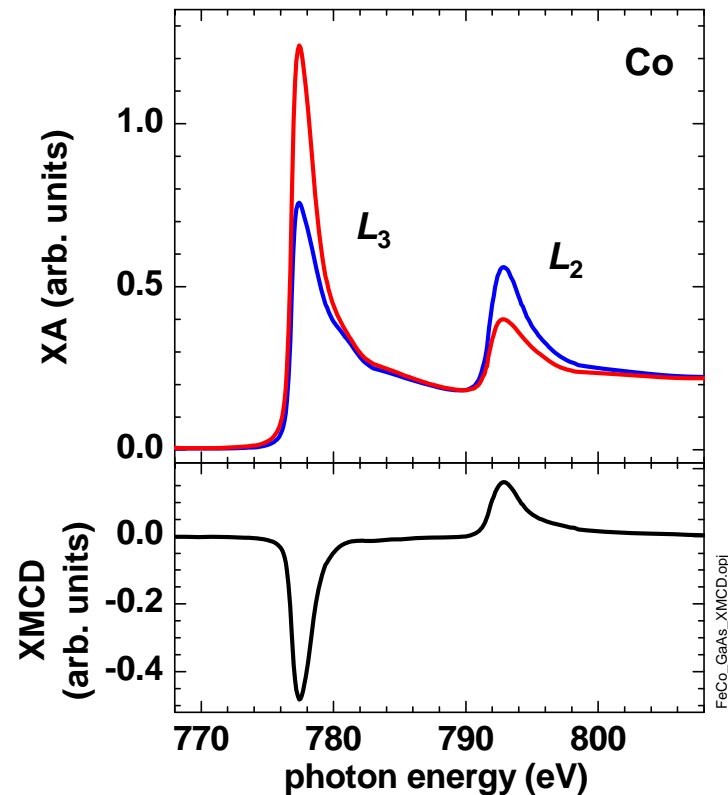
+ In fact:
Magnetic moments are not
fully aligned with applied fields
but precess around them.



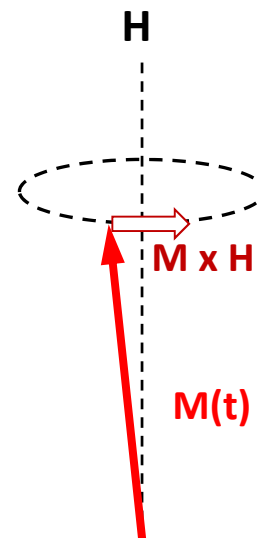
X-Ray Ferromagnetic Resonance



circularly
polarized

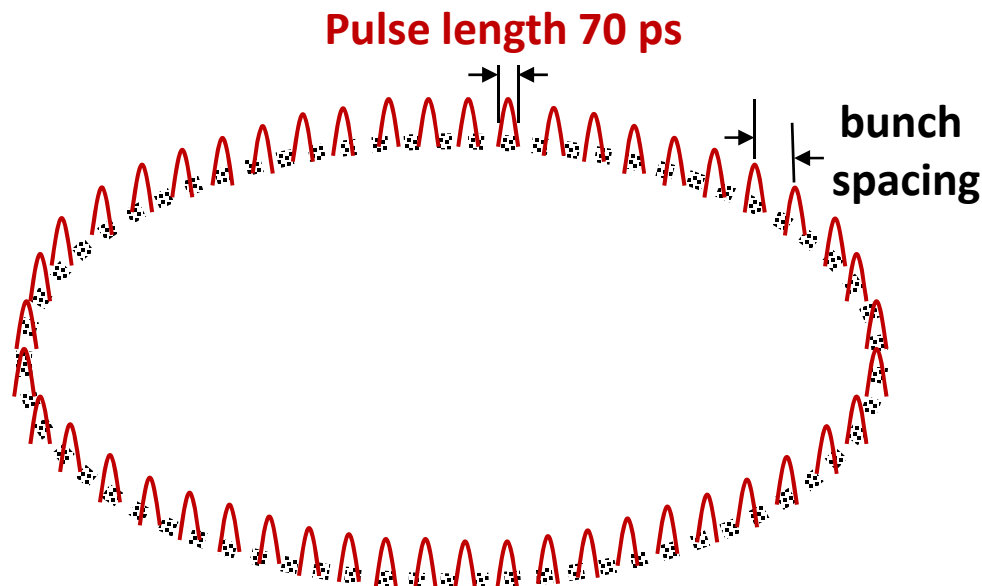


+ In fact:
Magnetic moments are not
fully aligned with applied fields
but precess around them.



+ Is it possible to measure the precession of magnetic moments
making use of the pulsed nature of synchrotron radiation and XMCD?

X-Ray Ferromagnetic Resonance

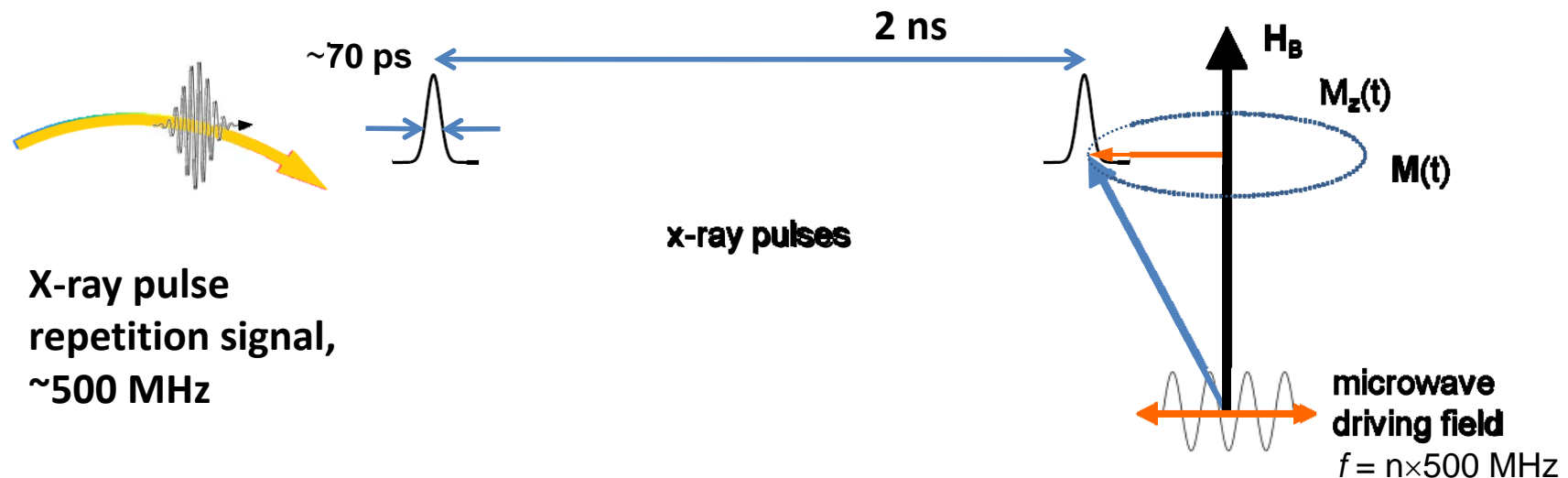


Pulsed nature of synchrotron radiation
Example: Advanced Light Source

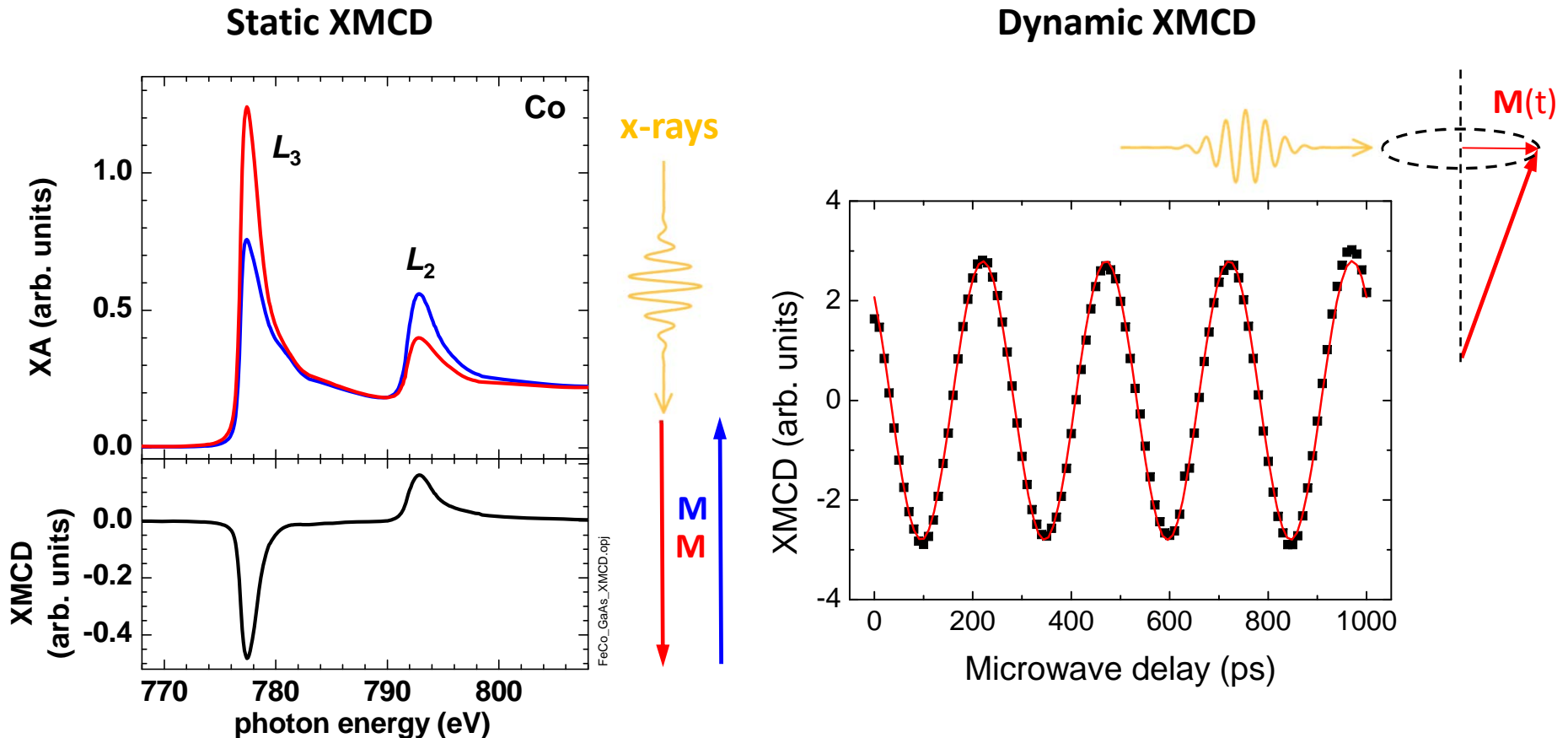
- + 256-320 bunches for 500mA beam current
- + Bunch spacing: 2 ns
- + Pulse length 70ps

X-Ray Ferromagnetic Resonance

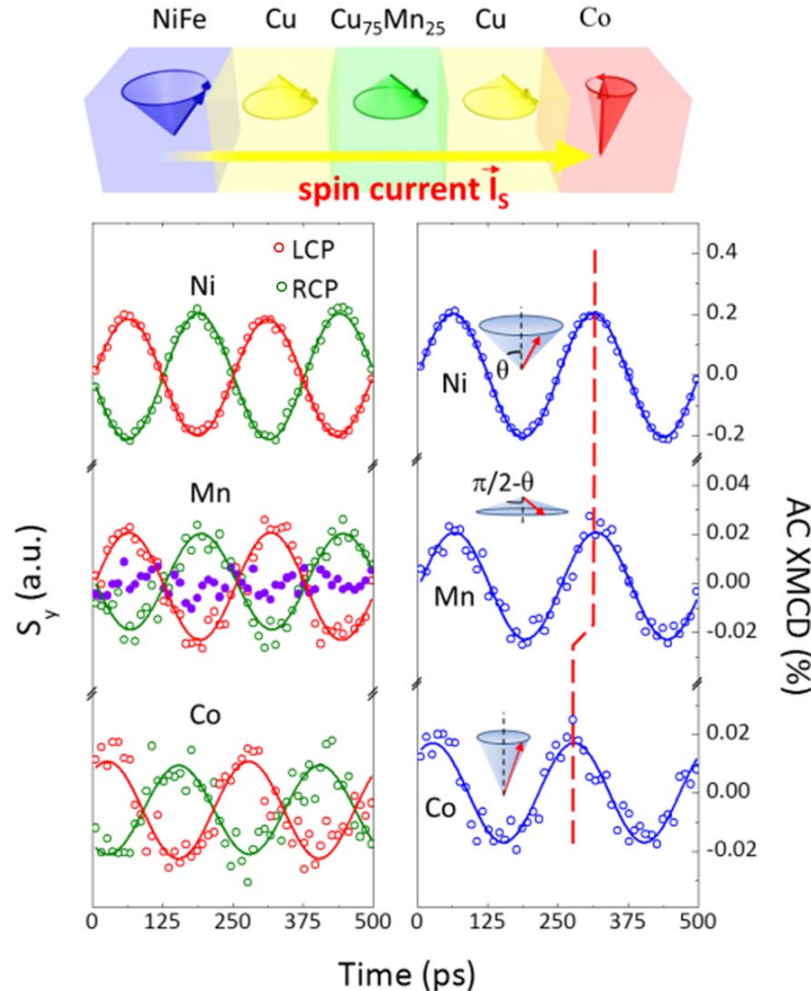
Dynamic XMCD measurement, i.e. synchronize x-ray pulses with FMR precession



X-Ray Ferromagnetic Resonance

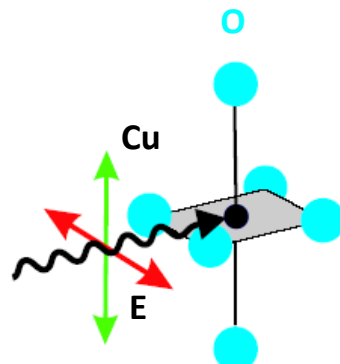


X-Ray Ferromagnetic Resonance

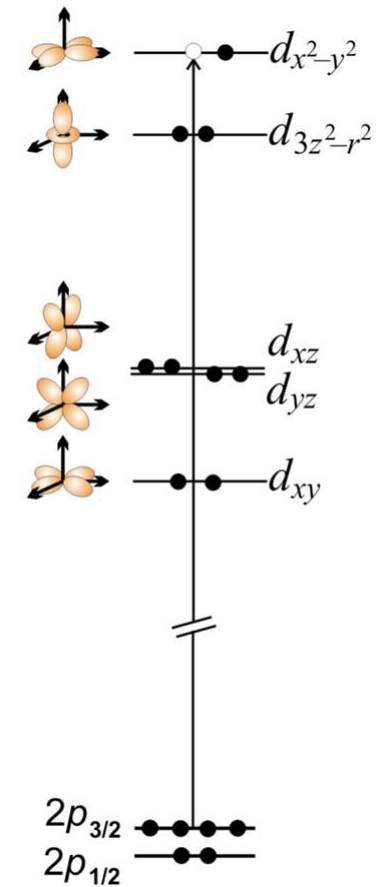
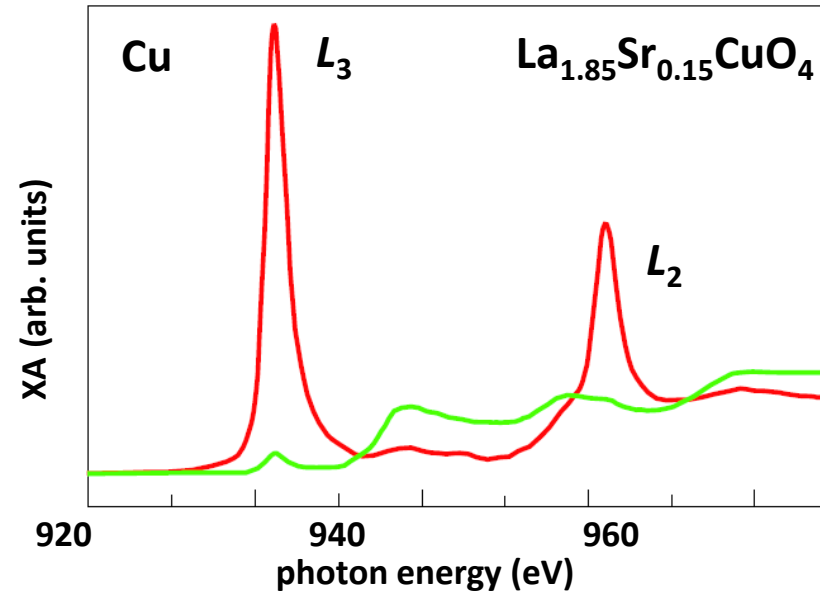


- Precession is resonantly excited in the NiFe layer with an 4 GHz RF field.
- The resonance field of the CO layer is higher, i.e. no precession is excited in the Co layer.
- Precession in Py, Cu₇₅Mn₂₅, and Co layers are probed by XMCD using left- and right-circularly polarized x-rays at Ni, Mn, and Co edges, respectively.
- The Cu₇₅Mn₂₅ spin precession is a direct indicator of the AC spin current through the structure.

X-Ray Linear Dichroism



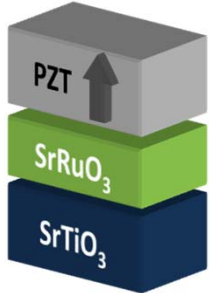
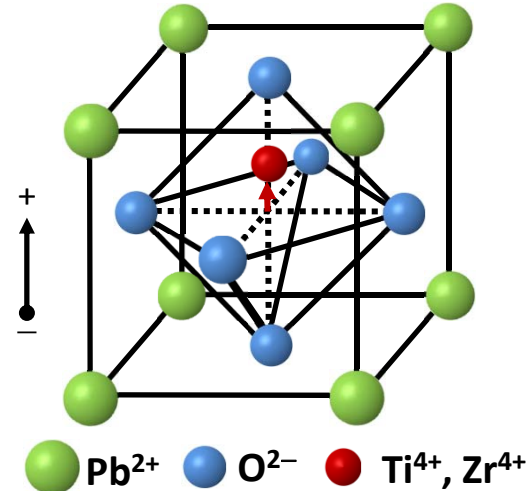
C. T. Chen *et al.*
PRL 68, 2543 (1992)



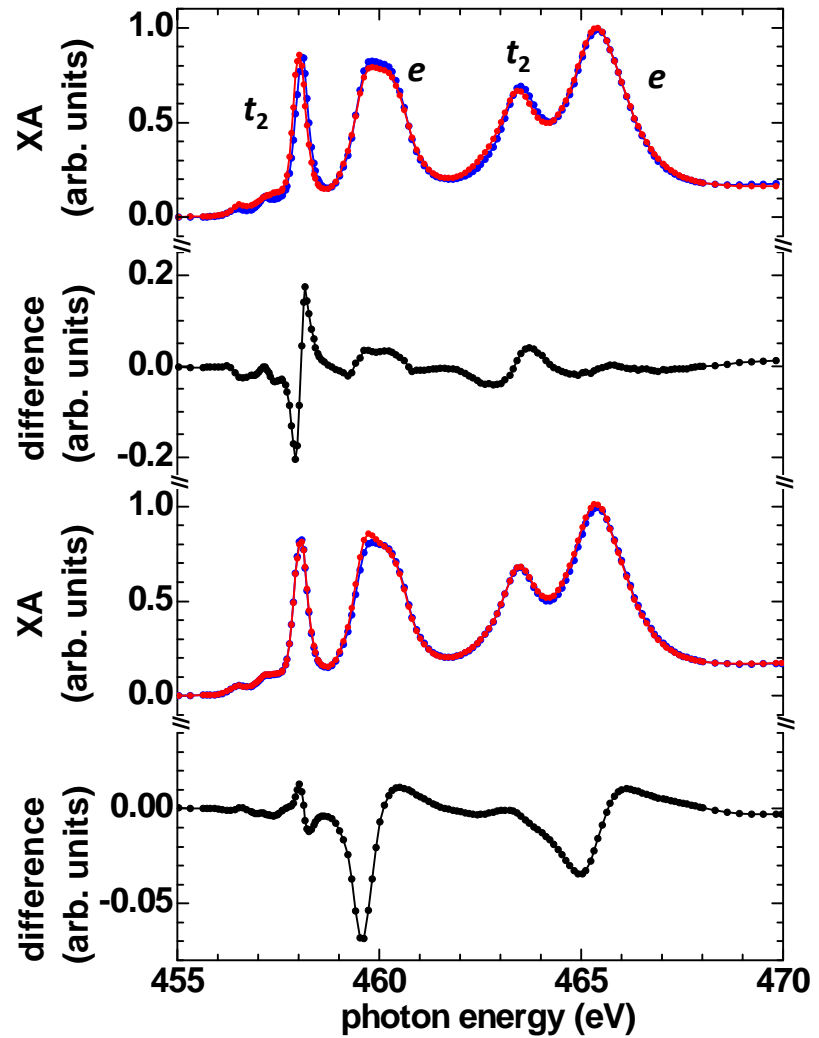
X-Ray Linear Dichroism:

- + Difference in x-ray absorption for different linear polarization direction relative to crystalline and/or spin axis.
- + Due to the anisotropic charge distribution about the absorbing atom caused by bonding and/or magnetic order.
- + “Search Light Effect”: X-ray absorption of linear polarized x rays proportional to density of empty valence states in direction of electric field vector E.

Structural Changes In $\text{PbZr}_{0.2}\text{Ti}_{0.8}\text{O}_3$



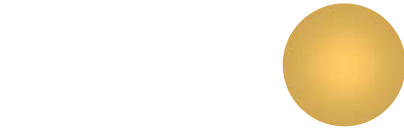
ferroelectric
polarization



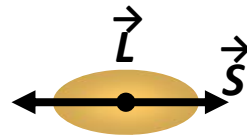
E. Arenholz *et al.*,
Phys. Rev. B **82**, 140103 (2010)

- + Spontaneous electric polarization due to off-center shift of Ti^{4+} , Zr^{4+} associated with tetragonal distortion \Leftrightarrow linear dichroism
- + Reversing ferroelectric polarization changes XA \Leftrightarrow Change in tetragonal distortion

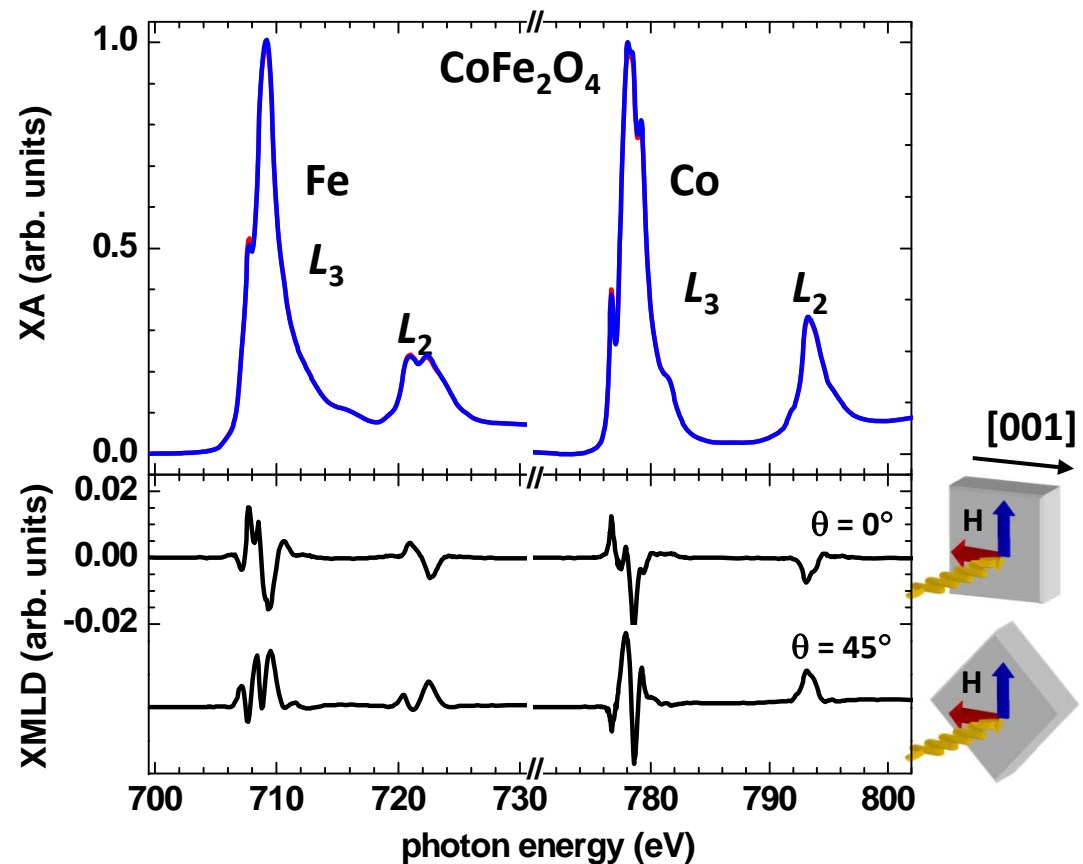
X-Ray Magnetic Linear Dichroism



Isotropic d electron charge density
⇒ No polarization dependence



Magnetically aligned system
⇒ Spin-orbit coupling distorts
charge density
⇒ Polarization dependence

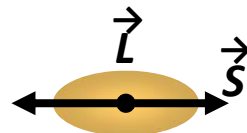


- + $I_{\text{XMLD}} = I_{||} - I_{\perp} \propto \langle m^2 \rangle$, $\langle m^2 \rangle$ = expectation value of square of atomic magnetic moment
- + XMLD allows investigating ferri- and ferromagnets as well as antiferromagnets
- + XMLD spectral shape and angular dependence are determined by magnetic order and lattice symmetry

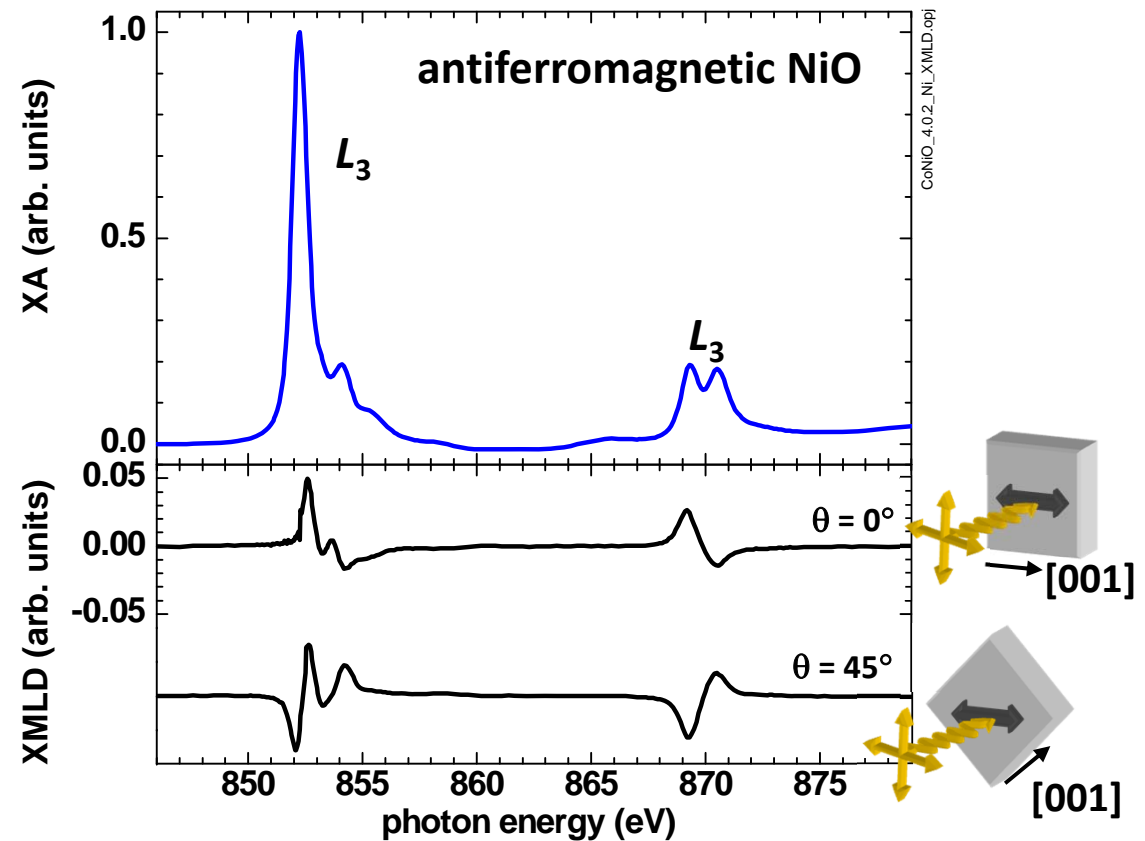
X-Ray Magnetic Linear Dichroism



Isotropic d electron charge density
⇒ No polarization dependence

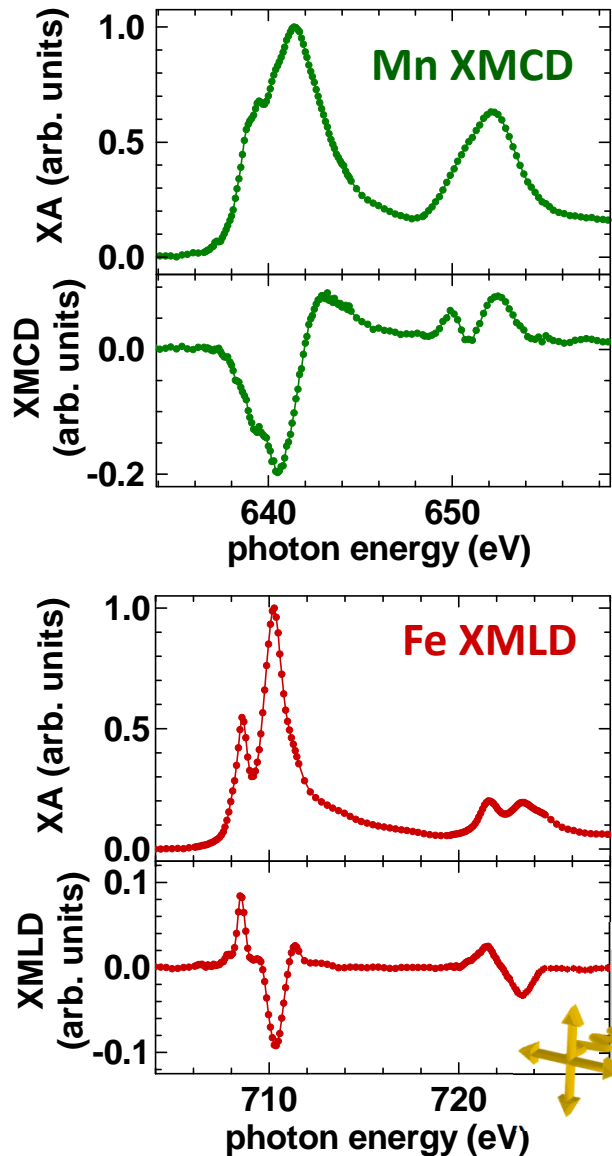


Magnetically aligned system
⇒ Spin-orbit coupling distorts
charge density
⇒ Polarization dependence

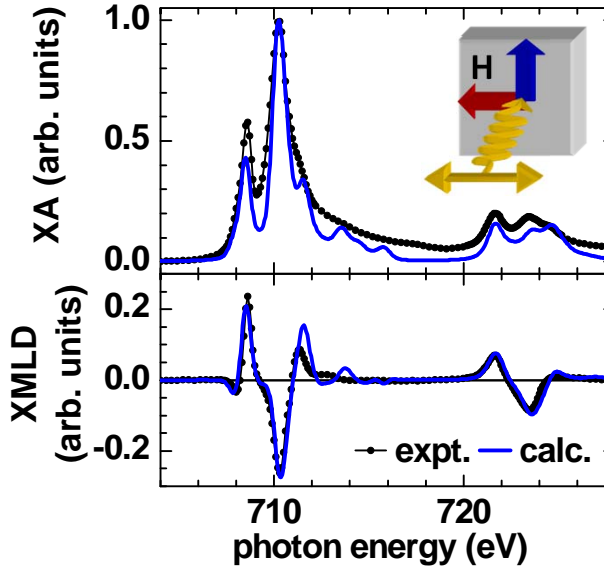


- + $I_{\text{XMLD}} = I_{||} - I_{\perp} \propto \langle m^2 \rangle$, $\langle m^2 \rangle$ = expectation value of square of atomic magnetic moment
- + XMLD allows investigating ferri- and ferromagnets as well as antiferromagnets
- + XMLD spectral shape and angular dependence are determined by magnetic order and lattice symmetry

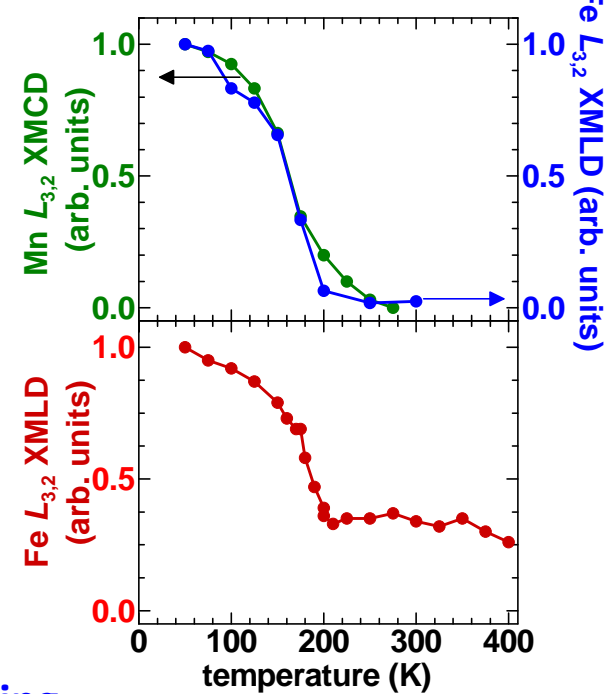
Magnetic Coupling At Interfaces



$\text{La}_{0.7}\text{Sr}_{0.3}\text{MnO}_3$ (LSMO)
ferromagnet
 $\text{La}_{0.7}\text{Sr}_{0.3}\text{FeO}_3$ (LSFO)
antiferromagnet

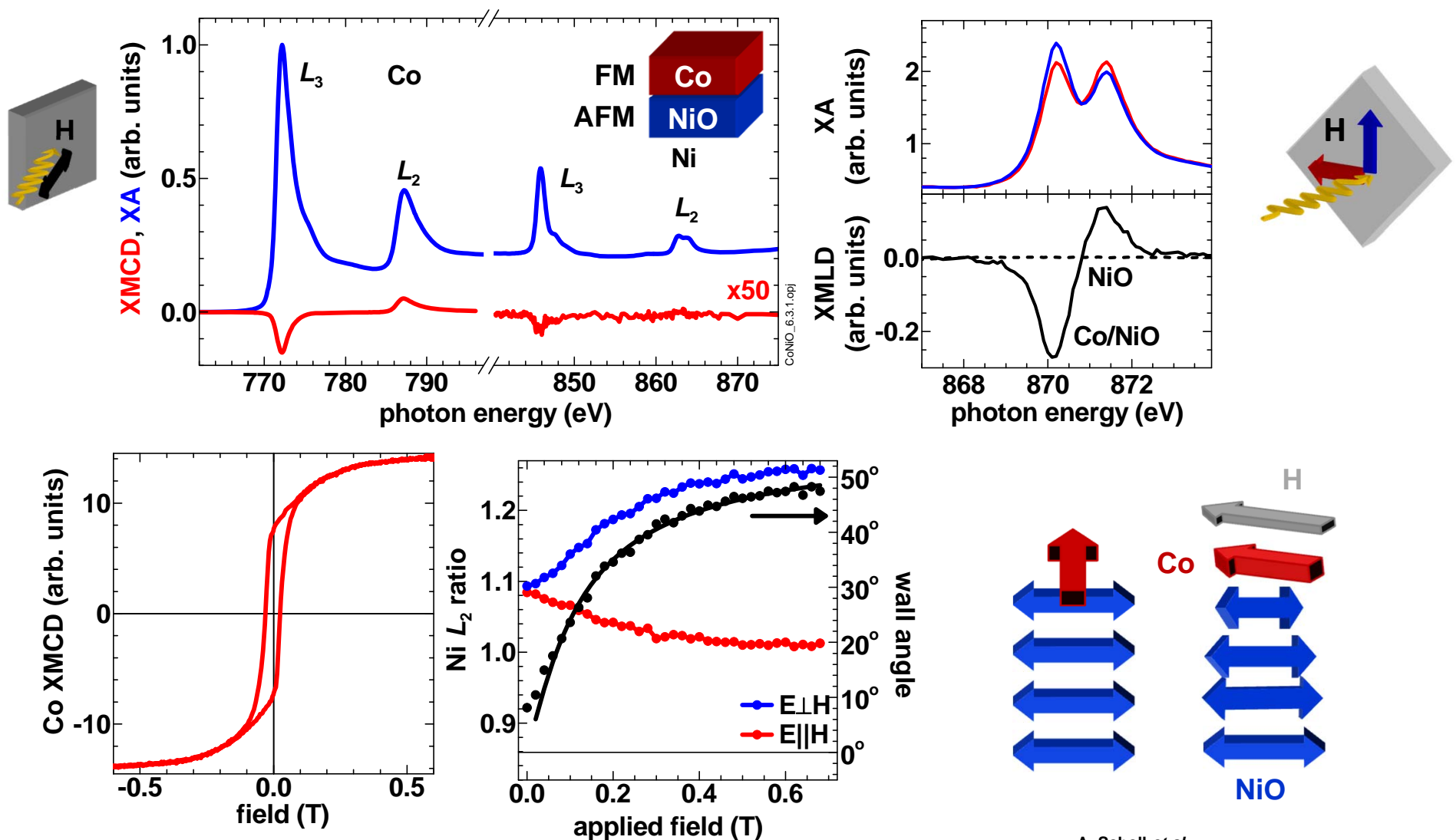


⇒ Perpendicular coupling
at LSMO/LSFO interface



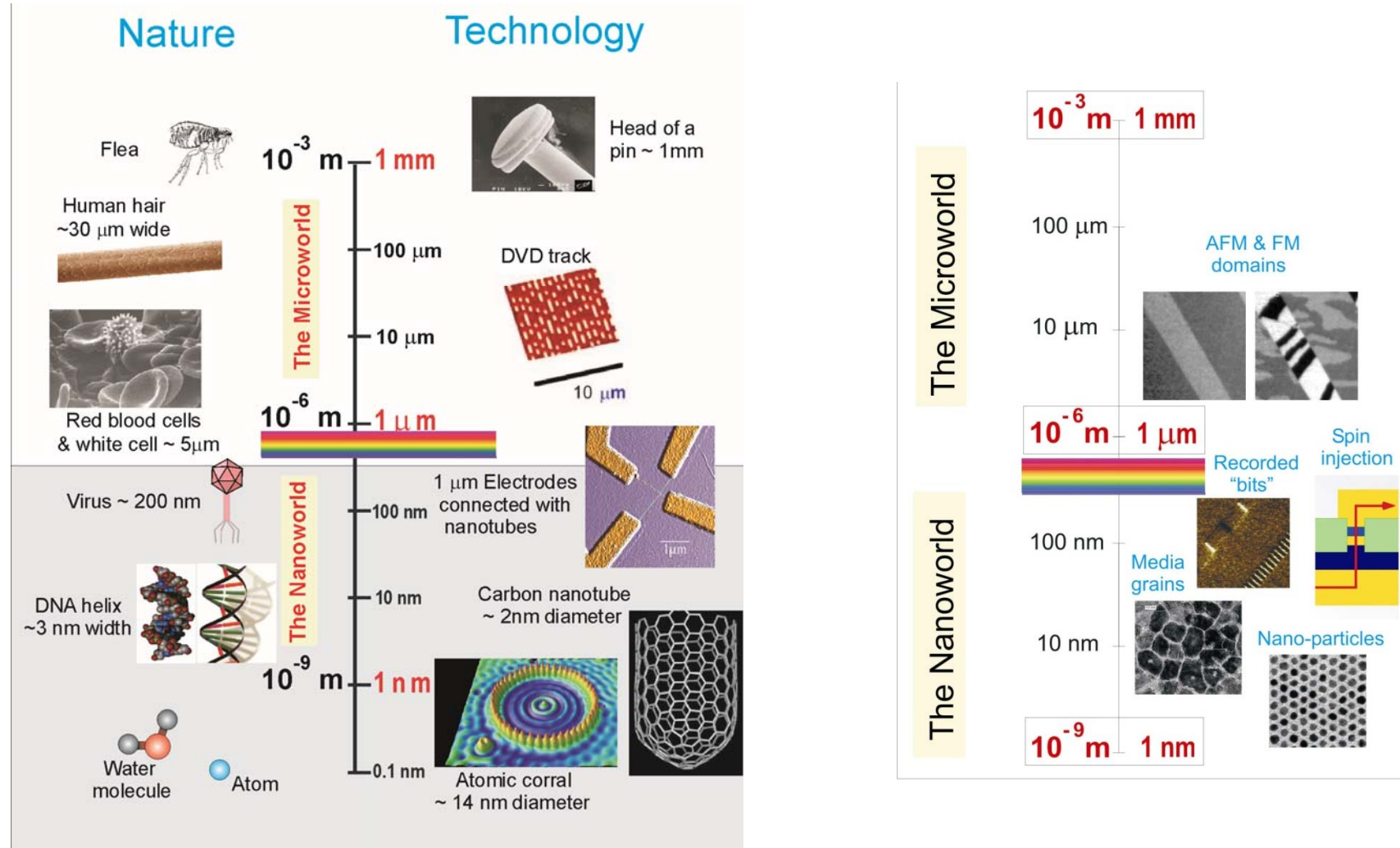
E. Arenholz *et al.*,
Appl. Phys. Lett. **94**, 072503 (2009)

Planar Domain Wall



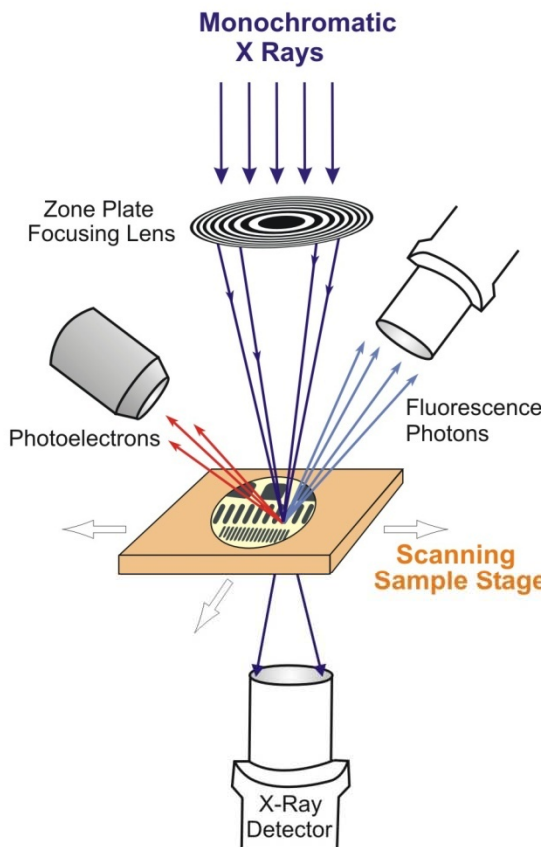
A. Scholl *et al.*,
Phys. Rev. Lett. 92, 247201 (2004)

Magnetic Microscopy

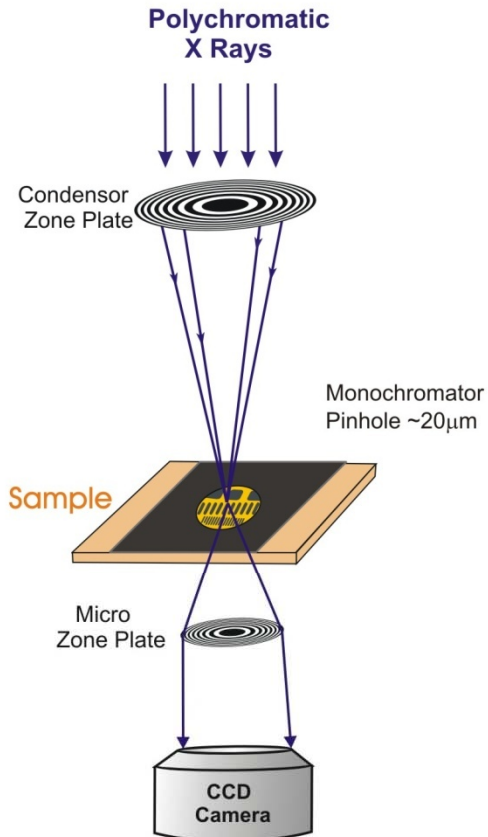


Magnetic Microscopy

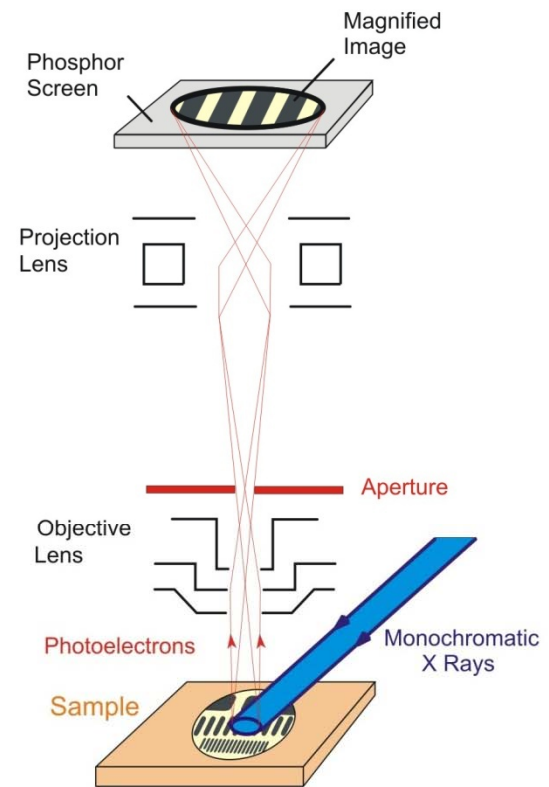
Scanning Transmission X-ray Microscopy
STXM



Transmission X-ray Microscopy
TXM



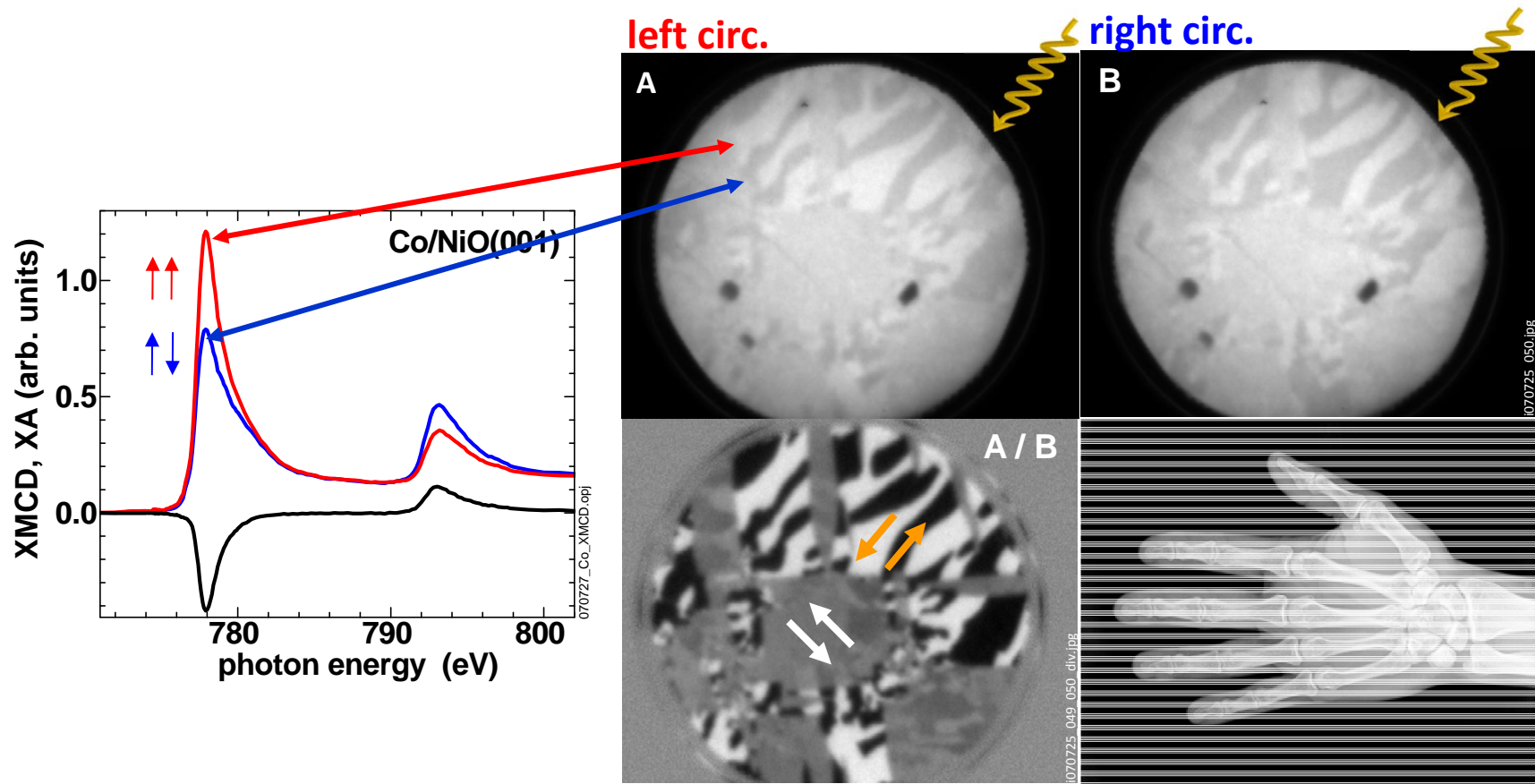
X-Ray Photoemission Electron Microscopy
XPEEM



10-50 nm spatial resolution

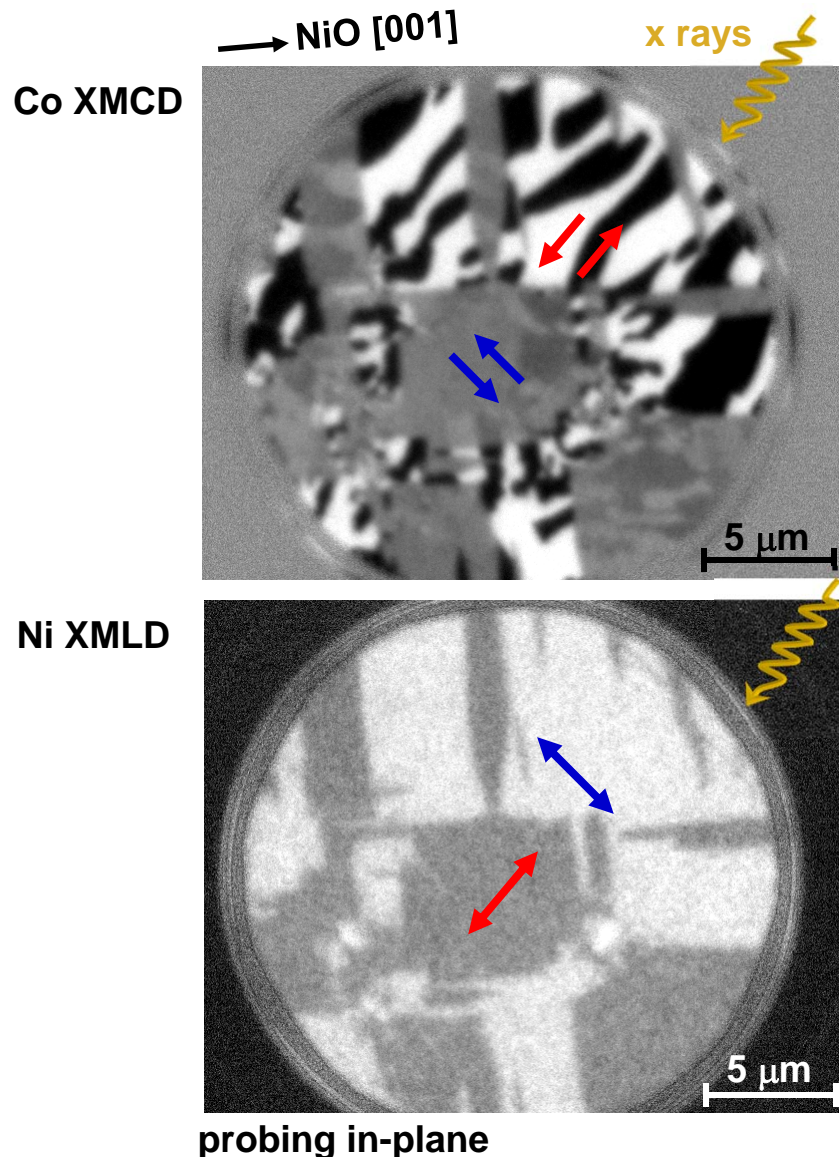
J. Stöhr, H.C. Siegmann,
Magnetism (Springer)

Imaging Magnetic Domains Using X-Rays



- + Images taken with left and right circularly polarized x-rays at photon energies with XMCD, i.e. Co L_3 edge, provide magnetic contrast and domain images.

Magnetic Coupling At Co/NiO Interface



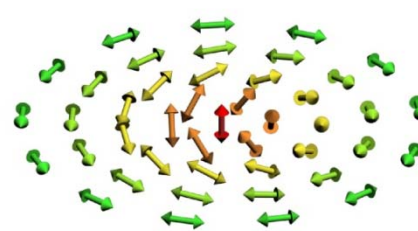
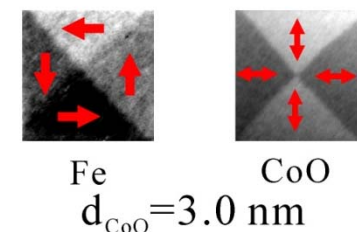
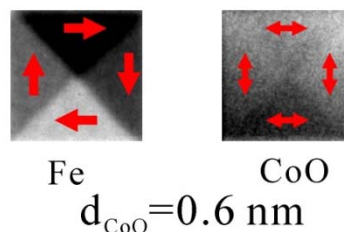
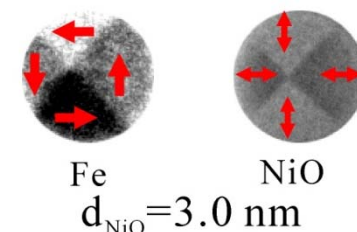
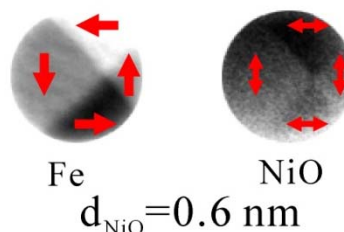
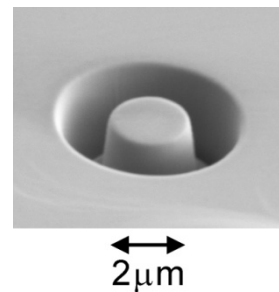
- + Taking into account the geometry dependence of the Ni XMLD signal
- ⇒ Perpendicular coupling of Co and NiO moments at the interface.

E. Arenholz *et al.*,
Appl. Phys. Lett. **93**, 162506 (2008)

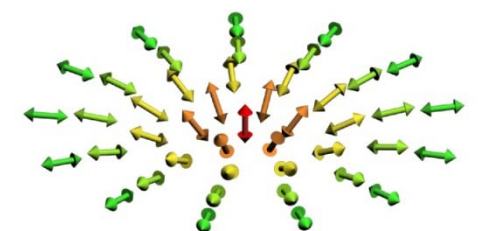
Magnetic Vortices

+ First direct observation of vortex state in antiferromagnetic CoO and NiO disks in Fe/CoO and Fe/NiO bilayers using XMCD and XMLD.

+ Two types of AFM vortices:
- conventional curling vortex as in ferromagnets
- divergent vortex, forbidden in ferromagnets
- thickness dependence of magnetic interface coupling



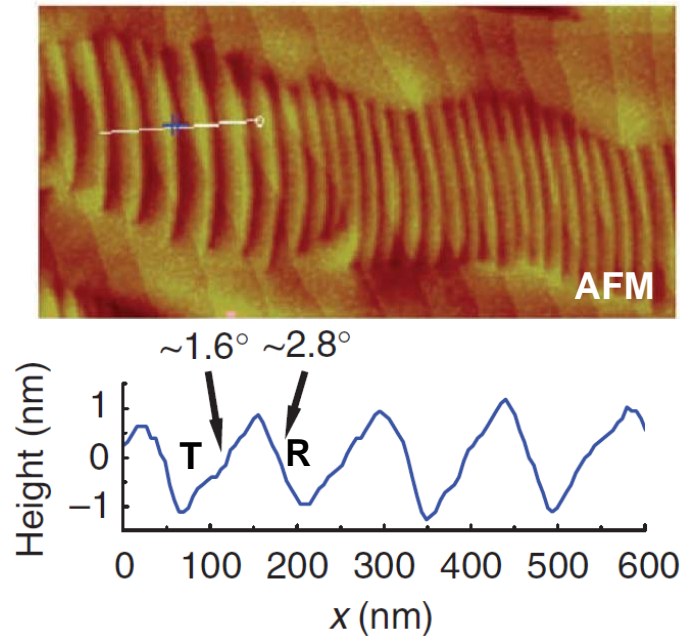
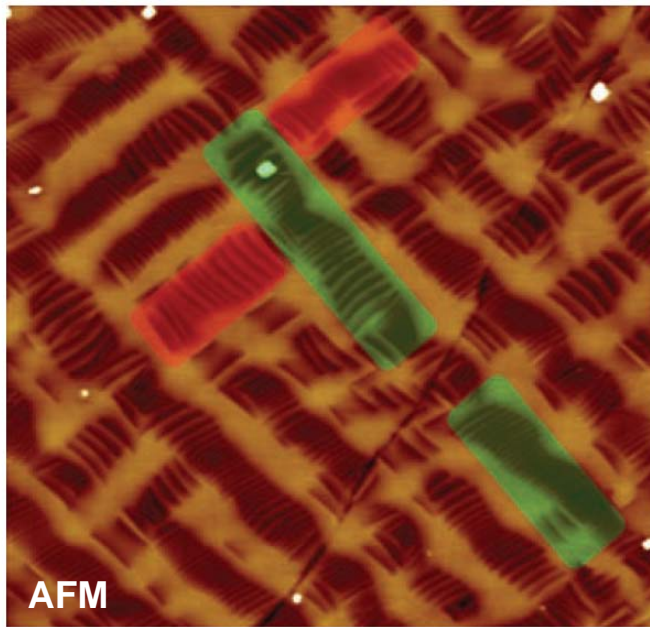
conventional curling vortex



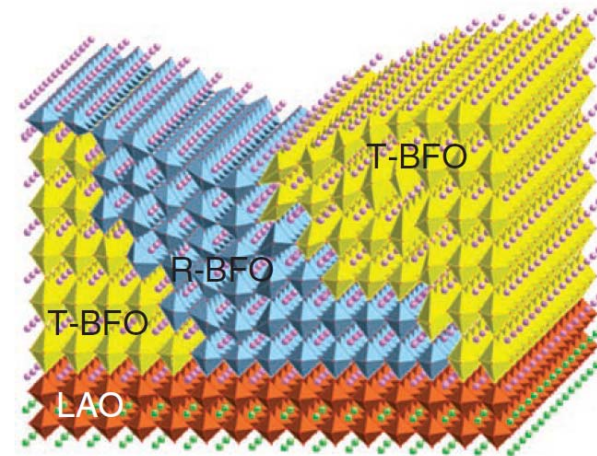
divergent vortex

J. Wu et al.,
Nature Phys. 7, 303 (2011)

Nanoscale Magnetic Phases

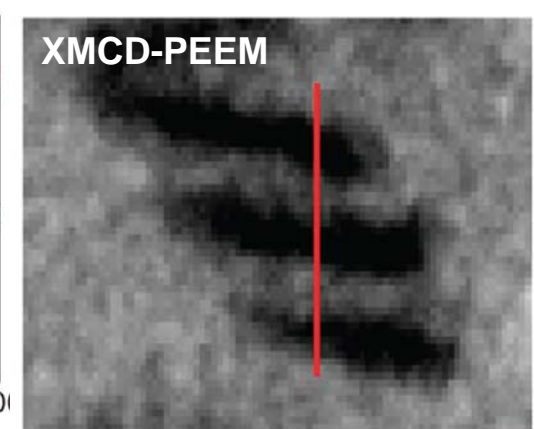
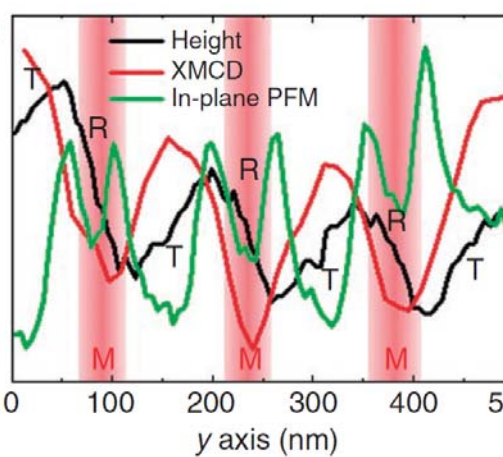
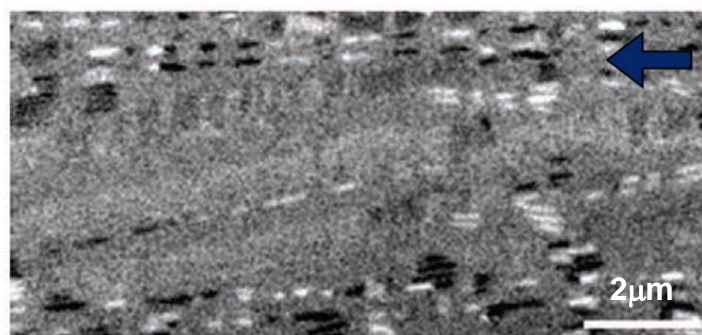
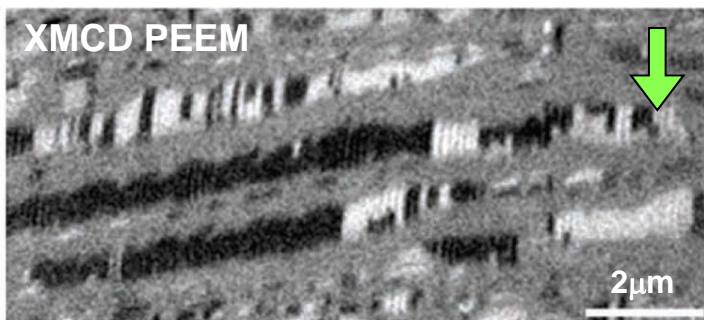
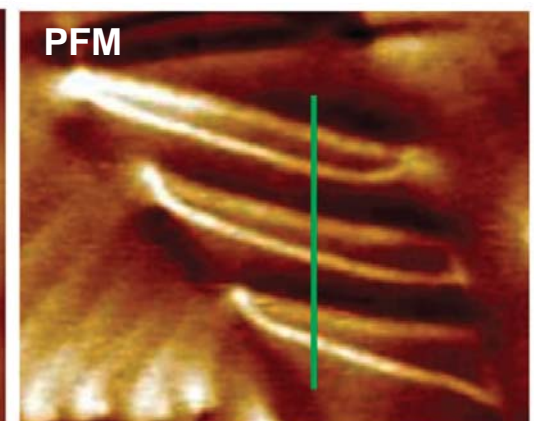
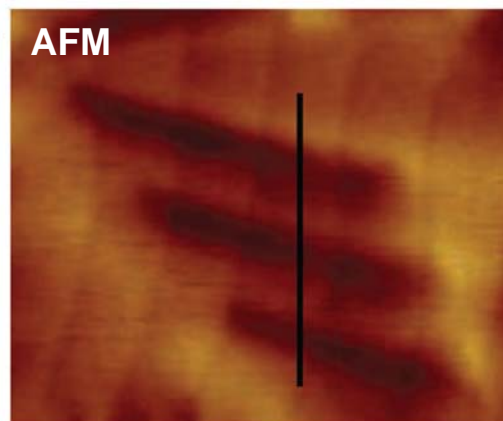
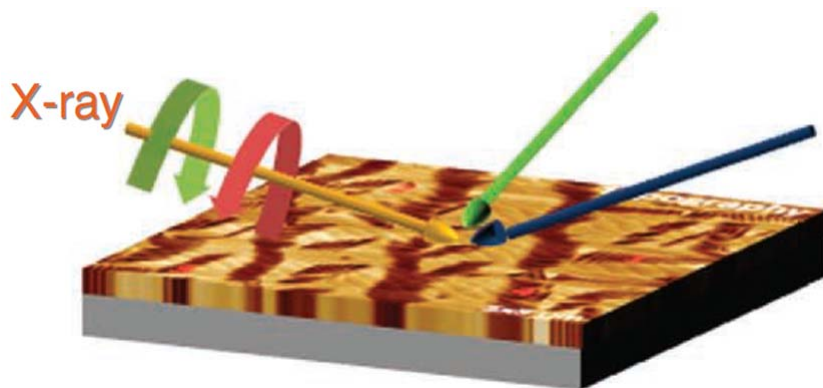


- + BiFeO_3 – multiferroic = ferroelectric + antiferromagnetic
- + Compressive strain on rhombohedral phase (R-phase)
induced by substrate
- ⇒ tetragonal-like phase (T-phase)
- + Partial relaxation of epitaxial strain
- ⇒ Formation of a nanoscale mixture of T- and R-phases



Q. He et al., Nature Comm. 2, 225 (2011)

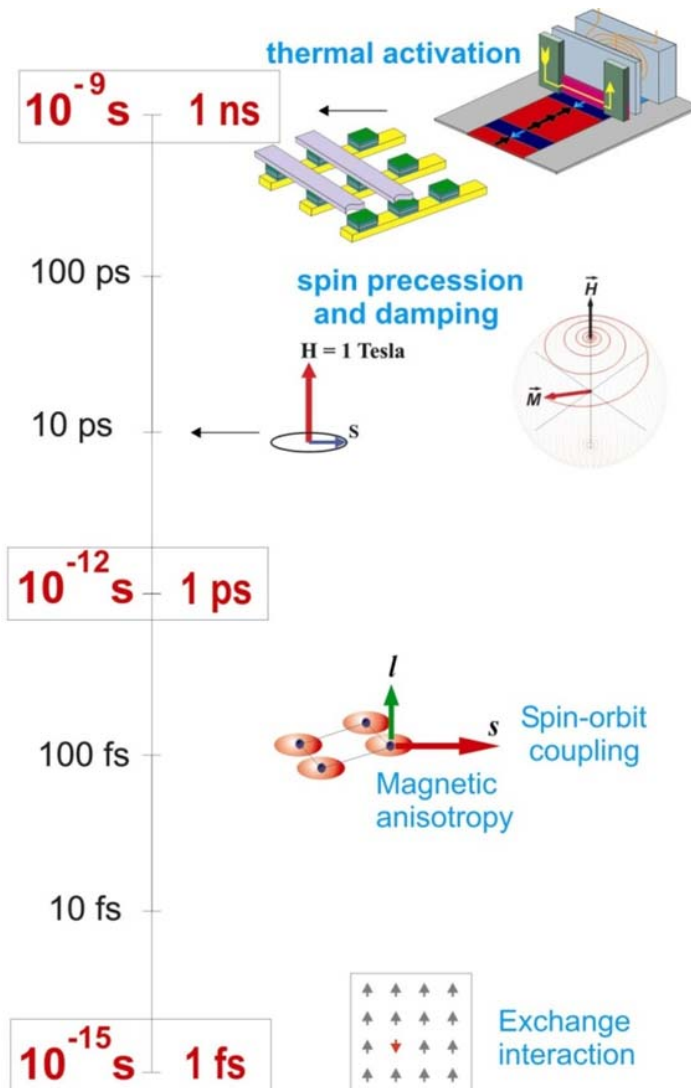
Nanoscale Magnetic Phases



- + Highly distorted R-phase is the source of enhanced magnetic moment in the XMCD image.

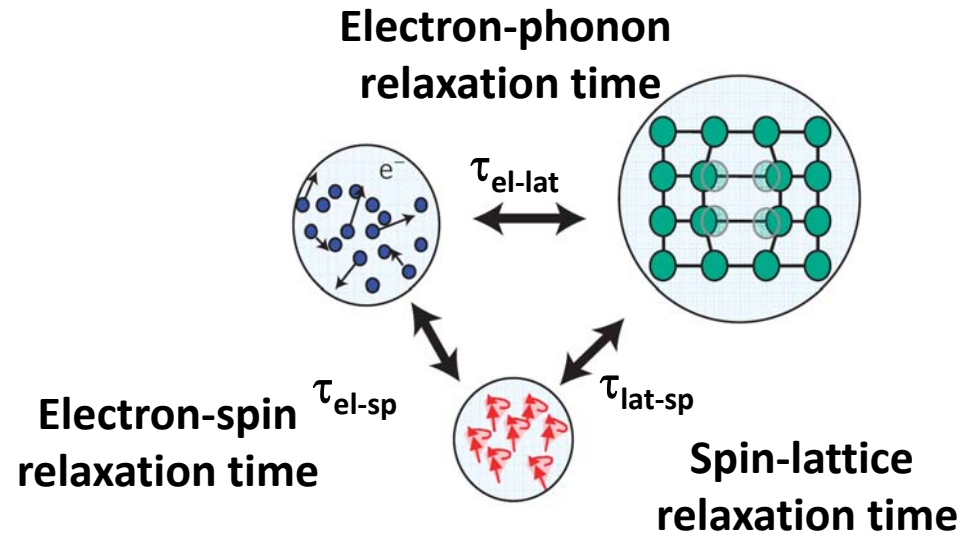
Q. He *et al.*,
Nature Comm. 2, 225 (2011)

Ultrafast Magnetism

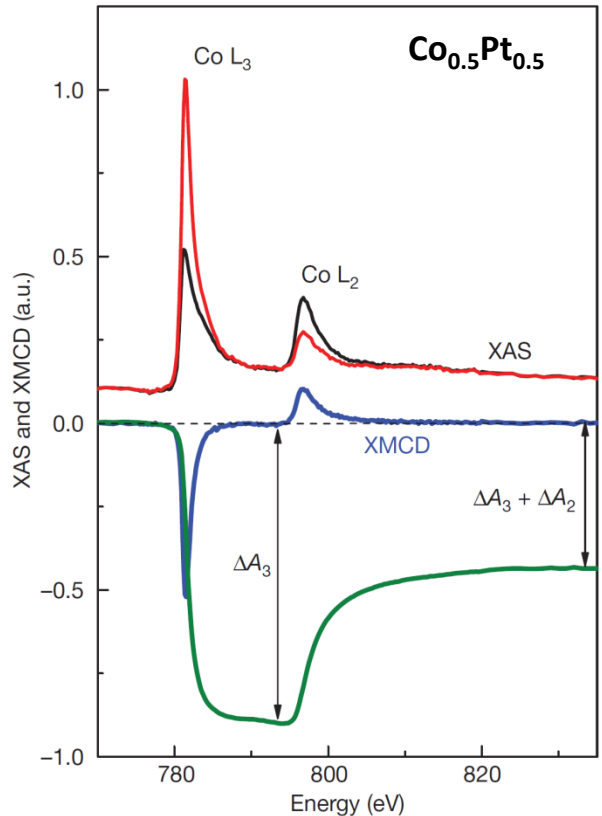


J. Stöhr, H.C. Siegmann,
Magnetism (Springer)

- + Energy reservoirs in a ferromagnetic metal
- + Deposition of energy in one reservoir
- ⇒ Non-equilibrium distribution and subsequent relaxation through energy and angular momentum exchange



Ultrafast Dynamics Of Spin And Orbital Moments

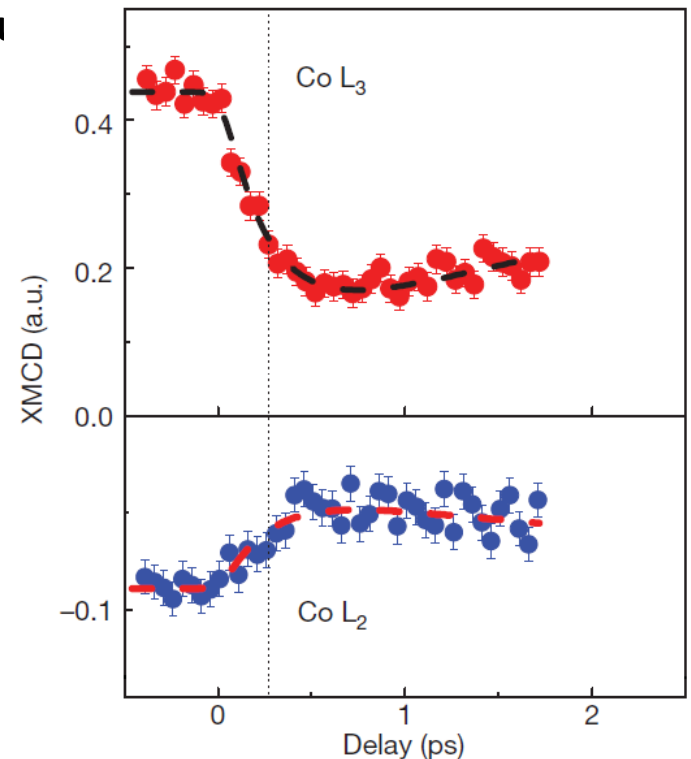


C. Boeglin, et al.,
Nature **465**, 458 (2010)

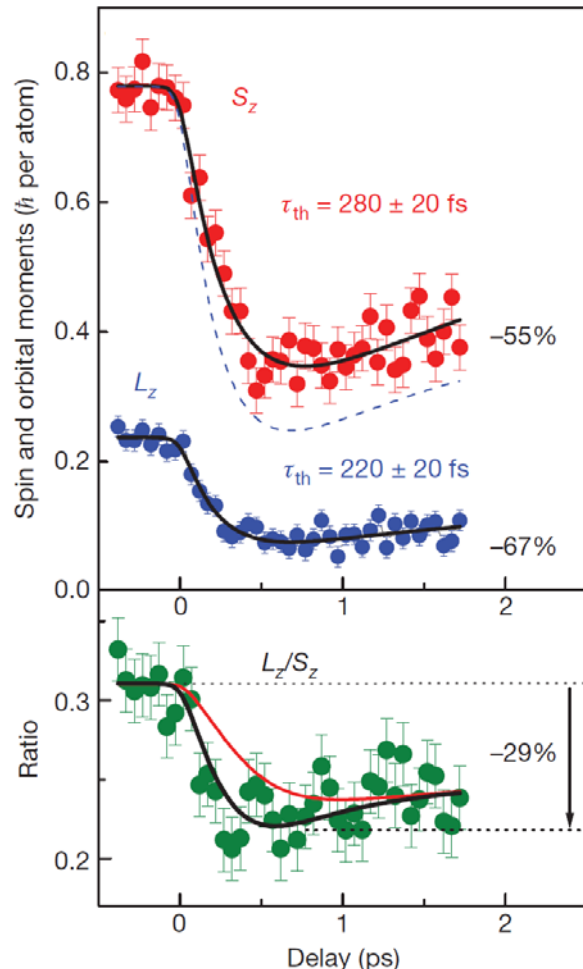
- + Orbital (L) and spin (S) magnetic moments can change with total angular momentum is conserved.
- + Efficient transfer between L and S through spin-orbit interaction in solids
- + Transfer between L and S occurs on fs timescales.

- + $\text{Co}_{0.5}\text{Pt}_{0.5}$ with perpendicular magnetic anisotropy
- + 60 fs optical laser pulses change magnetization
- + Dynamics probed with XMCD using 120fs x-ray pulses

- + Linear relation connects $\text{Co } L_3$ and L_2 XMCD with L_z and S_z using sum rules

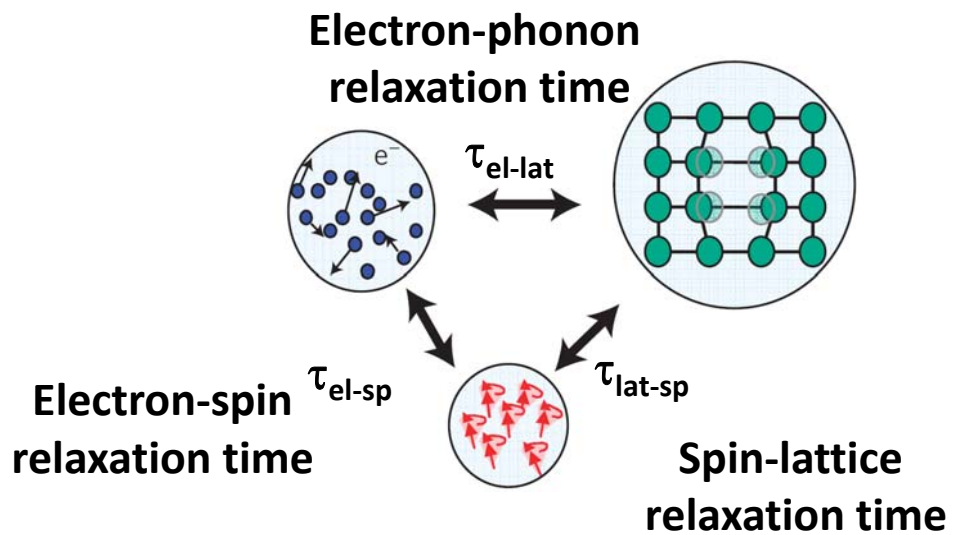


Ultrafast Dynamics Of Spin And Orbital Moments

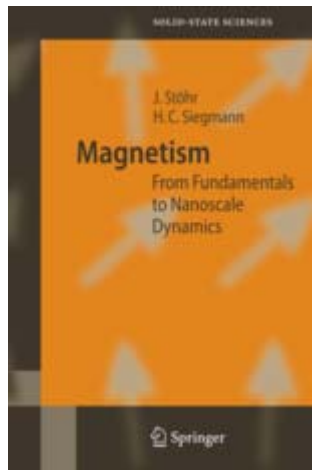


C. Boeglin, et al.,
Nature **465**, 458 (2010)

- + Thermalization: Faster decrease of orbital moment
- + Theory: Orbital magnetic moment strongly correlated with magnetocrystalline anisotropy
- + Reduction in orbital moment
 \Leftrightarrow Reduction in magnetocrystalline anisotropy
- + Typically observed at elevated temperatures in static measurements as well



References And Further Reading



J. Stöhr, H.C. Siegmann
Magnetism – From Fundamentals to Nanoscale Dynamics
Springer